UNITED STATES
NUCLEAR REGULATORY COMMISSION
WASHINGTON, D. C. 20555

December 17, 1982

Docket No. 50-133

MEMORANDUM FOR: The Atomic Safety and Licensing Board
for Humboldt Bay Boiling Water Reactor

FROM: Gus C. Lainas, Assistant Director
for Operating Reactors, DL

SUBJECT: U.S.G.S. OPEN FILE REPORT ON PROBABILISTIC ESTIMATES OF MAXIMUM ACCELERATION AND VELOCITY IN ROCK IN THE U.S. (BOARD NOTIFICATION NO. 82-123)

We have recently received a reprint of an Open File Report 82-1033 entitled, "Probabilistic Estimates of Maximum Acceleration and Velocity in Rock in the Contiguous United States" by S. T. Algermissen et al. of the U. S. Geological Survey (USGS) (attached). Open file reports are vehicles for providing rapid dissemination information and, as such, do not represent official positions of USGS. However, the NRC staff believes that this report may be of interest to the Indian Point Board since it has some relevant information to seismological aspects of the Indian Point Probabilistic Risk Assessment (PRA) study. The report is being sent to the other Boards for information.

The report consists of several sections. An introduction describing new information used since the publication of similar studies in 1976, followed by a discussion of the theory used in developing the probabilistic ground motion maps. Following the theory section, they discuss the earthquake model, magnitude distribution of earthquakes, the different seismic source zones in the contiguous U.S.A. and the different attenuation models used in the analysis. The last section provides a conclusion on what has been learned so far and what will be needed in the future.

The main contribution of this report is the six maps of horizontal velocity and acceleration in rock with 90 percent probabilities of not being exceeded in 10, 50 and 250 years for all parts of the contiguous United States. These probabilities are equivalent to annual probabilities of 1.1×10^{-2}, 2.1×10^{-3}, and 4.2×10^{-4}, respectively.

We are providing this review of seismic hazard levels in the U.S. as general background information. The acceleration levels in this study are arrived at in a different (that is, solely probabilistic) manner than those developed for individual nuclear power plant sites. We will be examining this study more fully in the NRC funded Lawrence Livermore National Laboratory program entitled, "Seismic Hazard Characterization of the Eastern U.S." We will inform the appropriate boards regarding any significant changes in the staff's position as a result of the evaluation.

Gus C. Lainas, Assistant Director
for Operating Reactors
Division of Licensing

Attachment:
As stated

cc: Board/Licensee Service List

Mr. P. A. Crane, V. President
& General Counsel, PG&E
77 Beale Street, 31st Floor
San Francisco, Calif. 94106

cc:

Mr. James Hanchett
Public Information Officer
Region V - IE
U. S. Nuclear Regulatory Commission
1990 N. California Boulevard
Walnut Creek, California 94596

Mr. Eric W. Hedlund
Humboldt County Board of Supervisors
County Courthouse
825 Fifth Street
Eureka, California 95501

Bruce Norton, Esq.
3216 N. Third Street, Suite 202
Phoenix, Arizona 85012

Michael R. Sherwood, Esq.
Sierra Club Legal Defense
Fund, Inc.
2044 Fillmore Street
San Francisco, California 94115

Linda J. Brown, Esquire
Donohew, Jones, Brown & Clifford
100 Van Ness Avenue, 19th Floor
San Francisco, California 94102

Dr. Perry Aminoto
Department of Conservation
Division of Mines & Geology
1416 9th Street, Room 1341
Sacramento, California 95814

Friends of the Earth
ATTN: Andrew Baldwin
124 Spear Street
San Francisco, California 94105

California Department of Health
ATTN: Chief, Environmental
Radiation Control Unit
Radiological Health Section
714 P Street, Room 498
Sacramento, California 95814

U.S. Environmental Protection
Agency
Region IX Office
Regional Radiation Representative
215 Freemont Street
San Francisco, California 94101

Robert H. Engelken
Regional Administrator, Region V
U.S. Nuclear Regulatory Commission
1990 N. California Blvd., Suite 202
Walnut Creek, CA 94596

Robert M. Lazo, Esq. Chairman
Administrative Judge
Atomic Safety and Licensing Board
U. S. Nuclear Regulatory Commission
Washington, DC 20555

Mr. Gustave A. Linenberger
Administrative Judge
Atomic Safety and Licensing Board
U. S. Nuclear Regulatory Commission
Washington, DC 20555

Dr. David R. Schink
Administrative Judge
Department of Oceanography
Texas A & M University
College Station, TX 77840

DISTRIBUTION LIST FOR BOARD NOTIFICATION

Before the Atomic Safety and Licensing Board

Humboldt Bay, Unit 3, Docket Nos. 50-133

Linda J. Brown, Esq.
Philip A. Crane, Jr., Esq.
Gretchen Dumas, Esq.
Friends of the Earth
ATTN: Andrew Baldwin
Robert M. Lazo, Esq.
Mr. Gustave A. Linenberger
Bruce Norton, Esq.
Dr. David R. Schink
Michael R. Sherwood, Esq.

Atomic Safety and Licensing
Board Panel
Atomic Safety and Licensing
Appeal Panel
Docketing and Service Section
Document Management Branch

ACRS Members

Dr. Robert C. Axtmann
Mr. Myer Bender
Dr. Max W. Carbon
Mr. Jesse C. Ebersole
Mr. Harold Etherington
Dr. William Kerr
Dr. Harold W. Lewis
Dr. J. Carson Mark
Mr. William M. Mathis
Dr. Dade W. Moeller
Dr. David Okrent
Dr. Milton S. Plesset
Mr. Jeremiah J. Ray
Dr. Paul C. Shewmon
Dr. Chester P. Siess
Mr. David A. Ward

United States Department of the Interior

Geological Survey

PROBABILISTIC ESTIMATES OF MAXIMUM ACCELERATION AND VELOCITY IN ROCK IN THE CONTIGUOUS UNITED STATES

by

S. T. Algermissen, D. M. Perkins, P. C. Thenhaus,
S. L. Hanson and B. L. Bender

Open-File Report 82-1033

1982

CONTENTS

Page

FIGURES

Page

Page

TABLES

PLATES

1. Map of horizontal acceleration (expressed as percent of gravity) in rock with 90-percent probability of not being exceeded in 10 years.

2. Map of horizontal acceleration (expressed as percent of gravity) in rock with 90-percent probability of not being exceeded in 50 years.

3. Map of horizontal acceleration (expressed as precent of gravity) in rock with 90-percent probability of not being exceeded in 250 years.

4. Map of horizontal velocity (expressed in centimeters per second) in rock with 90-percent probability of not being exceeded in 10 years.

5. Map of horizontal velocity (expressed in centimeters per second) in rock with 90-percent probability of not being exceeded in 50 years.

6. Map of horizontal velocity (expressed in centimeters per second) in rock with 90-percent probability of not being exceeded in 250 years.

ABSTRACT

Maximum horizontal accelerations and velocities caused by earthquakes are mapped for exposure times of 10, 50 and 250 years at the 90-percent probability level of nonexceedance for the contiguous United States. In many areas these new maps differ significantly from the 1976 probabilistic acceleration map by Algermissen and Perkins because of the increase in detail, resulting from greater emphasis on the geologic basis for seismic source zones. This new emphasis is possible because of extensive data recently acquired on Holocene and Quaternary faulting in the western United States and new interpretations of geologic structures controlling the seismicity pattern in the central and eastern United States.

Earthquakes are modeled in source zones as fault ruptures (for large shocks), as a combination of fault ruptures and point sources, and as point sources (for small shocks). The importance of fault modeling techniques is demonstrated by examples in the Mississippi Valley. The effect of parameter variability, particularly in the central and eastern United States is discussed. The seismic source zones used in the development of the maps are more clearly defined and are generally smaller than the seismic source zones used in the Algermissen and Perkins (1976) probabilistic acceleration map. As a result, many areas of high seismic hazard are more clearly defined on these maps than in the 1976 map, although in large areas of the country well defined geologic control for the seismic source zones is still lacking. The six probabilistic ground motion maps presented are multi-purpose maps useful in building code applications, land use planning, insurance analysis and disaster mitigation planning. As fault slip and related geological data become available, the further refinement of probabilistic ground motion maps through the use of time dependent models for earthquake occurrence will become feasible.

INTRODUCTION

The use of probabilistic ground motion maps to represent seismic hazard has evolved from experience with a number of other map representations and from a recognition of their drawbacks. Historical seismicity maps are factual and can serve to warn that earthquakes occur more widely than people usually recognize. However, their focus is on epicenters, and hence the maps lack two vital characteristics: (1) focus on hazardous ground motion, and (2) generalization to likely future areas of seismicity. Historic maximum intensity maps provide the focus on ground motion, but also lack generalization. Algermissen's 1969 generalization of historic maximum intensity achieved widespread acceptance as a hazard map, and slightly altered versions of it still remain in two important building codes. Shortly after the publication of this map, it was recognized that such a map overstates the hazard in those regions where earthquakes occur with greatly reduced frequency compared to the active areas of the country. The Algermissen and Perkins (1976) map introduced probability into the ground-motion description--the map depicted ground motions having the same probability of exceedance everywhere in the U.S. (annual exceedance probability of 1/500). Thus, the 1976 map responded to some criticism of earlier maps, but was perceived to have three new shortcomings: (1) lack of sufficient geological information in the generalization of the seismic history, (2) a focus on only one level of probability, and (3) description of seismic hazard in terms of only one ground-motion parameter, acceleration. The maps presented here are designed principally to answer these three shortcomings, and to improve our understanding of earthquake hazard in the United States.

Since the introduction of a probabilistic acceleration hazard map of the contiguous United States in 1976 (Algermissen and Perkins, 1972, 1976), advances in the understanding of many of the parameters in probabilistic hazard mapping have been significant. New information has become available to the extent that a revision of the 1976 probabilistic map provides important advances in the mapping of ground motion in the United States. Extensive mapping of Holocene and Quaternary faults, interpretations of the size of earthquakes represented by such faults, and recurrence estimates of large earthquakes based on such faults, have become available, particularly in California, Nevada and Utah. New geological and seismological research programs in the Mississippi Valley, New England, and the Charleston, South Carolina, area largely initiated since the publication of the 1976 probabilistic ground motion map have provided important new data and seismotectonic concepts.

Earthquake catalogs have substantially improved during the past five years through review and revision of regional and national earthquake catalogs. Examples of improved catalogs that we have made use of are the Utah Catalog by Arabasz and others (1979), the new catalog of the midwest by Nuttli and Herrmann (1978) and the USGS state seismicity maps and catalogs that have now been published for 27 states by Stover and others (1979-1981).

Considerable advances have also been made in the technique used in the computation of probabilistic hazard maps. The computer programs used in hazard analysis have been completely rewritten since 1976 (Bender, 1982, Bender and Perkins, 1982) and a number of support programs for the assembly of various kinds of data, analysis of completeness of seismological data and plotting routines have been completed. Despite improvements in the data base

and computational techniques since 1976, a number of the parameters in hazard analysis remain troublesome. These will be discussed as appropriate later in the text.

The decision was made to develop maps of acceleration and velocity for three exposure times: 10, 50 and 250 years. These maps provide significantly more information for the evaluation of ground motion for engineering purposes in the United States than can be obtained from the single, 50-year exposure time, acceleration map published in 1976. The velocity maps provide a useful additional measure of ground motion. The three exposure time maps indicate, for any point, the nature of the change in ground motion for various exposure times of interest. The additional maps together with the refinement of the parameters used in the development of the maps should provide appreciably improved ground motion estimates for building codes and for the design of structures in general.

CONCEPT OF HAZARD MAPPING

The concept of hazard mapping used here is to assume that earthquakes are exponentially distributed with regard to magnitude and randomly distributed with regard to time. The exponential magnitude distribution is an assumption based on empirical observation. The distribution of earthquakes in time is assumed to be Poissonian. The assumption of a Poisson process for earthquakes in time is consistent with historical earthquake occurrence insofar as it affects the probabilistic hazard calculation. Large shocks closely approximate a Poisson process, while small shocks may depart significantly from a Poisson process. The ground motions associated with small earthquakes are of only marginal interest in engineering applications and consequently the

Poisson assumption serves as a useful and simple model (Cornell, 1968). Spatially, the seismicity is modeled by grouping it into discrete areas termed seismic source zones. The most general requirements for a seismic source zone is as follows: (1) it have seismicity, and (2) it be a reasonable seismotectonic or seismogenic structure or zone. If a seismogenic structure or zone cannot be identified, the seismic source zone is based on historical seismicity. A seismotectonic structure or zone is taken here to mean a specific geologic feature or group of features that are known to be associated with the occurrence of earthquakes. A seismogenic structure or zone is defined as a geologic feature or group of features throughout which the style of deformation and tectonic setting are similiar and a relationship between this deformation and historic earthquake activity can be inferred.

The concept of probabilistic hazard mapping outlined above will be discussed in detail in the sections that follow.

THEORY

Development of probabilistic ground motion maps using the concepts outlined above involves three principal steps: (1) delineation of seismic source areas; (2) analysis of the statistical characteristics of historical earthquakes in each seismic source area; and (3) calculation and mapping of the extreme cumulative probability $F_{max,\ t}(a)$ of ground motion, a, for some time, t. These steps are shown schematically in figure 1. The general technique used here is essentially the same as that presented by Cornell (1968) with integrations replaced by discrete summations for flexibility in the representation of attenuation functions and source areas.

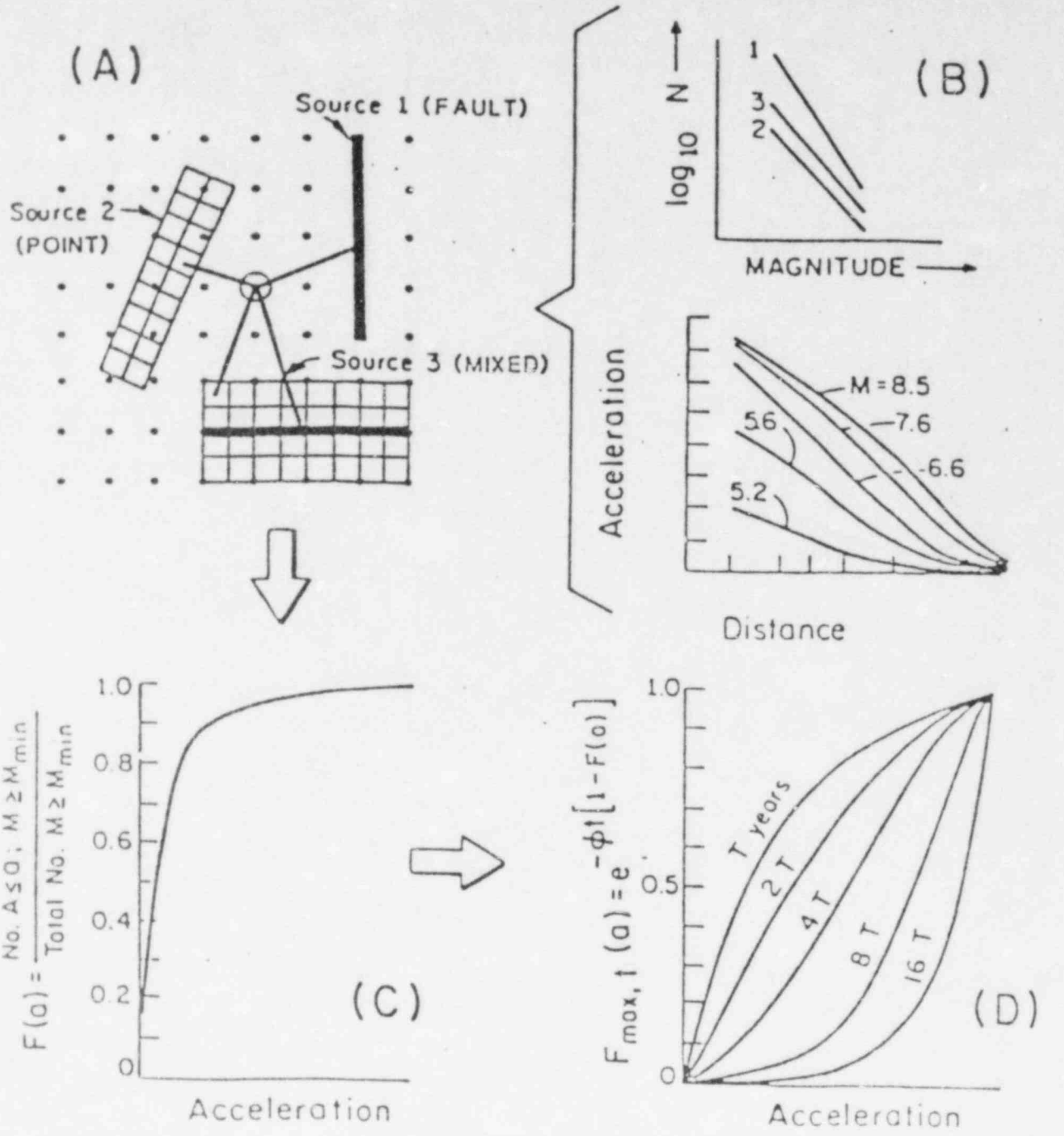

Figure 1 - Elements of the probabilistic hazard calculations.

(A) Typical source areas and grid of points at which the hazard is to be computed.
(B) Statistical analysis of seismicity data and typical attenuation curves.
(C) Cumulative conditional probability distribution of acceleration.
(D) The extreme probability $F_{max,\ t}(a)$ for various accelerations and exposure times (T).

Three idealized seismic source areas are shown in figure 1A. The earthquake within each source zone can be modeled as: (1) point sources in areas (used to represent earthquakes for which the fault rupture length is small compared with the map scale being used); (2) finite rupture lengths; or (3) as a mixed source, for example point sources for small earthquakes and fault (two dimensional) sources for larger earthquakes. These source areas are delineated on the basis of historical seismicity together with an evaluation of available geological evidence related to earthquake activity by methods to be detailed later.

After the zones are delineated, relationships of the form:

$$\log N = a - bM \qquad (1)$$

are determined for each source zone, where N is the number of earthquakes in a given magnitude range per unit time and a and b are constants to be determined. M is taken as M_s for shocks greater than or equal to 6.75 and is taken to be M_L for shocks less than 6.75. If the seismicity of individual source zones in a region is low, the b value (slope) in equation 1 is determined by considering the seismicity in an ensemble of source zones. Research (Bender, 1982) has shown that for zones in which the total number of earthquakes is less than about 40, significant errors in the computed b-values occur. The a-value for each source zone is determined by fitting a line with slope b through the seismicity data for each zone. Generally a minimum chi square regression was used for curve fitting although in the western portion of California a weighted least squares technique was used (Thenhaus and others, 1980). The two techniques yield equivalent results with earthquake

sample sizes of about 40 or more. The distribution of earthquakes in each source zone is then characterized by the parameters of equation 1, up to some maximum magnitude which is assigned for each zone.

The future spatial occurrence of earthquakes in each source zone is assumed to be uniform throughout each source area. That is, if each seismic source area is divided into n small divisions (such as shown in fig. 1A) and if the number of earthquakes likely to occur in any magnitude range is N, then the number of earthquakes likely to occur in this magnitude range in each small division or block of a source area is

$$\frac{N}{n} \qquad (2)$$

If seismicity is distributed along a fault of length L, the distribution of earthquakes is somewhat more complicated. We have used the relationship between fault rupture length (L) and magnitude (M) suggested by Mark (1977):

$$\log (L) = 1.915 + 0.389\ M \qquad (3)$$

where L is the average fault rupture length in meters and M is as already defined. If there are $N_{M_2 - M_1}$ earthquakes in the magnitude interval M_2-M_1 that have an average length of rupture (determined from equation 3) of L_{ave} and we are modeling a fault of length X, the earthquakes are distributed at the rate of

$$\frac{N_{M_2 - M_1}}{X - L_{ave}} \qquad (4)$$

earthquakes per unit of length along the fault. If one end of a fault is located at X_1 and the other end at X_2, the earthquake rupture centers are assumed to occur uniformly

between $X_1 + \frac{L_{ave}}{2}$ and $X_2 - \frac{L_{ave}}{2}$ along the fault.

Once the distribution of earthquakes likely to occur in each small division of the source or along a fault is decided upon, the effect at each site due to the occurrence of earthquakes in each small division of the source or for each fault can be computed using suitable ground motion attenuation curves such as those shown in Figure 1B. In practice, the distribution of ground motion is computed for a number of sites located on an appropriate grid pattern (fig. 1A).

From the distribution of ground motion at each site (part C of fig. 1) it is possible to determine directly the expected number of times a particular amplitude of ground motion is likely to occur in a given period of years at a given site, and, thereby, the maximum amplitude of ground motion in a given number of years corresponding to any level of probability. The relationship between return period $R_y(a)$, exposure time, T, and probability of exceedance during that exposure time, $1-F_{max,t}(a)$ is best explained by the following development.

First, the distribution of the expected number of occurrences of ground motion at each location is calculated. The peak ground motion, for example, the peak acceleration corresponding to some extreme probability, is then calculated from the distribution of the expected number of occurrences in the following manner. Let the peak acceleration be a , then

$$F(a) = P[A<a \mid M>M_{min}] \qquad (5)$$

is the probability that an observed acceleration A is less than or equal to the value a, given that an earthquake with magnitude M, greater than some minimum magnitude of interest, has occurred. The calculation at a given grid point or along a fault is performed for every acceleration a of interest using:

$$F(a) = \frac{\text{expected number of occurrences with } A<a \text{ and } M>M_{min}}{\text{total expected number of occurrences } (M>M_{min})}$$

A typical F(a) is shown in figure 1C.

Assume N independent events with accompanying accelerations A_i. The cumulative distribution of the maximum accleration of the set of N accelerations is given by

$$F_{max}(a) = P[\text{The largest of the N accelerations is less than or equal to a}]$$

$$= P[\text{each of the N accelerations is less than or equal to a}]$$

$$= P[A_1 \leq a]\ P[A_2 \leq a] \ldots P[A_n \leq a], \text{ since the events are independent}$$

$$= F(a)^N, \text{ if the events are identically distributed} \qquad (6)$$

If N itself is a random variable

$$F_{max}(a) = F(a)^0 \cdot P(N=0) + F(a)^1 \cdot P(N=1) + \ldots + F(a)^j \cdot P(N=j) + \ldots$$

$$F_{max}(a) = \sum_{j=0}^{\infty} F(a)^j \, P(N=j) \tag{7}$$

If N has a Poisson distribution with mean rate λ,

$$F_{max}(a) = \sum_{j=0}^{\infty} F(a)^j \frac{\lambda^j e^{-\lambda}}{j!} = e^{-\lambda} \sum_{j=0}^{\infty} \frac{(\lambda F(a))^j}{j!} = e^{-\lambda} e^{\lambda F(a)}$$

$$F_{max}(a) = e^{-\lambda (1-F(a))} \tag{8}$$

Now if $\lambda = \phi t$, where ϕ is mean rate of occurrence of earthquakes $M \geq M_{min}$ per year and t is number of years in a period of interest, then:

$$F_{max,t}(a) = e^{-\phi t[1-F(a)]} \tag{9}$$

In the program, a table of accelerations (a) and F(a) is constructed. For a particular exposure time $t = T$, $F_{max,t}(a)$ is calculated, and the value of a for a given extreme probability, say $F_{max,t}(a) = .90$, is found by interpolation.

It is convenient here to define the term return period as:

$$R(a) = \frac{1}{1-F(a)} \tag{10}$$

where R(a) is the average number of events that must occur to get an acceleration exceeding a. The return period in years is given approximately by

$$R_y(a) = \frac{R(a)}{\text{Expected number of events per year } (M \geq M_{min})} \tag{11}$$

We obtain from (10) and (11):

$$\phi t(1-F(a)) = \frac{t}{R_y(a)} \tag{12}$$

thus,

from (9) and (12): $F_{max,t}(a) = e^{-t/R_y(a)}$ (13)

and $\ln (F_{max,t}(a)) = -\frac{t}{R_y(a)}$ (14)

For an extreme probability of .90 and an exposure time of t=10 years:

$$\ln (.90) = -\frac{10}{R_y(a)}$$

or $$R_y(a) = \frac{10}{.1054} = 94.9 \text{ years}$$

Thus, the average return period for the accelerations we have mapped is about 95 years. For the same extreme probability (.90), exposure times of 50 and 250 years yield average return periods of 474.4 and 2371.9 years.

It may be useful to point out that using equation (13) and setting the exposure time equal to the average return period R_y (a); that is

$$t = R_y(a),$$

we have

$$F_{max,\ t}(a) = e^{-1} = 0.37. \qquad (15)$$

Thus the acceleration with a return period of $R_y(a)=t$ years has a probability of

$$1 - F_{max,\ t}(a) = 1 - 0.37 = 0.63 \text{ or } 63\%$$

of being exceeded in t years. The point is that accelerations (or any other parameter) with a particular return period have a 63-percent probability of being exceeded during an exposure time equal to that return period. Because the acceleration with a return period of R years is often incorrectly associated with zero probability of exceedance in less than R years, it is preferable to explicitly state the probability of exceedance and exposure time T associated with a particular ground motion. In addition the earthquakes which produce the R-year <u>return period</u> ground motion at a site may have <u>recurrence intervals</u> in the source region of one-third to one-tenth R, depending on the area of the source zone. Avoiding the use of return period will hopefully avoid the identification of the return period of ground motion with the recurrence interval of earthquakes.

Frequently, it is convenient to express the maximum ground motion in terms of the annual probability of exceedance. Let $r_T(a)$ be the probability of exceedance of ground motion a in T years; then

$$F_{max,\ T}(a)=1-r_T(a)=e^{-T/R_y(a)} \tag{16}$$

and

$$r_T(a)=1-e^{-T/Ry(a)}. \tag{17}$$

For T = one year, (17) becomes

$$r_T(a) = 1-e^{-\frac{1}{Ry(a)}}$$

when R_y (a) is sufficiently large (say, greater then ten years),

$$r_T\ (a) = \frac{1}{R_y(a)}$$

DEVELOPMENT OF THE PROBABILISTIC MODEL

The development of a probabilistic model for earthquake hazard analysis requires data and assumptions concerning parameters such as the earthquake rupture length, the magnitude distribution and the sequence of occurrence in time of the earthquakes, the geometry of the seismic source zones and the attenuation of seismic waves. The general concept and theory of the model have already been discussed.

Earthquake Model

The earthquakes were modeled in a very simple way. The earthquakes are all assumed to be shallow shocks similar to the California earthquakes used in the development of the Schnabel and Seed (1973) acceleration curves, with the exception of the intermediate focal depth shocks in the Puget Sound, Washington, area. Earthquakes were modeled as (a) point sources, or as (b) line rupture sources, the length of faulting being obtained from equation (3).

Magnitude Distribution

The magnitude distribution was taken to be exponential and of the form given by equation 1. The earthquakes in each seismic source zone were corrected for completeness using the technique suggested by Stepp (1973). As previously discussed, b-values were determined for groups of seismic source zones where the historical seismicity was low in individual zones. The a-values for each zone were then obtained by a minimum chi-square fit through the earthquake data for each zone, holding the b-value constant. For seismic source zones with high historical seismicity, b-values were often obtained for each seismic source zone independently. The seismic source zones used in the preparation of the maps are shown in Figures 2 and 3. The slope, b, and the number of intensity V earthquakes per year in each zone are listed in Table 1. Earthquakes with magnitudes less than M_L=4.0 or intensities less than V were not considered in the computation of the ground motion. For each seismic source zone the maximum magnitude was determined from a consideration of (1) the largest historical earthquake that had occurred (in zones with high rates of activities); (2) the tectonic setting of any particular zone; (3) technical opinions expressed at the workshop in which the source zone was considered;

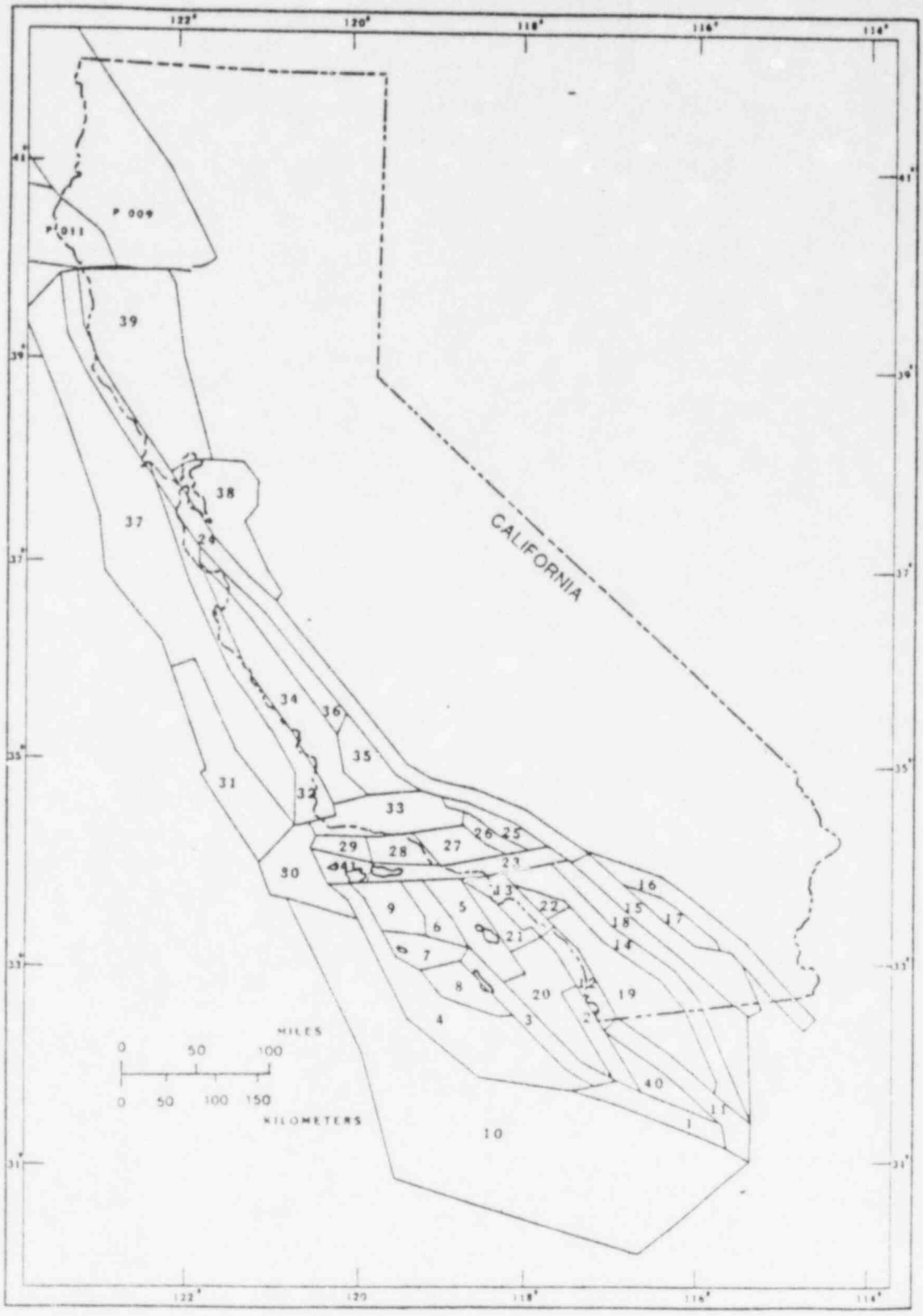

Figure 2 - Seismic source zones in western California and the adjacent offshore area. The numbers in the source zones are used to identify each zone in the discussion in the text and in Table 1. Zones 1-39 are preceded by "c" in Table 1.

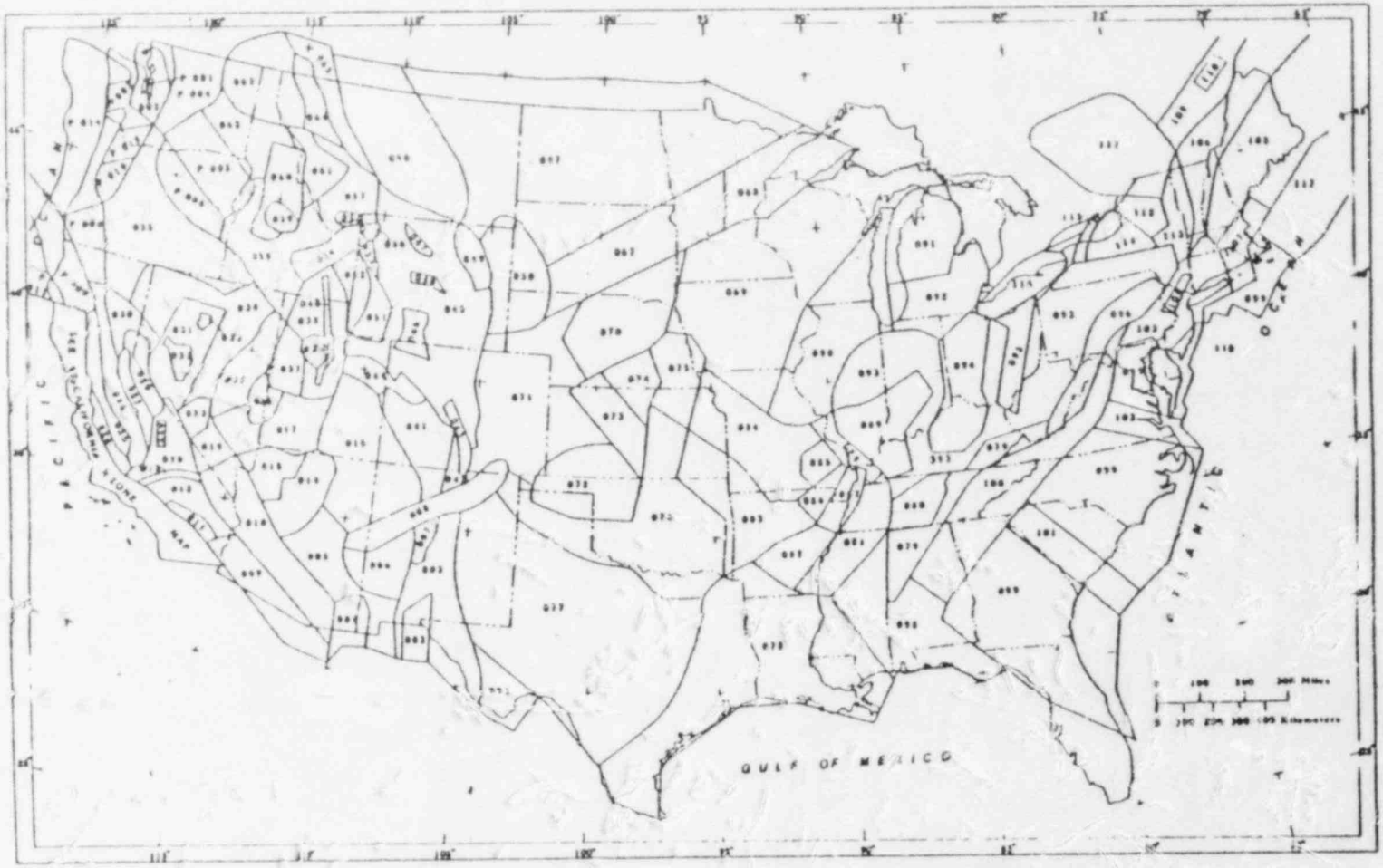

Figure 3 - Seismic source zones in the contiguous United States (other than those shown in Figure 2). The numbers in the source zones are used to identify each zone in the discussion in the text and in Table 1.

(4) and combinations of the above sources of information. The magnitudes used in this paper have been obtained in two ways: (1) from earthquake catalogs containing instrumentally determined magnitudes, and (2) by computing the magnitude obtained from the maximum intensity I_o using the relationship $M = 1.3 + 0.6\ I_o$ (Gutenberg and Richter, 1942). The magnitudes used by Gutenberg and Richter in deriving the above $M - I_o$ relationship were principally M_L for shocks with M_L of about 6 3/4 or less and M_s for larger earthquakes. Since instrumental magnitudes are not available for many important earthquakes, extensive use was made of the $M - I_o$ relationship. Thus, the maximum magnitudes used for the seismic source zones are, in general, expressed as M_s magnitudes. Table 1 lists pertinent information concerning the magnitude distribution of earthquakes assumed for each seismic source zone. In the Nevada seismic zone, the maximum magnitude was reduced to $M_L = 6.0$ in zones in which large historical earthquakes had occurred (zones 022, 032 and 033 in Figure 3). The assumption is that in the Nevada seismic zone large earthquakes are not likely to reoccur in the same zones where they have already occurred historically, at least in the time period of interest of the hazard maps (up to exposure times of 50 years). This assumption is consistent with current thinking concerning the temporal and spatial distribution of large shocks in western Nevada (Wallace, 1977a, 1978c; Ryall, 1977; Ryall and others, 1966; Van Wormer and Ryall, 1980; Ryall and Van Wormer, 1980). Historical earthquakes with magnitudes greater than 6.0 in zones 022, 032 and 033 were distributed into the surrounding zone. For example, the earthquakes with magnitudes greater than 6.0 in zones 032 and 033 were distributed into zone 031. The larger shocks in zone 022 were distributed into 020.

Occurrences of Earthquake in Time

The distribution of earthquakes in time is assumed to be Poissonian. The southern California earthquake catalog, after removal of aftershocks, has been shown to be Poissonian (Gardner and Knopoff, 1974). The important observation is that the occurrence of large shocks tends to be Poissonian while small shocks often are not. However, the ground motions associated with small shocks are of only marginal interest in engineering applications (Cornell, 1968).

Seismic Source Zones

The probabilistic ground motion calculations use as input a model of the future seismicity. This model consists of source zones and their associated rates of activity for earthquakes of various magnitudes up to the maximum magnitude assumed for each zone. Within each source zone, which may be a fault or an area, the seismicity is assumed to be uniformly distributed spatially. The size of the source zone reflects the following:

(1) The amount and applicability of geological and seismological information available.

(2) A reasonable generalization from the seismic history, based both on (1) and the period of interest for which the resulting probabilistic maps are to apply.

(3) The scale of mapping. For a national-scale map, some of the detail available for local or regional mapping would not be useful.

The seismic source zones used for the national map (Figs. 2 and 3) are the result of a concerted effort to introduce more seismotectonic information into the development of source zones (Thenhaus and others, 1982a). Figure 4 indicates areas considered in various workshops and other meetings concerned with the presentation and discussion of seismotectonic data useful in the development of seismic source zones. The initial, new mapping effort was focused on Alaska and the offshore areas adjacent to the eastern and western contiguous United States. Liaison was maintained with Survey geologists in Menlo Park and Alaska during the development of the west coast (Perkins and others, 1980; Thenhaus and others, 1980) and Alaska maps (Thenhaus and others, 1982). As a result, the seismotectonic basis for the seismic source zones for the new national map in areas A and B of Figure 4 rely heavily on data developed and discussions held with a number of U.S. Geological Survey geologists and geophysicists during the preparation of the offshore hazard maps.

As the work on the national map proceeded, a more formal series of meetings evolved and five workshops were conducted to consider five additional regions: (1) the Great Basin (area C, Figure 4); (2) the northern and central Rockies (area D, Figure 4); (3) the southern Rockies and the southern Great Basin (area E, Figure 4); (4) the central interior (area G, Figure 4), and (5) the northeast (area H, Figure 4). The seismotectonics of the southeast United States were discussed at two U.S. Geological Survey meetings conducted during the preparation of eastern offshore hazard maps. The workshops held for areas D, E, and G also considered some aspects of the seismotectonics of area F (figure 4).

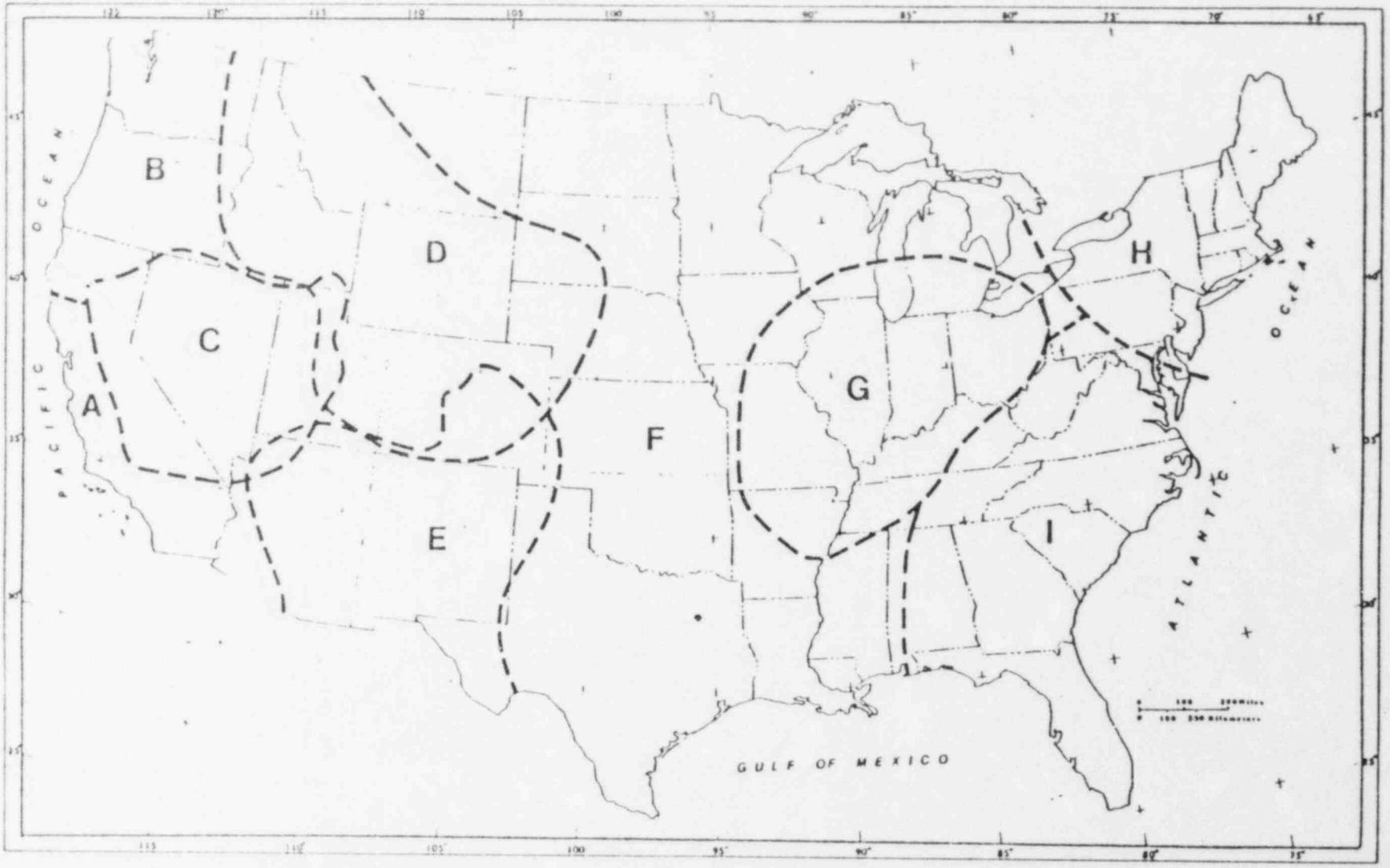

Figure 4 - Location map indicating areas considered in various workshops and other meetings concerned with the presentation and discussion of seismotectonic data used in the development of seismic source zones. See text for discussion of each lettered area.

The meetings were very useful as a forum for outlining seismotectonic ideas and for the presentation of new hypotheses for earthquake occurrence in the various regions. Typically, the workshop participants took one or a combination of several of the following approaches in outlining the seismotectonics of a region. The approaches may be characterized (Thenhaus, 1982a) as (1) seismotectonic zoning on individual faults, or the areal extent of faulting where the faults show late Quaternary or Holocene displacements, or have a distinct association with the historical seismicity; (2) zoning primarily on regional structural style; (3) zoning on the basis of the spatial distribution of seismicity in the absence of any aspects of (1) and (2) that could be used. The zones developed by the participants in these meetings or workshops provided an invaluable source of information for the development of the zones used to prepare the probabilistic ground motion maps. The zones that were developed at the meetings could not always be used directly as seismic source zones in the probabilistic model. For example, a number of zones were outlined by the workshops which had little or no historical seismicity or geologic data such as fault slip that could be used to establish a rate of seismic activity for the zone, even though the zone might be considered by the workshop participants to have earthquake potential. Thus, many of the zones developed as a result of the meetings had to be altered or divided in such a manner that it was possible to develop rates of earthquake occurrence. As previously noted the final seismic source zones are shown in Figures 2 and 3. The seismic source zones organized by area are discussed in the following section to provide more detail concerning the techniques used.

Coastal and Southern California (Area A, Figure 4): In coastal and southern California (Figure 2) faults of regional extent are recognized as seismic source zones if they can be associated with historic seismicity or if they show evidence of historic or Holocene surface rupture. Although fault displacements are dated for much of coastal California area (Ziony and others, 1974; Buchanan-Banks and others, 1978; Pampeyan, 1979; Herd and Helley, 1976) we made no attempt to zone segments of faults on the basis of age of latest displacements. Instead, we assume that Holocene or historic rupture on any segment of a fault or fault zone indicates that the entire fault or fault zone is active; we also assume that earthquakes are equally likely along the entire fault length. We recognize major faults in the San Andreas fault system as independent seismic source zones (Figure 2). Large earthquakes (M_s>6.75) are modeled as ruptures of appropriate length on these faults. Small shocks (M_L<6.75) are modeled as point sources throughout a zone 10 km wide on either side of the fault. The faults are (1) San Andreas fault (zone c24); (2) southern San Andreas (zone c16); (3) San Jacinto-Imperial Valley (zone c15); (4) Elsinore (zone c14); (5) Newport-Inglewood-Rose Canyon (zones c13, c12, and c11); (6) San Clemente (zone c3); (7) Agua Blanca (zone c1); (8) Santa Monica, Cucamonga and associated faults of the southern margin of the Western Transverse Ranges (zones c23 and c41); (9) San Gabriel-Eastern San Fernando (zone c26); and the far offshore (c10) and the San Gregorio-Hosgri (zone c32). Other zones which appear somewhat broader, contain parallel to sub-parallel arrangement of primary faults. These are (1) zone c33 containing the Santa Ynez and Big Pine faults of the northern block of the Western Transverse Ranges; (2) zone c34

enclosing the west margin of the Salinian Block and containing the Rinconada and Nacimiento Faults; (3) zone c38 containing the Hayward and Calavaras faults of the San Francisco Bay area; and (4) zone c39 containing the Maacama, Rodgers Creek, and Green Valley faults north of the San Francisco Bay area.

The source zones of coastal California are described more fully by Thenhaus and others (1980); however a few points will be reiterated here. Some source zone boundaries in the coastal California region are based solely on seismicity where historic seismicity shows a persistent nonuniform distribution in an area of otherwise apparently homogeneous geologic character. The best example is the Ventura Basin (zone c28) where historic seismicity has been concentrated in the eastern portion of the Santa Barbara Channel (Hamilton and others, 1969; Lee and Vedder, 1973). Other areas showing like geologic character but distinguished by the nonuniform geographic distribution of seismicity are the San Pedro Basin (zones c20 and c21), the Newport-Inglewood-Rose Canyon fault trend (zones c13 and c12), the margins of the Salinian Block (zones c34 and c35) and the region from San Francisco Bay to Clear Lake (zones c38 and c39).

This procedure of differentiating zones on the basis of distinctive rates of seismicity was not followed for the San Andreas fault north of the Transverse Ranges (zone 24). There are substantial differences in activity rates and style of deformation along segments of the fault, and equally marked differences in interpretation. On the one hand, Bakun and others (1980) argue that the central, creeping section of this fault cannot cause high accelerations or large-magnitude events in the future. On the other hand, it can be argued, on the basis of the similarity of creep behavior to incipient fracture in metals and rocks, that this region is a likely region for the next

large earthquake to occur (see for example, Stuart, 1979). Burford and Harsh (1980) have addressed this question in terms of strain accumulation and have concluded that between the two hypotheses, a correct choice based on physical arguments is not possible at this time. Accordingly, we treat the entire San Andreas fault as one zone, which implies that the creeping section is capable of generating a large magnitude earthquake. This appears to be prudent in light of the conflicting physical arguments.

Along the coast of central California, we have defined the San Gregorio-Hosgri fault zone (zone 32) as a single seismic source zone. Historic seismicity relocated by Gawthrop (1975) shows an association with the Hosgri fault zone. Although there is considerable controversy about the possible connection of the Hosgri and San Gregorio faults, Silver (1978a,b) concludes that the faults are linked and that together they constitute the longest subsidiary fault zone of the San Andreas system. More recent work (Leslie, 1981) shows a probable connection between the Hosgri and San Simeon fault zones that further supports a probable connection between the Hosgri and San Gregorio faults. On the basis of this model, we have extended zone 32 northward to include the San Gregorio fault, which has both geomorphic evidence and stratigraphic offset that indicate Holocene movement (Buchanan-Banks and others, 1978). This model produces more conservative ground motions than one in which the faults are distinct.

Pacific Northwest (Area B, Figure 4): The mostly broad, generalized seismic source zones of the Pacific Northwest region shown in Figure 3 are in strong contrast to the detailed seismic source zones of the coastal California region. Whereas individual seismogenic faults and general Cenozoic tectonic

development are well known in coastal California on a regional scale, the Pacific Northwest lacks a unifying regional tectonic model for Cenozoic tectonism. If such a model were to become available, it could have significant ramifications for defining future regional seismic source zones in this region. Results of recent paleomagnetic studies indicate large post-Eocene rotations of the Cascade-Coast Ranges block of Washington and Oregon (Simpson and Cox, 1977; Magill and others, 1982). Also post-Miocene rotation of the Coast Ranges is indicated with perhaps the Cascade Range acting as a tectonic boundary between the Columbia Plateau area and the Coast Ranges block (Magill and others, 1982). An important question related to the tectonic development of the Pacific Northwest is the origin of intermediate depth seismicity in the Puget Sound area. Two damaging earthquakes in recent times had focal depths of 40 km or greater with NNW oriented normal focal mechanisms (Algermissen and Harding, 1965). Riddihough (1977, 1978), Riddihough and Hyndman (1977), Kulm and Fowler (1974), and Atwater (1970), among others, provided geophysical, stratigraphic, or tectonic arguments as to why subduction could be occurring in the northwest; however, other seismological (Crosson, 1972; Hill, 1978), petrologic (White and McBirney, 1978), and tectonic evidence (Stacey, 1973) can be used to argue against subduction.

In lieu of a unifying regional tectonic model, observations on the geographical distribution of seismicity as it relates to geological features are useful. The youngest orogenic province in the region is the Cascade Range which has large volumes of Quaternary volcanic rocks. The range itself, however, has no clear association with a regional seismicity trend (Perkins and others, 1980). The diffuse seismicity of the northern Basin and Range province in southeastern Oregon also seems to characterize the southern

Cascade Range. The basin and range structure of southern Oregon and northern California merges with the north-south structure of the southern Cascade Mountains (Hammond, 1979; Magill and others, 1982; Lawrence, 1976). The Eugene-Denio Zone and Mt. McLoughlin Zone are regions of northwest-trending right-lateral shear that extend from the northern Basin and Range province and offset the Pleistocene-Holocene trend of the southern Cascades by about 10 to 20 km (Lawrence, 1976). The merging of the Quaternary structure of the Basin and Range province with the southern Cascades and the characteristically diffuse seismicity across both provinces indicates that perhaps both are within a similar seismotectonic regime. The two areas are combined into zone 035.

Perkins and others (1980) have noted that the geographic distribution of seismicity is not continuous across the Northern Cascade Mountains of Washington. The majority of the earthquake activity is along the extreme western edge of the province and is probably related to the tectonism of the Puget Sound area. On the eastern flank of the Cascades (zone P004) seismicity clusters around the Lake Chelan area. A distinctly different history of Cenozoic tectonic development between the northern Cascades and the southern Cascades across a boundary coincident with the Olympic-Wallowa lineament (Hammond, 1979), along with a distinctly different geographic pattern of historical seismicity, serve as bases for distinguishing zone P004 from 035.

Within the Puget Sound area itself (zones P001, P002) zone boundaries are based on seismicity alone as there are no known dominant faults or known specific geologic structures that govern the spatial pattern of seismicity. The Puget Sound zones are within a broad region that encloses the Puget Sound-Willamette Depression. A zone encloses the Portland, Oregon, area (zone P018)

and is based on a general northeast trend of seismicity through the area (Perkins and others, 1980). West of the Puget Sound-Willamette Depression, zone P014 includes the western Coast Ranges and adjacent continental shelf area. On the south, the Puget Sound-Willamette Depression terminates against the Klamath Mountains (zone P008).

In northeastern Oregon and southeastern Washington, zone P005 has a northwest trend sub-parallel to the Intermountain Seismic Belt in western Montana (Smith and Sbar, 1974). Zone P005 represents a regional northwesterly trend of seismicity ($Io \geq V$) noted by Perkins and others (1980) and also appears to be only part of a more regional belt of moderate strain release that extends to the southeast into the western Snake River Plain of Idaho (Algermissen, 1969, Fig. 2). There is a strong northwest trending structural control of the geologic features in the zone (Newcomb, 1970; Walker, 1977) most significant of which are features of the Olympic-Wallowa lineament (Skehan, 1965) and the Vail Zone (Lawrence, 1976). However, the control of these northwest-trending structural zones on the regional distribution of seismicity is not well understood. To date the most recent surface deformation (probably by fault movement) noted on the Columbia Plateau is Holocene in age and occurs on the flanks of the Toppenish Ridge anticline (Campbell and Bentley, 1981); a member of the east-west family of anticlines belonging to the Yakima folds section of the Columbia Plateau (Thornbury, 1965). Also, the largest earthquake to occur in the Columbia Plateau, the 1936 Milton-Freewater earthquake ($M_s = 5.75$), has been relocated from a location near the Olympic-Wallowa lineament to a location nearer the northeast trending Hite fault system (Woodward-Clyde Consultants, 1980). Both the Yakima folds section and the Hite fault system appear to have some structural

relationship, as yet undefined however, to the more regional northwest structural grain. The east-west trends of the Yakima folds deflect to the southeast along a broad northwest-southeast zone coincident with the Olympic-Wallowa lineament. Southeast of the Hite fault system, numerous northwest trending normal faults bounding the La Grande Graben align with the strikes of faults of the extreme western Snake River Plain area. At the intersection with the Hite fault system, normal faulting is deflected north and then northwest along the more northwesterly trend of the Olympic-Wallowa lineament (see Newcomb, 1970). Because of the currently unclear nature of specific seismogenic features, the area (zone P005) has been modeled as a broad zone that emphasizes only regional trends of geologic structure and seismicity. Expression of more local structure is at variance with the overall trend of zone P005, yet local structure either deflects, or is deflected by, the overall northwest strike of the regional trends indicating genetic relationships as yet undefined in a regional tectonic model.

Great Basin (Area C, Figure 4): The Nevada Seismic Zone (zone 031) has been distinguished from a more regional zone generally characterized by Holocene fault displacements (zone 34) (Wallace, 1977a,b; 1978a,b,c). Similarly, the Southern Nevada Seismic Zone (zone 017) has been separated from a broad area of the southern Great Basin characterized by late Quaternary fault displacement (zones 017, 018 and 019). Zones 032 and 033 within the Nevada seismic zone are based on the aftershock zones of large surface rupturing historic earthquakes.

Zones outlined at the seismic source zone meetings and defined only on geologic criteria may divide tight clusters of seismicity. This is the case in the Reno-Carson City-Lake Tahoe area of western Nevada. Boundaries of four zones drawn at the seismic source zone meetings, based on fault information, join in this area and segment the northern part of a regional seismicity trend that follows the Sierra Nevada-Great Basin boundary zone (See Thenhaus and Wentworth, 1982). Distributing this seismicity into the zones defined at the meeting would have resulted in zones of relatively low seismicity that extend into northeastern California, western Nevada and the central Sierra Nevadas. This would have resulted in a lower rate of earthquake occurrence in the immediate Reno-Carson City-Lake Tahoe area. We have chosen to preserve the influence of the Sierra Nevada-Great Basin boundary on seismicity in this area. For this reason we have modified the source zones defined at the meeting and extended zone 029 along the Sierra Nevada-Great Basin Boundary Zone north to include the Reno-Carson City-Lake Tahoe area.

Zones 037, 038, 039 and 040 encompass and include the Wasatch fault zone at the eastern margin of the Great Basin. The zones are based on studies of ages of latest surface displacements along faults in this area as summarized by Bucknam and others (1980). The zones have been generalized somewhat from Bucknam and others (1980) to reflect the regional geographic distribution of historical seismicity. Except for zone 039, which is characterized by late Quaternary faulting, zones conterminous to, and including, the Wasatch fault (zone 040) are characterized by faults having Holocene age displacements.

Northern Rocky Mountains (Area D, Figure 4): Seismic source zones of the northern Rocky Mountains (Figure 3) were drawn to strongly reflect structural sub-provinces of that region. This approach provides a reasonable organization for historic seismicity in the region.

Zone 064 is an area of pre-late Pleistocene Basin and Range-type faulting and includes the seismically active Flathead Lake area of Northwestern Montana (Witkind, 1977; Sbar and others, 1972). The zone is bounded on the east by the north-northwest-striking imbricate thrust sheets of the Disturbed Belt of western Montana (zone 065) (Mudge, 1970). Both zone 064 and 065 are bounded on the south by the west-northwest trending St. Marys fault trend (zone 057). A broad zone of seismicity extending from Helena to the Flathead Lake area (Stickney, 1978) is coincident with the overall west-northwest structural trend in this area. South of the St. Marys trend, zone 057 is characterized by mixed northeast, northwest and east-west trending faults. The Intermountain Seismic Belt (Smith and Sbar, 1974) follows a broad northerly trend through this area but historic seismicity appears to concentrate in the Three Forks Basin area (Qamar and Hawley, 1979).

Zone 055 is an east-west-trending zone that includes the historically active areas of Hebgen Valley, Madison Valley and Centennial Valley of extreme southwestern Montana (Smith and Sbar, 1974). Zone 056 is the volcano-tectonic area of Yellowstone National Park.

The highly seismic areas included in zones 056 and 055 are in strong contrast to the aseismic nature of the eastern Snake River Plain (zone 054). Perhaps the warm, thin crust of the eastern Snake River Plain cannot store enough elastic strain to generate earthquakes. The cooler, thicker western part of the Plain (included in zone 058) however, has had historic seismic

activity. An intensity VII was felt at Shoshone, Idaho, on the western part of the Plain in 1905 (Greensfelder, 1976). Zone 058 includes an area of Basin and Range-type extensional tectonics north of the Snake River Plain and on the western edge of the Idaho Batholith. Except for the Challis geothermal area (zone 059), which is characterized by swarm activity, the Idaho Batholith (zone 060) exhibits very little earthquake activity. Southeast of the Snake River Plain, the Intermountain Seismic Belt crosses the Overthrust Belt of southeastern Idaho and southwestern Wyoming (zone 052). Long normal faults with probable Holocene movements (Thenhaus and Wentworth, 1982) are superimposed on the older Laramide age thrusts in the Overthrust Belt. An earthquake focal mechanism in the Caribou Range of southeastern Idaho indicates normal faulting generally on strike with mapped normal faults in this area (Sbar and others, 1972).

In the Central Rocky Mountains of Wyoming and northern Colorado, seismicity appears to be primarily associated with the faulted Laramide age mountain uplifts (zone 045) whereas the Laramide age basins in the area show very little seismic activity (Powder River Basin, zone 049; Big Horn Basin, zone 047; Wind River Basin, zone 048; Green River Basin, zone 051; and the Washaki Basin, zone 046). Interpretations of a deep crustal seismic reflection line from the Green River Basin, across the southern end of the Wind River Mountains and into the Wind River Basin, indicate low angle thrusting along a narrow zone extending through the entire crust to depths of 25 to 30 km. (Smithson and others, 1978). Significant deformation of the basin sedimentary sequence occurs where the thrust overrides the basin, however the central basin area shows no deformation of comparable scale.

Southern Rocky Mountains (Area E, Figure 4): In the southern Rocky Mountain region, areas of Holocene fault displacement bound the Sangre De Cristo Range of southern Colorado (Figure 3, zone 043) (Kirkham and Rodgers, 1981) and the southern margin of the Albuquerque Basin on the La Jencia fault (Machette, 1978) (zone 007). Areas of possible Holocene age displacements are located in the southern Rio Grande Rift (zone 002) and extreme southeastern Arizona (zone 004) just north of the 1877 Sonora earthquake area (zone 004). Sanford and others (1979; 1981) consider the Rio Grande Rift (zones 042, 007 and 003) to be the most seismically active area in New Mexico in historic times with the majority of seismic activity occurring in the Albuquerque Basin (zone 007). They also note the apparent association of seismicity with the Jemez Lineament (zone 008). The northeast margin of the San Juan Basin, San Juan Volcanic field and Uncompahgre uplift area (zone 041) exhibit a moderate level of seismicity.

The structural continuity of the southwest margin of the Colorado Plateau is broken by northeast-trending, Precambrian faults which not only have controlled the northeastern migration of volcanic activity in the San Francisco Volcanic field, but also apparently influence the regional distribution of seismicity (zone 014) (Shoemaker and others, 1978).

The central part of the Colorado Plateau (zone 016) exhibits significantly less earthquake activity than its seismically active margins.

Great Plains and Gulf Coast (Area F, Figure 4): In the northern Great Plains there is an apparent association between a northeast-striking trend of seismicity through South Dakota and western Minnesota and the Colorado Lineament as defined by Warner (1978) (Figure 3, zones 067, 068). In

Minnesota, seismicity is associated with the Great Lakes Tectonic Zone (Simms and others, 1980; Mooney and Morey, 1981). This zone is generally on strike with the Colorado Lineament to the southwest. Elsewhere throughout the Great Plains, seismicity tends to be associated with basement highs such as the Sioux Uplift, Souixana Arch, and Cambridge Arch (zone 070), central Kansas Uplift (zone 073), Nemaha Ridge (zones 075 and north part of zone 076), the Wichita Uplift (also known as the southern Oklahoma Aulacogen; southern area of zone 076) and the Seminole Arch (southeast area of zone 076). Intervening basin areas of the Forest City Basin (western part of zone 069), Salina Basin (zone 074), Denver Basin (zone 071), and the Williston Basin (zone 097) show a much lower rate of seismic activity. The Anadarko Basin (zone 072) is somewhat of an exception having four $I_o \geq$ IV earthquakes.

Large seismic source zones enclose the Gulf Coast area (zones 078 and 098). The thick cover of Tertiary sediments in this region obscures the association of seismicity with what perhaps are deeply buried structures.

Central Interior (Area G, Figure 4): A number of geological and geophysical investigations have defined reactivated zones of faulting associated with an ancient crustal rift in the northern Mississippi Embayment (Hildebrand and others, 1977; Heyl and and McKeown, 1978; Russ, 1979, 1981; Hamilton and Russ 1981; Zoback and others, 1980) (Figure 3, zone 087). The great 1811 and 1812 New Madrid earthquake series are located in this zone. Zone 082 extends southwest from the New Madrid Zone. Regional gravity and magnetic studies suggest that this area may be a possible continuation of the rift structure. Another possible interpretation is that the seismicity of zone 082 may be associated with structures of the Ouachita Mountains where they are buried

beneath Coastal Plain Tertiary sediments.

Zones 086 and 081, adjacent to the main zone of the Reelfoot Rift, are based on the distribution of seismicity. Zone 086 contains a pronounced northeast trend in seismicity that extends along the geologic contact of Paleozoic strata of the Ozark Dome with Tertiary Coastal Plain sediments. This seismicity trend has persisted for a long span of historic time (see figures 1-4 of Herrmann, 1981) but causative structures are unknown. The trend appears to be distinct from the main zone of faulting within the Rift in zone 087. Zone 088 is a northwest trending, narrow zone having a relatively high concentration of seismic activity. Zone 088 bounds the Ozark Dome on the northeast and is central to the recently defined St. Louis arm of the Reelfoot Rift (Braile and others, 1982). Zone 089 includes a large portion of the Illinois Basin, the Wabash Valley Fault Zone and a possible continuation of the Reelfoot Rift into Indiana (Braile and others, 1980; 1982). The zone has been highly seismic historically.

The remaining zones of the central Interior follow the theme evident in the Great Plains region: seismicity appears to be associated with high basement features and margins of Paleozoic basins. Zones 084, 090, 094 and 080 follow the trends of the Central Missouri High, Mississippi River Arch-Wisconsin Arch, Cincinnati Arch and Nashville Dome respectively. Zones 092 and 095 are along the gently dipping margins of the Wisconsin Basin (zone 091) and the Appalachian Basin (east part of zone 093).

Northeast United States (Area H, Figure 4): The most notable change in the seismic source zones in this region from the previous source zone map (Algermissen and Perkins, 1976) is the segmentation of the diffuse northwest-

trending zone of seismicity previously associated with the Boston-Ottawa trend (Diment and others, 1972; Sbar and Sykes, 1973). An area of low seismic activity (Figure 3, zone 106) about 100 km wide extending northward through eastern Vermont and western New Hampshire serves to break the Boston-Ottawa trend into two discrete segments. In eastern Massachusetts (zone 107), seismicity has concentrated in the Boston area and offshore. This seismic activity coincides with the eastern Massachusettes thrust province characterized by northwest-over-southeast thrusting. The zone of thrusting is near the western margin of the Avalonian Platform, an island arc assemblage accreted to the North American continent perhaps in late Precambrian time (Rast, 1980). Zone 107 includes the thrust province but also extends into the Avalonian Platform in eastern Massachusettes to include an area of moderate seismicity around Narragansett Basin. It is interesting to note that in northeastern Massachusetts the strike of the thrust province is normal to the regional maximum compressive stress axis (Zoback and Zoback, 1980). These faults may be reactivated in the current stress regime.

Earthquake activity in southern New Hampshire, previously considered part of the Boston-Ottawa zone, is combined with seismicity in eastern Maine (zone 108). The zone follows the Merrimack Synclinorium which is a regional tectonic feature of northeastern New England inherited from compressional tectonism of the Acadian Orogeny (Moench, 1973).

Zones 105, 109 and 111 distinguish the seismically active regions of the St. Lawrence River and the western Quebec-northern New York area. The zones are generally similar to those of Basham and others (1979). Zone 113 encloses a north-trending zone of seismicity peripherial to the Adirondack Mountains (zone 112) and along the Hudson River.

The Clarendon-Linden fault and its possible northeastern extension across Lake Ontario (Hutchinson and others, 1979) comprise zone 115. Small earthquakes have occurred along the fault; some of these are due to solution mining of salt but others appear to be of tectonic origin (Fletcher and Sykes, 1977). The 1929 intensity VIII Attica earthquake is included in this zone although it is not entirely clear that the earthquake occurred on the Clarendon-Linden fault.

Zone 103 was drawn primarily on the distribution of historic seismicity but includes the Connecticut Valley graben, Newark Basin and Gettysburg Basin. The Ramapo fault (zone 104) has been shown to be a locus of seismic activity in the region (Aggarwal and Sykes, 1978) although other faults parallel in strike to the Ramapo may also be associated with seismicity (Yang and Aggarwal, 1981).

Southeast United States (Area I, Figure 4): Seismic source zones in this area generally follow those of Perkins and others (1979). The regional geologic bases of zones are (1) the fold belt of the Appalachian Mountains (zone 096); (2) the thrust faulted Appalachian trend (zone 100); and, (3) a broad zone including the Piedmont and Coastal Plain (zone 099) that extends offshore to the western margin of the large Jurassic basins of the Continental Shelf (zone 118). Zone 099 can be characterized as a Mesozoic extensional terrain containing graben and half-graben of Triassic age that were superimposed on an older compressional terrain during the incipient opening of the Atlantic Ocean.

Wentworth and Mergner-Keefer (1981) have suggested that perhaps early Mesozoic normal faults are reactivated in the current stress regime with high angle reverse movement (as along the Ramapo fault) and are responsible for the

present day seismicity along the eastern seaboard including the 1886, Modified Mercalli Intensity X, Charleston, South Carolina earthquake. Alternatively, however, Armbruster and Seeber (1981) suggest that the 1886 Charleston earthquake was the result of backslip on a low-angle detachment indicated by COCORP reflection profiling (Cook and others, 1979; 1981). Recent reinterpretation of COCORP profiles in the region suggest, however, that the decollement zone might have roots beneath the southern Appalachians and therefore does not extend into the Coastal Plain (Inverson and Smithson, 1982).

The unresolved question of the origin of the Charleston earthquake has led us to retain the northwest-trending zones (zone 101 and 102) as used in the 1976 hazard map (Algermissen and Perkins, 1976), although the Charleston zone (zone 101) has been narrowed to include only the larger size events in the zone. These northwest-trending zones are consistent with the trend of historical seismicity in the area.

Attenuation

Acceleration attenuation curves developed by Schnabel and Seed (1973) were used in the western United States (from the Rocky Mountains westward). The Schnabel and Seed acceleration was also used in a modified form for acceleration attenuation in the central and eastern part of the country (Figure 5). The modification of the Schnabel and Seed curves for the central and eastern United States is that proposed by Algermissen and Perkins (1976). In the Puget Sound area for those earthquakes modelled at intermediate depths, the Schnabel and Seed curves were modified to reflect the greater depth of focus.

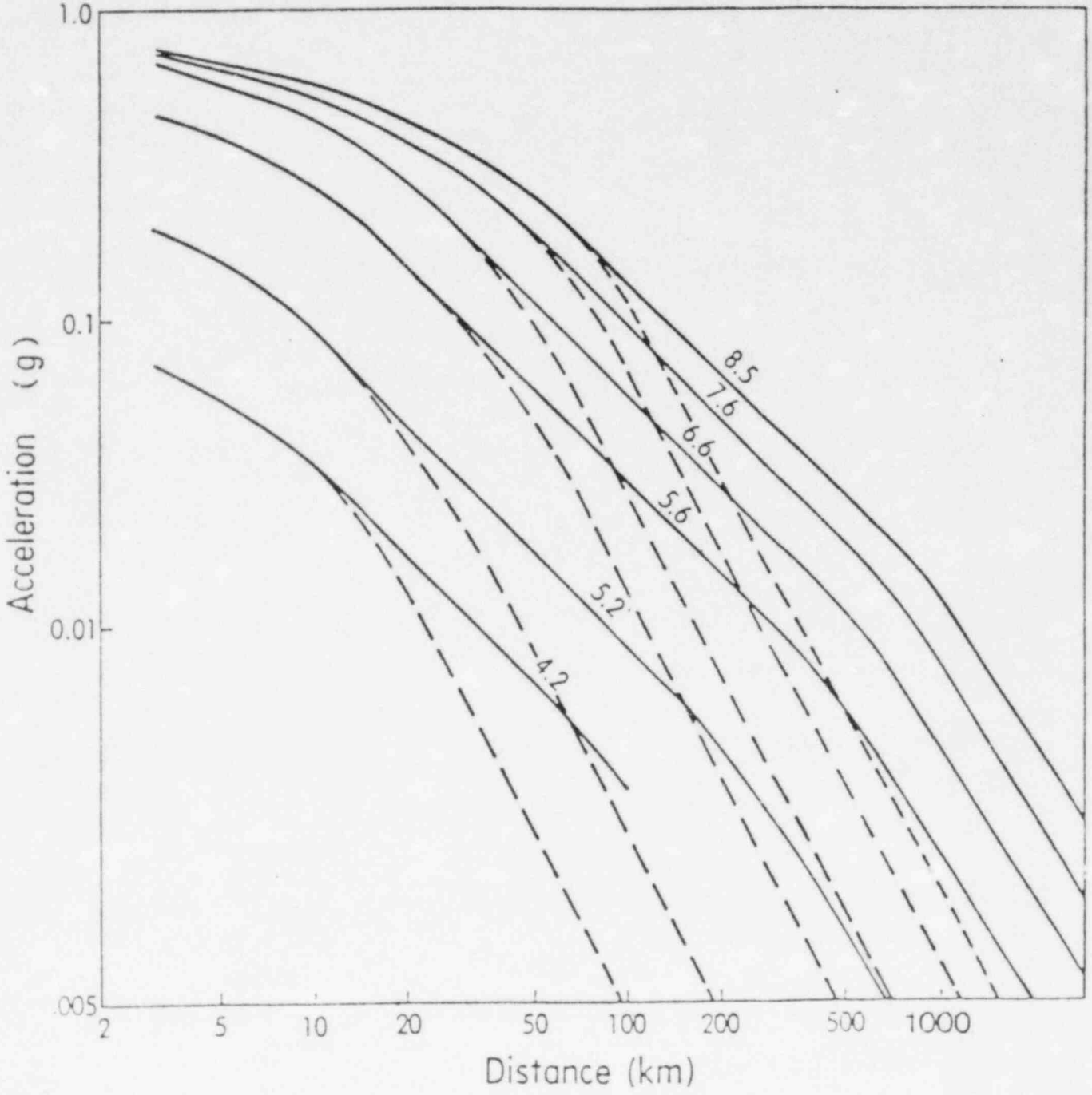

Figure 5 - Acceleration attenuation curves (Algermissen and Perkins, 1976). The solid lines are curves used for the eastern region (see text for definition). The dashed lines together with solid lines at close distances are the attenuation curves used for the western region and are taken from Schnabel and Seed (1973).

The attenuation curves used for velocity were developed by D. M. Perkins, S. T. Harding and S. C. Harmsen (Perkins, 1980) using the same general techniques and a portion of the ensemble of strong motion records used by Schnabel and Seed (1973) in their study of acceleration. Velocity attenuation curves were developed for the western United States (from the Rocky Mountains westward) and for the central and eastern United States (Figure 6). The velocity attenuation curves were developed such that they would satisfy three principal requirements: (1) they should have magnitude dependent attenuation shapes; (2) the magnitude dependence should be specified in terms of magnitudes present in the historical catalogs, M_L for earthquakes less than 6.75 and M_s for larger magnitudes; and (3) the velocity attenuation curves should be compatible with the Schnabel and Seed (1973) acceleration attenuation used for the acceleration hazard maps. That is, the curves should be derived by a similar technique for a similar set of earthquakes.

A computer program was designed to attenuate observed strong motion records, taking into account both anelastic attenuation and geometric attenuation of body waves in the manner similar to that of Schnabel and Seed.

For anelastic attenuation, the observed strong motion velocity record was Fourier-analyzed into its constituent frequency components. The components were adjusted to standard distances, R_i, using the factor

$$e^{\frac{-w}{vQ}(R_i - R_o)}$$

where R_o is the distance from the fault rupture at which the strong motion was recorded. Q is a regional characteristic of attenuation, as the frequency of the Fourier component and v is a shear wave velocity. At the standard distances the adjusted components were inverse transformed to produce an

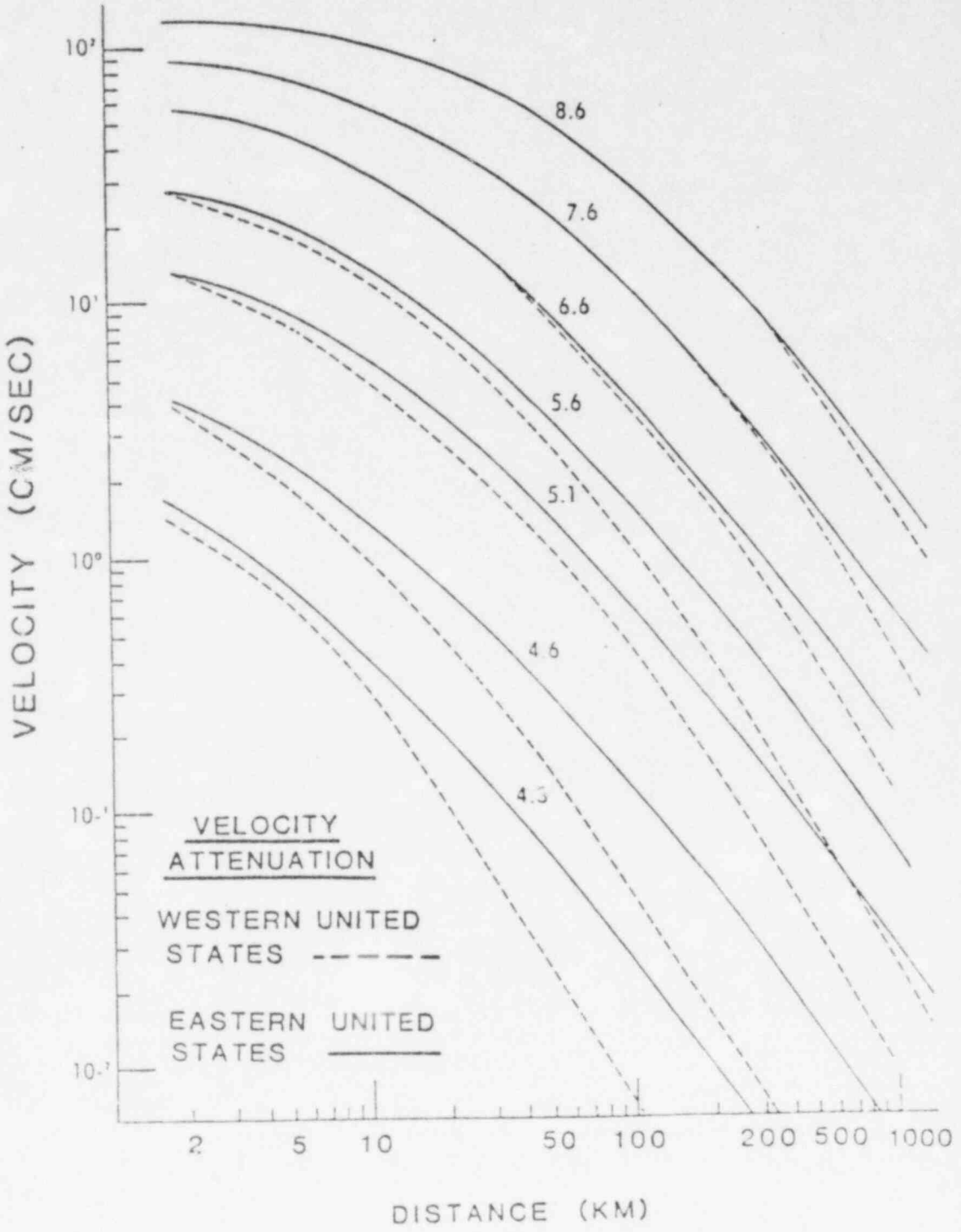

Figure 6 - Velocity attenuation curves (Perkins, 1980). The solid lines are curves used for the eastern region. The dashed lines together with solid lines (in some instances) at close distances are the attenuation curves used for the western region.

adjusted strong motion record, from which an adjusted peak velocity could be measured. Because the ground motions due to different magnitudes have different predominant frequencies, this anelastic attenuation is implicity magnitude dependent.

For geometric attenuation, the adjusted peak velocities were further adjusted by the factor

$$[E(R_o)/E(R_i)]^{\frac{1}{2}}$$

where

$$E(r) = 2LW + 2\pi rW + 2\pi rL + 4\pi r^2$$

E(r) represents the area of a surface at a distance r from a rectangular rupture of length L and width W. This surface is a rectangular block whose edges and corners are circularly rounded with radius r. This surface represents a surface over which the ground motion energy is distributed. The energy per unit surface decreases as the distance r increases. Because the energy in a signal is proportional to the square of the amplitude, the ground motion amplitude should derease with the square root of the energy and hence in inverse proportion to the square root of the surface E(r).

The rupture length L, and to some extent the width W, are a function of the earthquake magnitude, and hence the source size effect is magnitude-dependent for distances of the same order as the rupture size. In the far-field, the size-effect factor reduces to Ro/Ri.

This dual-factor process yielded a suite of curves that were smoothed to produce average velocity attenuation curves. Attenuation curves for the western United States were derived using Q = 250. For the eastern United States the same source characteristics were used but the Q was changed to 1200.

This process guarantees that the attenuations for eastern and western United States earthquakes will produce the same near-field ground motions for the same epicentral intensities.

Because the inverse transform process yields results that are less and less like impulsive earthquake records the further the standard distance is from the recorded distance, beyond 500 km the individual earthquake curves tended to behave unstably. Therefore, far-field attenuations were constrained to have the same slopes. This required finding a slope in the far field consistent with the smoothed behavior of all the curves. To facilitate this, far-field curves were recalculated for point sources. The far-field slopes found were -1.77 for the western United States attenuation and -1.46 for the eastern United States attenuation.

The development of the velocity attenuation curves is briefly described in Perkins (1980).

DISCUSSION

A number of factors related to the development and computations of the new national hazard maps were examined. The factors of most importance to be discussed here are (1) the influence of several different fault modeling techniques; (2) various attenuation factors; (3) variability in fault rupture length–magnitude relationship; and (4) variability in attenuation functions. Finally, the new maps are reviewed in order to point out significant differences between the new maps and the Algermissen and Perkins (1976) map.

Faul[illegible]ag

It is a good deal faster in the hazard mapping program to model the effects of point sources than linear ruptures. Hence there is an advantage in modeling earthquakes as point sources when the approximation does not greatly distort the effective exceedance rates for the mapped accelerations.

Now, for a given acceleration, the rate of exceedance at an arbitrary point in the source region is directly governed by the area over which that acceleration is exceeded. Given a magnitude and an arbitrary source, the attenuation function gives the distance from the source within which a given acceleration is exceeded. When an earthquake is modeled as a point source, the area over which that acceleration is exceeded is a circle. If that same earthquake is modeled instead as a rupture source, the area is given by two halves of that point-source circle joined by a rectangular section of width equal to the diameter of the circle and length equal to the rupture length. Now when the ruptures are small, as with small magnitude earthquakes, or when the radial distance is large, as with small accelerations, the area given by a point source can approximate that given by the rupture source. On the other

hand, when accelerations are large, as are those which are close to the source, or when ruptures are large, as for large magnitude earthquakes, the area of exceedance may be many times larger for the rupture source than for the point source, the usual ratio is from 3 to 10 times.

Accordingly, for sources having low seismicity, for which the mapped accelerations are low, we have used point sources up to magnitude 6.4. For very active sources, or for sources with large maximum magnitudes, we have used rupture sources for magnitudes over 5.8.

Rupture lengths were determined using the equation developed by Mark (1977). This equation depends heavily on California strike-slip fault data. A number of investigators (for example, Evernden, 1975) have suggested that the fault rupture lengths for earthquakes in the midwest and eastern United States may be substantially shorter than fault rupture lengths in the west. We examined the significance of assuming a shorter fault rupture length in the midwest and east as compared with the west by computing the 10, 25, and 250 year, 90-percent extreme probability accelerations at three cities in the midwest (Charleston and St. Louis, Missouri, and Memphis, Tennessee) using (1) Mark's (1977) equation; and (2) fault rupture lengths of one half the fault rupture length in (1). In both cases above, the earthquakes in zone 087 (figure 3) were modeled as occurring on parallel faults 5 km apart, filling the zone. The model faults were given strikes parallel to the northwestern boundary of zone 087 (figure 7). The results are shown in figure 8. The largest difference (less than 15 percent) in acceleration resulting from the two fault rupture length models occurs at Charleston, Missouri. Charleston is on strike and near the northern end of seismic source zone 087 and could be assumed to represent a site that would receive the maximum change in ground

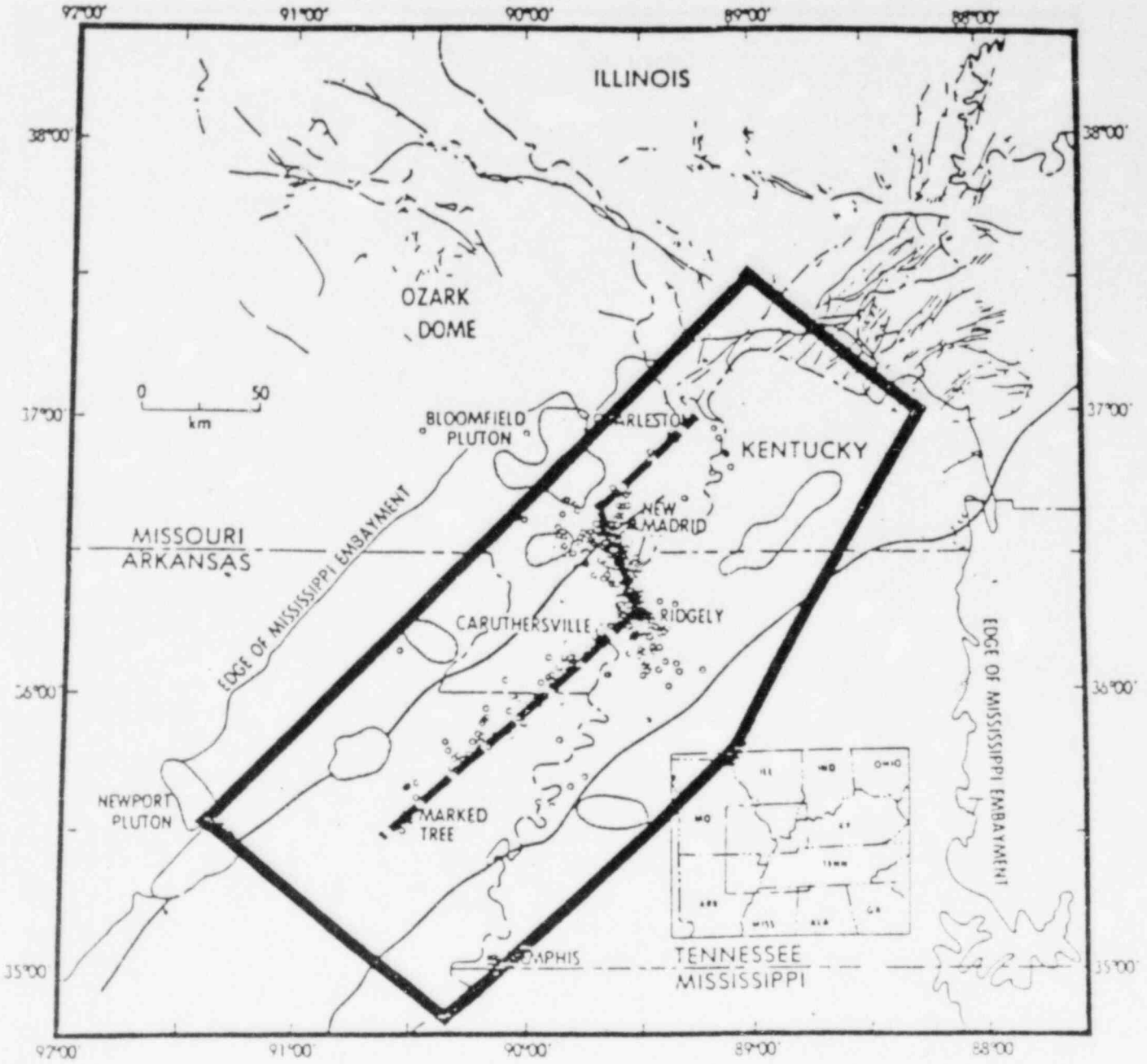

Figure 7 - Map of southeast Missouri and adjacent area showing recent seismicity (1977-1980), faults, graben boundaries, and plutons (hachured). Adopted from Hamilton and Zoback, (1982). The heavy black line outlines seismic source zone 087 (see Figure 3). The heavy dashed line represents the "single fault" model discussed in the text. The "multiple fault" model discussed in the text consists of faults parallel to the northwest edge of zone 087, spaced 5 km apart across the zone.

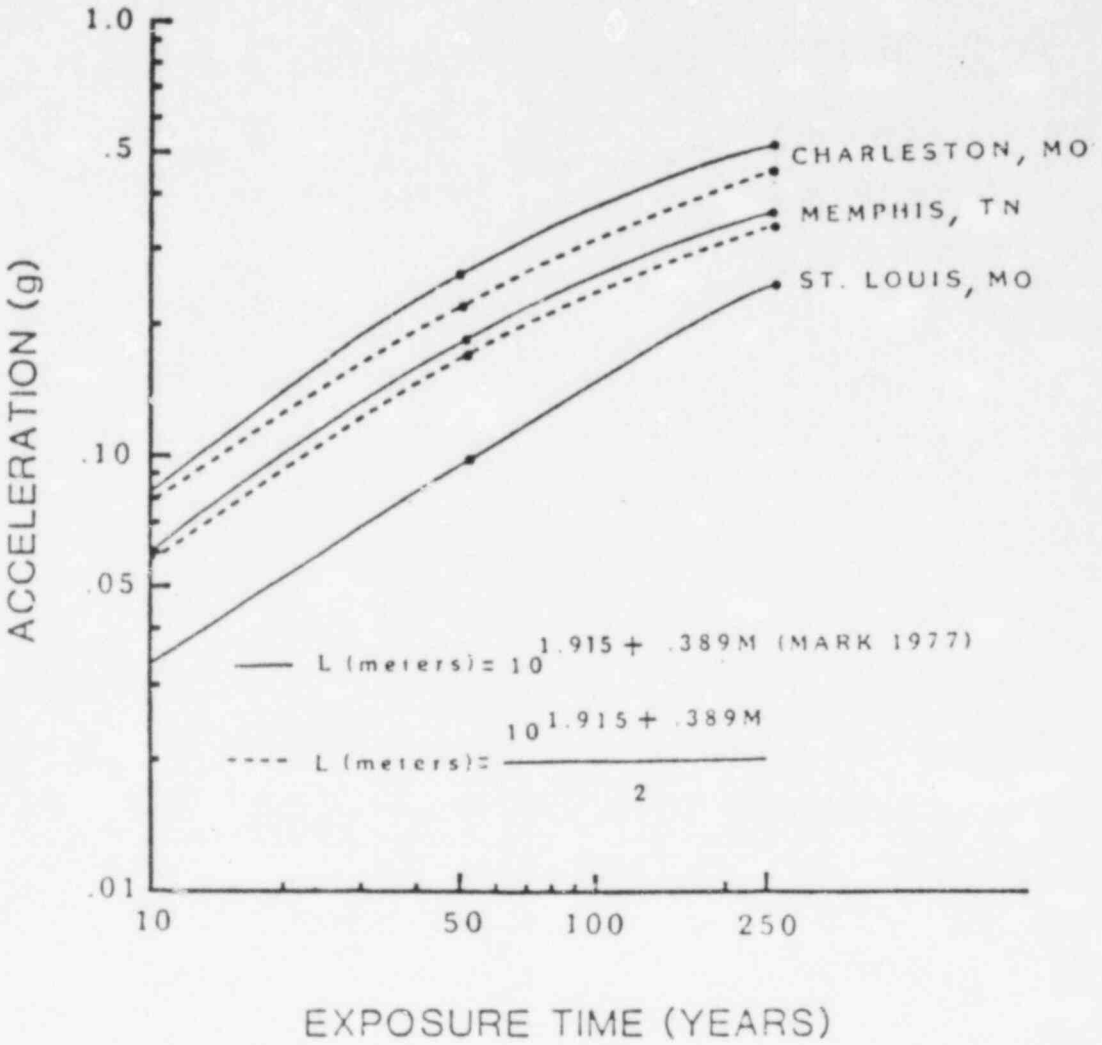

Figure 8 - Comparison of acceleration at Charleston and St. Louis, Missouri, and Memphis, Tennessee, for various exposure times with a 90-percent extreme probability. The solid lines indicate accelerations resulting from fault rupture length modeling using the relationship developed by Mark (1977). The dashed lines are the accelerations resulting from modeling the faults using one-half the fault rupture lengths given by Mark (1977). For accelerations at St. Louis, the solid and dashed lines are approximately the same. See text for discussion.

motion as a result of the two models. At Memphis, the difference in the acceleration produced by the two models is somewhat less, about ten percent. The difference in acceleration resulting from the two models is very small at St. Louis, Missouri, about 190 km northwest of the northern boundary of seismic source zone 087. The conclusion is, then, that in an area of moderate seismicity (but with a potential for very large earthquakes), reduction in the fault rupture lengths as given by Mark (1977) (equation 3, this paper) of 50 percent results in a maximum decrease in acceleration of less than 15 percent for exposure times greater than about 20 years. For shorter exposure times the differences in acceleration resulting from the two models are very small regardless of the site selected.

The effect of another possible variation in fault modeling is illustrated in the Mississippi Valley again using seismic source zone 087. Recent studies (Zoback and others, 1980) have shown that seismicity during the past few years has been concentrated in a narrow zone within seismic source zone 087. Using the recent seismicity as a guide, the fault zone within zone 087 was modeled as two faults parallel to, and 2.5 km to either side of the dashed line shown in figure 7. This is essentially a "single fault" model. The accelerations for a range of exposure times at three cities, Charleston and St. Louis, Missouri and Memphis, Tennessee resulting from the "single fault" model are compared with the accelerations computed at the same three cities using multiple closely spaced faults throughout zone 087 having strikes parallel to the northwestern side of zone 087. This second model is the "multiple fault" model used to model the seismicity in zone 087 for the new national hazard maps. The comparison between the "single fault" and "multiple fault" model is shown in Figure 9. As might be expected, the largest differences in ground

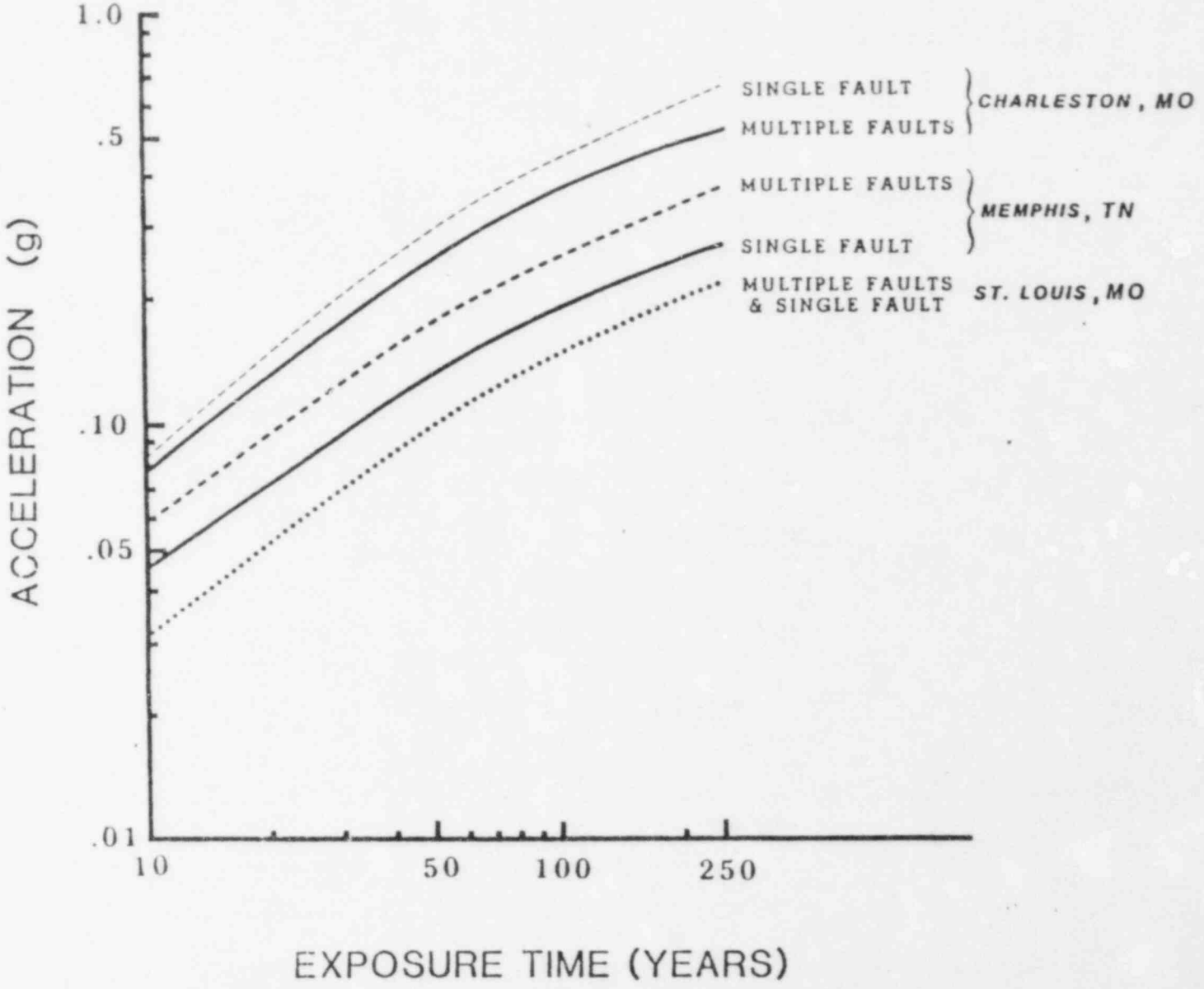

Figure 9 - Acceleration with a 90-percent extreme probability at Charleston and St. Louis, Missouri, and Memphis, Tennessee, for various exposure times resulting from the "single fault" model and the "multiple fault" model used in the computation of the national maps (see Figure 7). At St. Louis the accelerations resulting from both models are essentially the same.

motion between the two models occur for the largest exposure time considered, 250 years. Significant differences between the accelerations occur only at Charleston, Missouri and Memphis, Tennessee. The accelerations over a fairly wide range of exposure times is essentially the same at St. Louis. The differences between the accelerations generated by the two models at Charleston and Memphis are interesting. Note that at Charleston, Missouri, the acceleration resulting from the "single fault" model is larger than the acceleration generated by the "multiple fault" model by about 30 percent. This result occurs because Charleston, Missouri is located at the north end of the "single fault" model. The "multiple fault" model disperses the seismicity around Charleston resulting in a lower acceleration. Memphis, Tennessee is near the eastern boundary of seismic source zone 087 such that for the "multiple fault" model, some faults occur very near Memphis causing a higher acceleration at Memphis than the "single fault" model. Memphis is about 70 km east of the "single fault" model and consequently the ground motion at Memphis is less when the "single fault" model is used.

As already mentioned, we used the "multiple fault" model to model the seismicity in zone 087 for the national maps because there is, in our opinion, insufficient evidence to postulate that future large earthquakes within the time span of interest in this investigation (10 to 250 years) should be restricted to a single fault. From the above examples it is clear that the "multiple fault" model is not conservative for all sites. These results show the importance of refinement of seismic source zones through additional geologic and geophysical research.

Attenuation

Attenuation of acceleration and velocity with distance is poorly known for the central and eastern United States because of the lack of recordings of strong ground motion and the relatively poor quality of the available Modified Mercalli isoseismal maps. The larger shocks in the central and eastern United States occurred, for the most part, in the 19th century before the development of instrumental seismology and before the careful, systematic examination of earthquake effects. Consequently, differences in attenuation curves for these areas may be large and it is of interest to examine the effects of these differences. Figures 10 and 11 show selected acceleration and velocity attenuation curves recently developed by Nuttli and Herrmann (1981) for the midwest and eastern United States. Also shown in Figure 10 and 11, for comparison, are selected acceleration and velocity attenuation curves used in this study. The Nuttli and Herrmann (1981) curves have been redrawn with magnitudes appropriate for comparison with the attenuation curves used by us. The national acceleration and velocity maps discussed here were essentially complete before the Nuttli and Herrmann (1981) curves were available. It is therefore interesting to compare ground shaking at selected points using the two sets of attenuation curves. Figures 12 and 13 show comparisons between accelerations and velocities computed at St. Louis, Missouri, and Memphis, Tennessee, using the attenuation curves adopted for this study and using the curves of Nuttli and Herrmann (1981). The accelerations computed at St. Louis and Memphis using the two different attenuation curves are considerably different for an exposure time of 10 years, particularly at St. Louis. This effect is probably caused by the contribution of small to moderate earthquakes to the acceleration at St. Louis

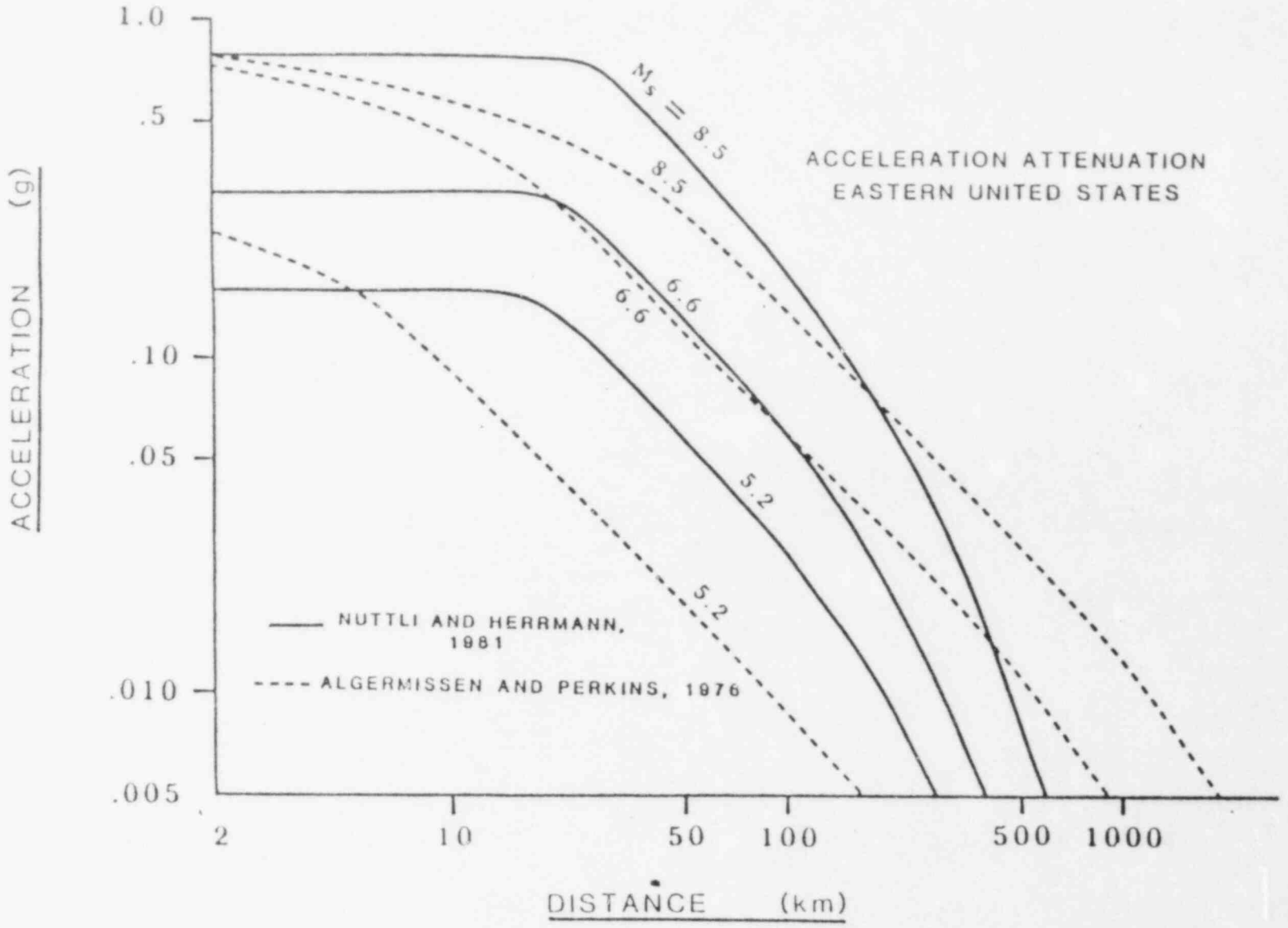

Figure 10 - Comparison of Algermissen and Perkins (1976) and Nuttli and Herrmann (1981) acceleration attenuation curves for the eastern and central United States.

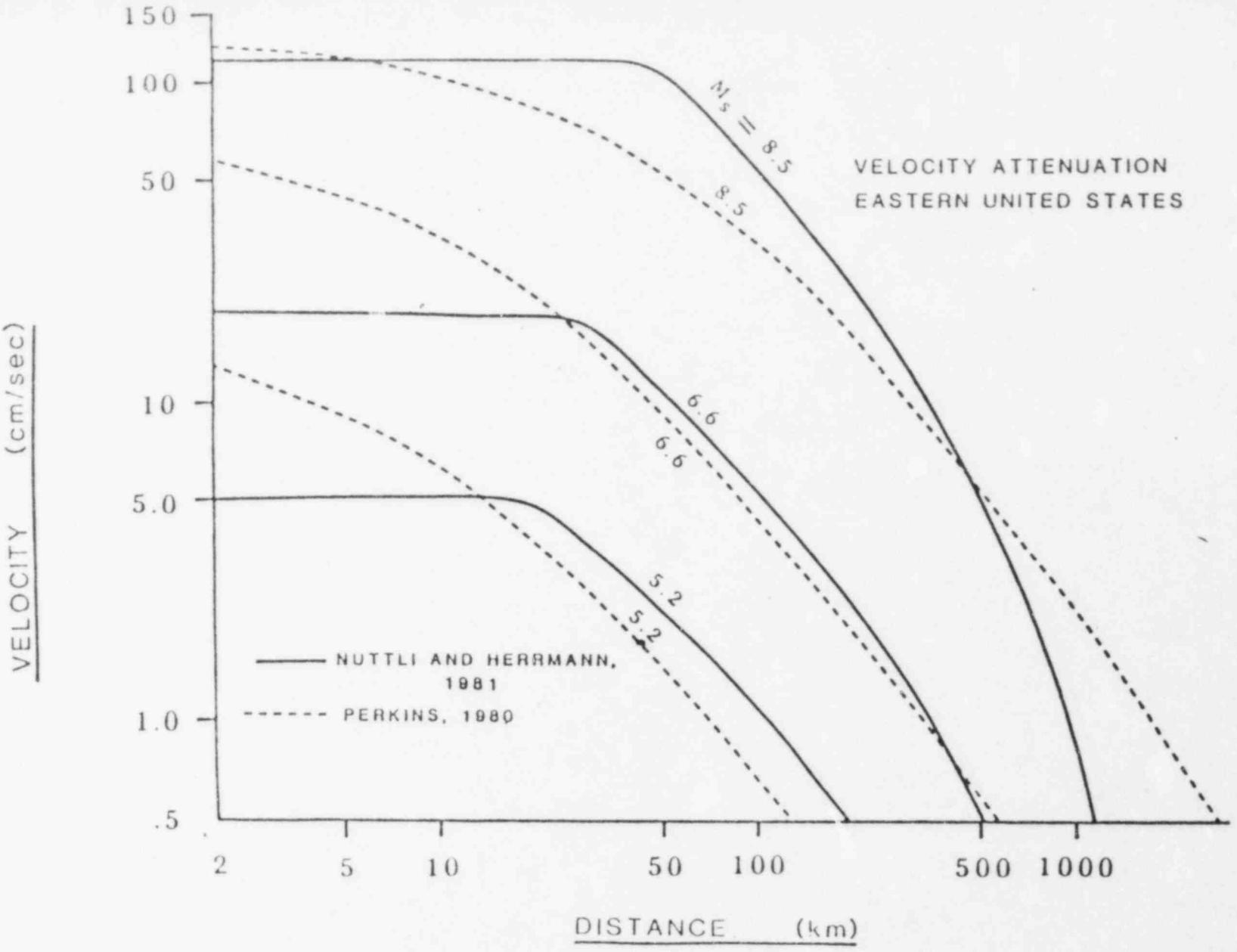

Figure 11 - Comparison of Perkins (1980) and Nuttli and Herrmann (1981) velocity attenuation curves for the central and eastern United States.

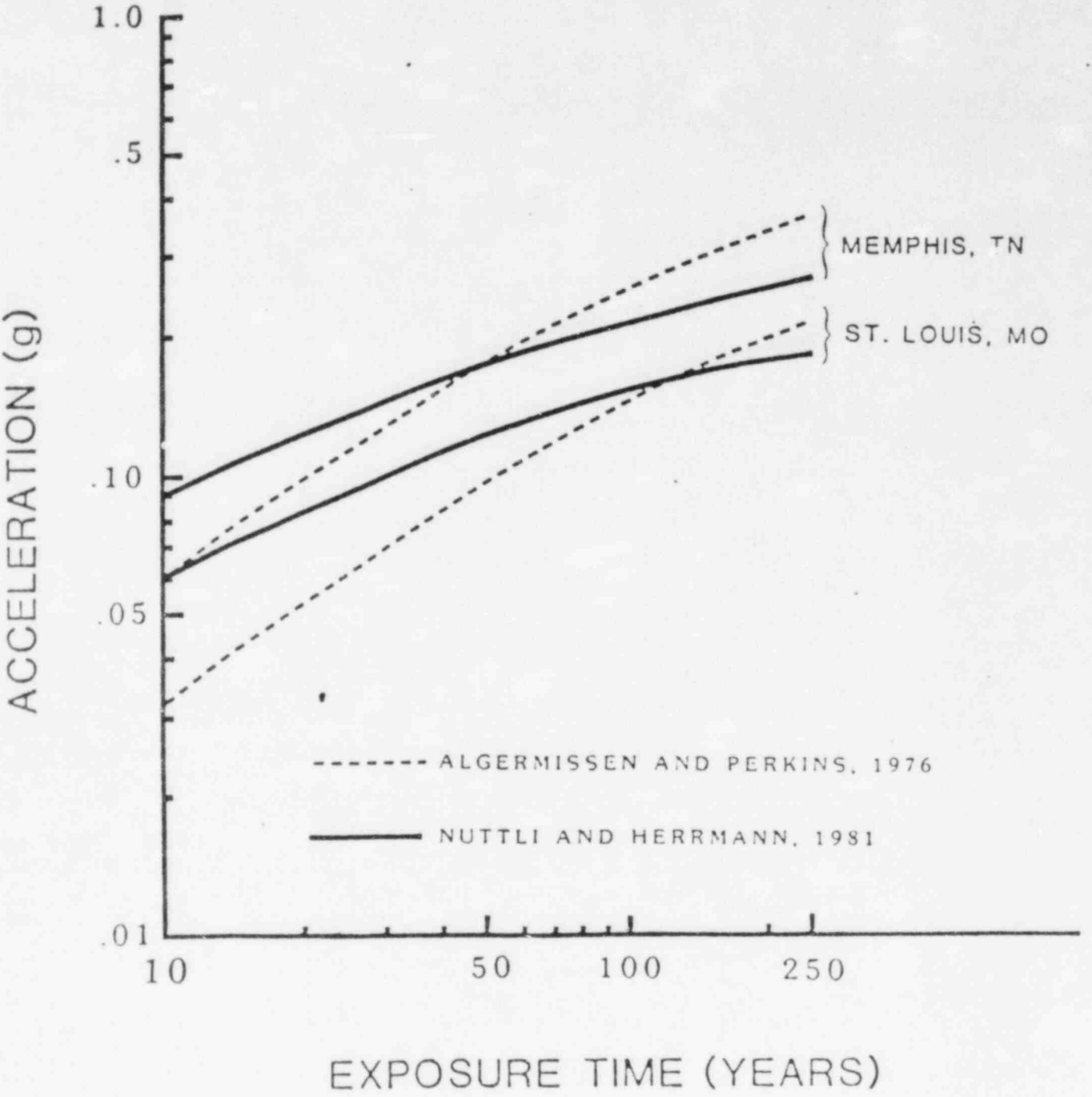

Figure 12 - Comparison of 50-year exposure time, 90-percent extreme probability acceleration at St. Louis, Missouri, and Memphis, Tennessee, computed using different acceleration attenuations.

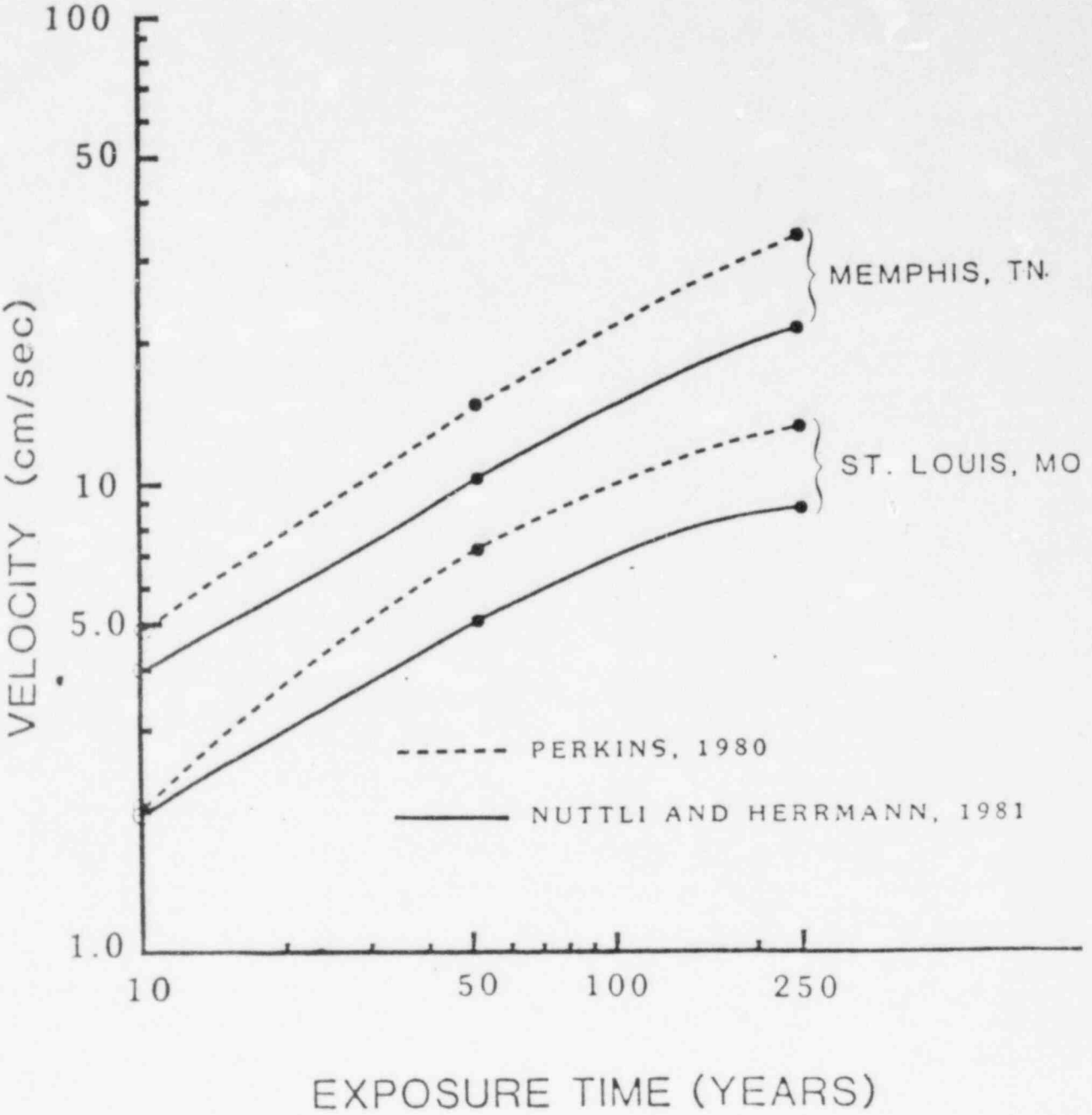

Figure 13 - Comparison of 50-year exposure time, 90-percent extreme probability, velocity at St. Louis, Missouri, and Memphis, Tennessee, computed using different velocity attenuation.

and the appreciable difference in the attenuation curves for small to moderate shocks. For longer exposure time (greater relative contribution to the ground motion from larger shocks) the agreement between the accelerations is somewhat closer. Velocity values for moderate exposure times (50 and 250 years) computed using the two different attenuation curves differ by a factor of about 1.5. For the 10-year exposure time the agreement is somewhat closer. This result comes from the fact that the two sets of attenuation curves are quite similar at large distances. At short return periods, a significant part of the exceedances of the mapped ground motions comes from distant earthquakes. At long return periods, high accelerations are mapped, these are governed by the near-field ground motions of rare, high magnitude events. In the near field, the attenuation functions differ strongly.

Another method of estimating uncertainty in the computed ground motions is to include parameter variability in the probabilistic ground motion calculation. Variances are not directly available for the Schnabel and Seed (1973) acceleration curves or the Perkins (1980) velocity attenuation curves. McGuire (1978) has estimated the standard deviation σ_a for the Schnabel and Seed curves as 0.50, and the standard deviation σ_L of the Mark (1977) fault rupture length relationship as 0.60. For purposes of illustration, variances of 0.50 are assumed for the acceleration and velocity curves used in this study. A variance of 0.60 is assumed for the fault rupture length relationship of Mark (1977). Figure 14 is a map showing the location of representative profiles of velocity and acceleration computed two ways: (1) without variability in fault rupture length and attenuation; and (2) including variability in fault rupture length and attenuation. The

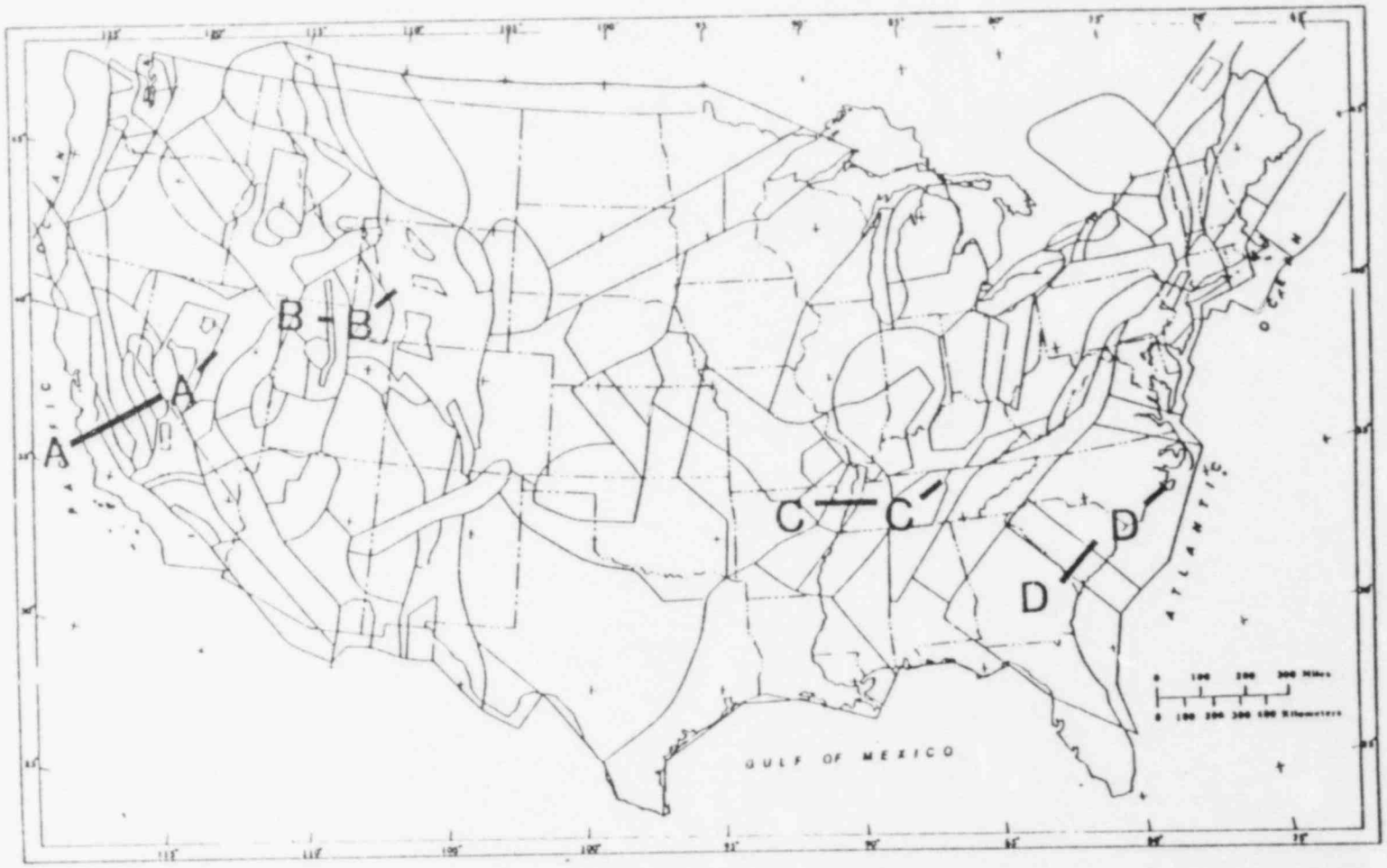

Figure 14 - Location map for acceleration profiles shown in Figures 15, 16, 17 and 18. The seismic source zones are also shown (except in coastal and southern California) for reference.

profiles are shown in Figures 15, 16, 17 and 18. Examination of the four representative profiles indicates that accounting parameter variability using this technique results in ground motion increases of from about 5 to 50 percent.

Review of the National Maps:

The main features of the new maps (Plates 1-6) will be reviewed by region in the following sections together with a discussion of the differences between the new set of maps and the Algermissen and Perkins (1976) acceleration map.

Coastal and Southern California (Region A, Figure 4): The major differences between the Algermissen and Perkins (1976) map and the new national maps result from the greater detail of the seismic source zones used in the new maps. Considerably more geological information was available for the development of the new maps (Thenhaus and others, 1980) than was available in the period 1972-1975 when the Algermissen and Perkins (1976) map was prepared. This is particularly true in southern California and in the coastal areas. Comparison of the 1976 mapped ground motion with the new maps shows that the levels of ground motion along the major features such as the San Andreas fault are approximately the same for the 1976 and the new national maps. The levels of ground motion in the coastal area of southern California are considerably higher on the new national maps than they are on the 1976 map; this results from the more extensive delineation of individual faults as sources zone for the new maps. Additional details of technique and of the mapped ground motion in coastal and southern California area are provided by Thenhaus and others (1980).

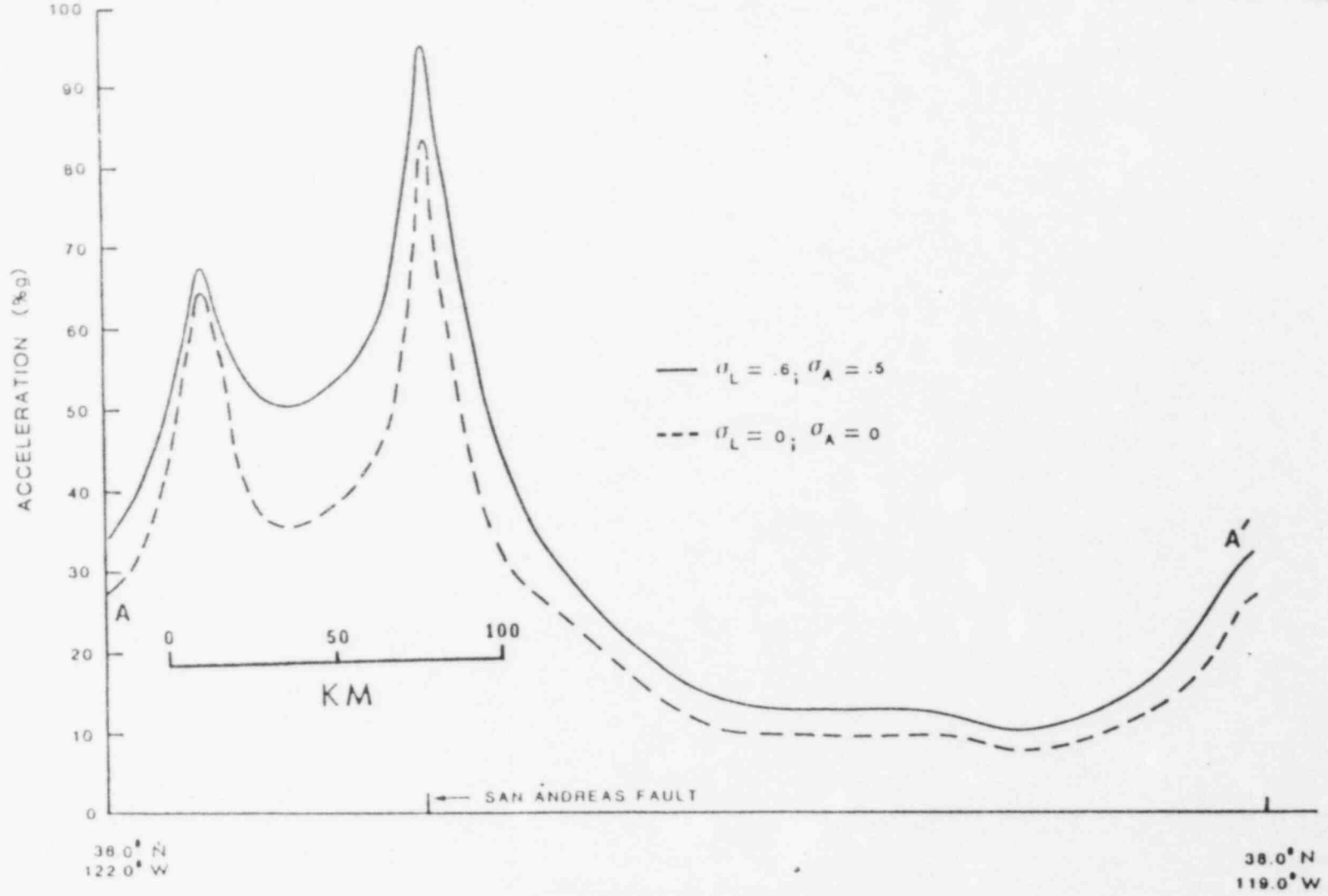

Figure 15 - Acceleration profile A-A' (see Figure 14 for location). The accelerations are for exposure times of 50 years with a 90-percent extreme probability.

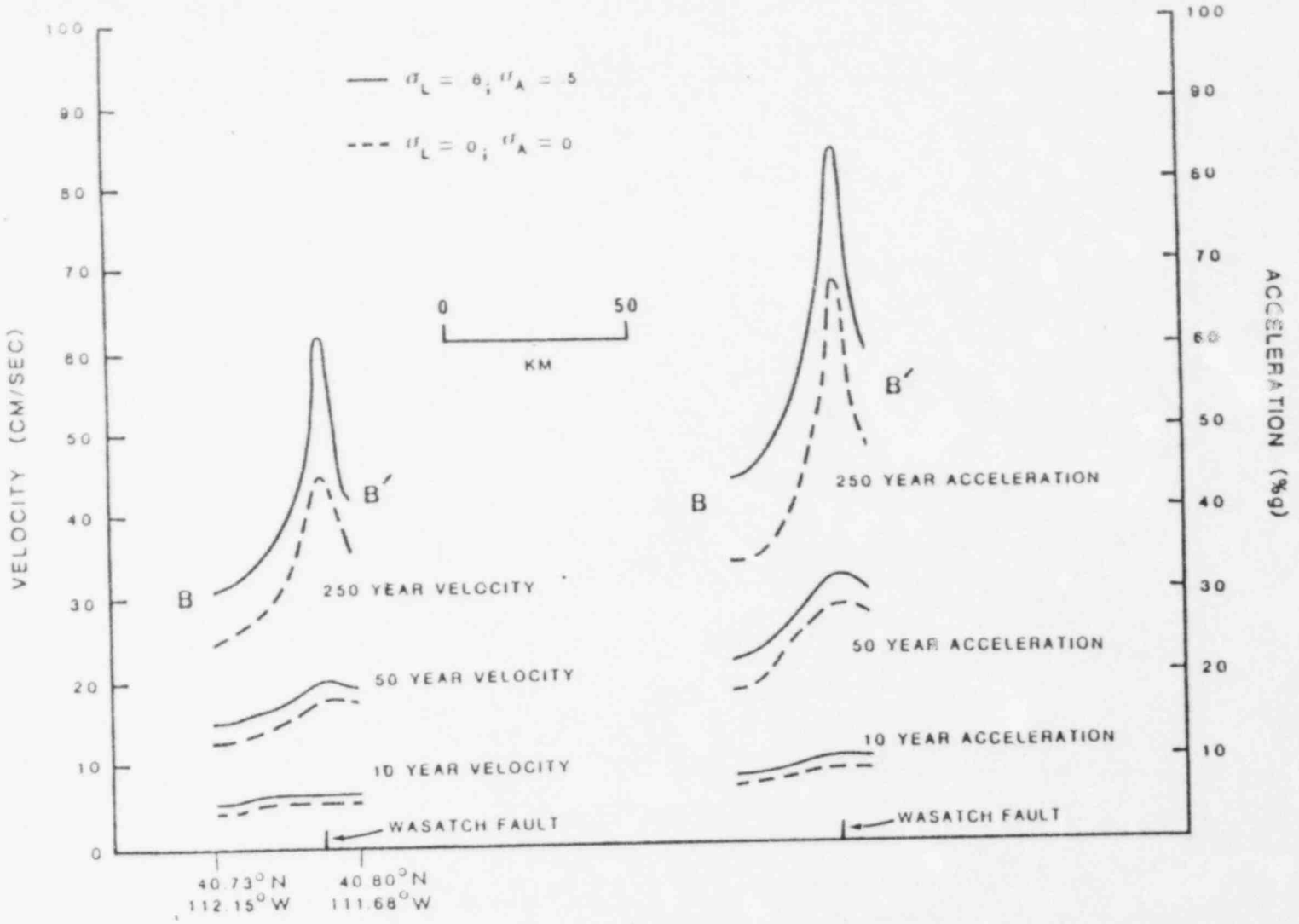

Figure 16 - Velocity and acceleration B-B' profiles (see Figure 14 for location). The velocities and accelerations are for exposure times of 50 years and a 90-percent extreme probability.

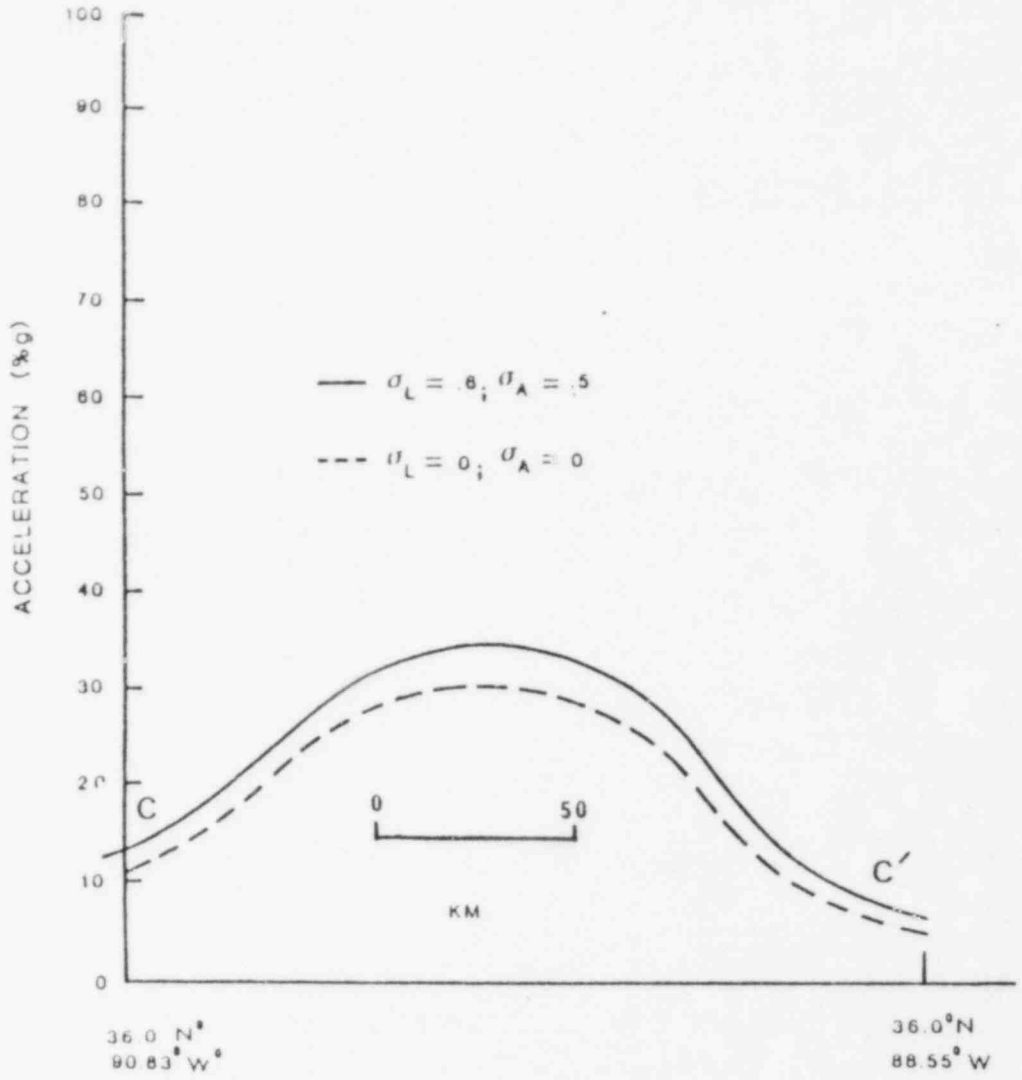

Figure 17 - Acceleration profile C-C' (see Figure 14 for location). The accelerations are for exposure times of 50 years with a 90-percent extreme probability.

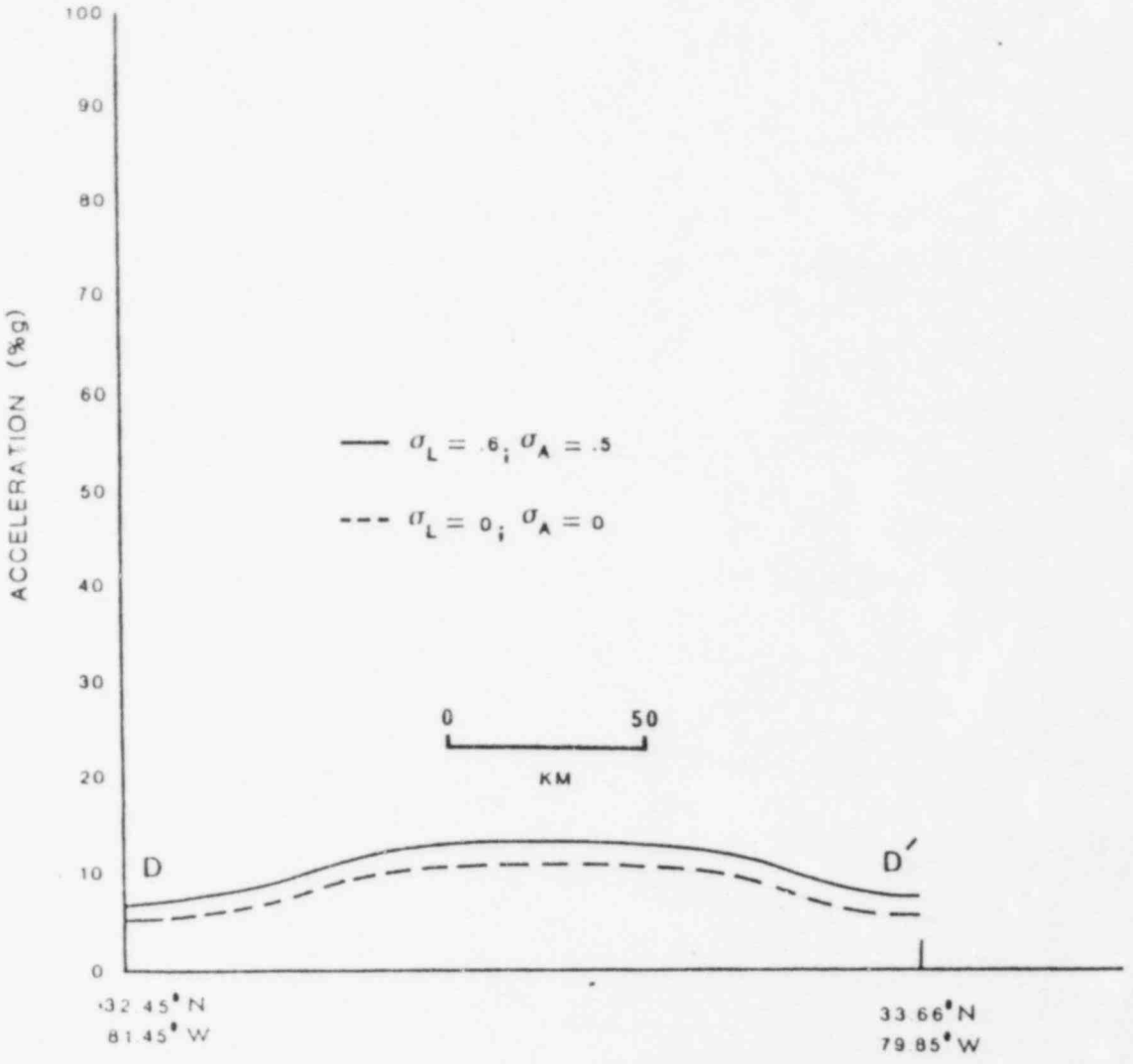

Figure 18 - Acceleration profile D-D' (see Figure 14 for location). The accelerations are for exposure times of 50 years with a 90-percent extreme probability.

Pacific Northwest: Historically, significant seismic hazard in this region is associated with the large (for example, M_s = 7.1 in 1949) earthquakes that occur at depths of 50-60 km in the Puget Sound Depression. In the 1976 map, these earthquakes make the major contribution to the probabilistic ground motion hazard. Since the preparation of the Algermissen and Perkins (1976) map, the importance of the December 14, 1872 central Washington earthquake has become established (Hopper and others, 1982). Also the possiblity of significant surface faulting has been established. As a result of modeling these new influences, the new national maps show significantly higher levels of ground motion in the Puget Sound area than the 1976 acceleration values. For example, the new 50-year exposure time, 90-percent extreme probability map shows a maximum acceleration of 0.30 g in the Puget Sound area as compared with a maximum of 0.15 g on the 1976 map.

These increases result from a change in the approach to modeling the earthquakes in the Puget Sound area. Because of uncertainty regarding the probability of occurrence of large shallow earthquakes (M_s > 6.4, depths of the order of 15 km) in the Puget Sound area, 25 percent of the large earthquakes were modeled as occurring at shallow depth and 75 percent were modeled as occurring at a depth of 50 km in the computation of the new national maps. Earthquakes smaller than M_L = 6.4 were modeled at shallow depth. In the computation of the 1976 acceleration map all of the large earthquakes were modeled as occurring at depths of 60 km. A more conservative position was taken in the preparation of the new national maps because there is some evidence that the 1872 shock may have occurred at shallow depths and because of the magnitude of the 1872 shock (M_s ~ 7.0). Furthermore, there is evidence of Holocene surface faulting in the western Puget Sound area (Gower,

1978) which may indicate the occurrence of relatively large, shallow earthquakes in the recent geologic past. Figure 19 shows the range of ground motions possible in the central Puget Sound area assuming various percentages of earthquakes $M_s > 6.4$ occur at shallow depth and modeling all earthquakes smaller than $M_s = 6.4$ at shallow depth.

A small increase in the level of ground motions in central Washington resulted from the reevaluation of the 1872 earthquake data. The ground motions in central Washington remain low, however, because of the generally low level of historical seismicity per unit area.

Great Basin (Area C, Figure 4): The level of ground motion in western Nevada is generally somewhat lower, but dispersed over a broader area than is shown on the 1976 acceleration map. This result occurs for two reasons. First, the greater geological input available for the new maps, particularly in the western Nevada - eastern California area resulted in an entirely different treatment of the source zones for the new maps in this area. Second, the maximum magnitude in the areas outlined by the aftershock zones of the major historical earthquakes in western Nevada were limited to $M_L = 6.0$, while the maximum magnitude of the surrounding zones was $M_s = 7.3$. This approach was taken because it is assumed that, for the exposure times considered, large shocks are likely to occur in the Nevada Seismic Zone, but not in the areas where major earthquakes have occurred historically. This view is consistent with what is presently known concerning Holocene fault movement in western Nevada.

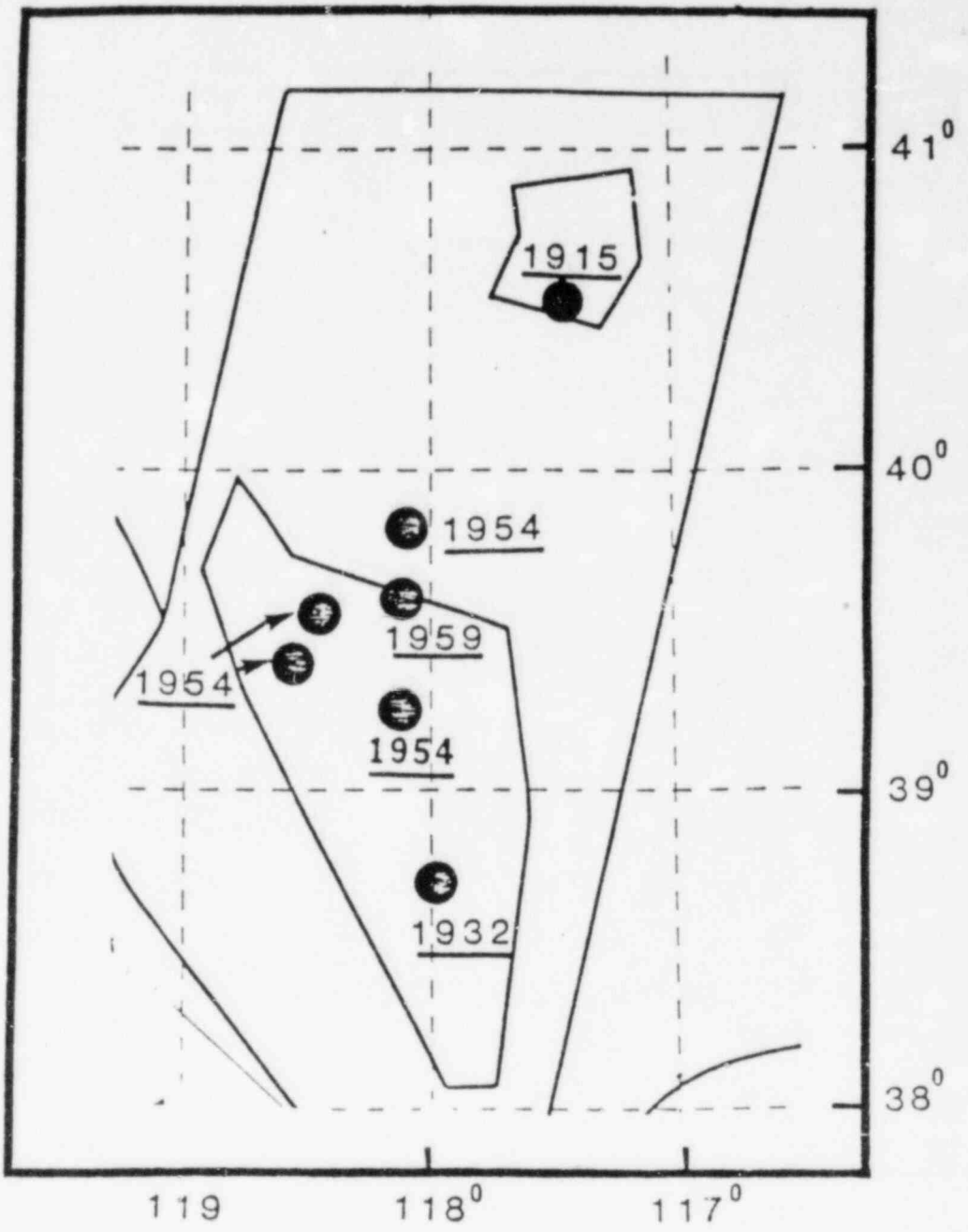

Figure 19 - Source zones in a portion of the Nevada Seismic Zone. The location of large earthquakes in 1915, 1932, 1954 and 1959 are also shown.

Specifically, the maximum magnitudes of seismic source zones 022, 032 and 033 were limited to M_L = 6.0, because these seismic source zones are areas in which large earthquakes (and their aftershocks) are known to have occurred historically (Figure 3). The seismic source zones surrounding zones 022, 032 and 033, namely zones 020 and 031, are considered as more likely loci of future large shocks (at least for the periods of interest for the hazard mapping considered here). The maximum magnitudes for zones 020 and 031 were set at M_s = 7.3. The historical seismicity (for M_L > 6.0) is taken from zones 022, 032 and 033 and used in the development of magnitude distributions for earthquakes in zones 020 and 031. The assumption is that large earthquakes will occur in the future in the Nevada Seismic Zone with about the same frequency as in the recent past, but they will not occur in the areas where large historical earthquakes have occurred. It is further assumed that they are more likely in the seismic source zones surrounding the aftershock zones of historical earthquakes (zones 020 and 031).

The modeling process and the resulting distribution of ground motion can be more clearly seen in Figures 20 and 21 which shows a portion of the Nevada Seismic Zone already discussed. Figure 20 shows seismic source zones 031, 032 and 033 together with the epicenters of large earthquakes that occurred in 1915, 1932, 1954 and 1959. The resulting 250-year exposure time, 90-percent extreme probability, velocity is shown in Figure 21. In this type of modeling, the area between seismic source zones 032 and 033 becomes a kind of seismic gap with high expected ground motions in the future.

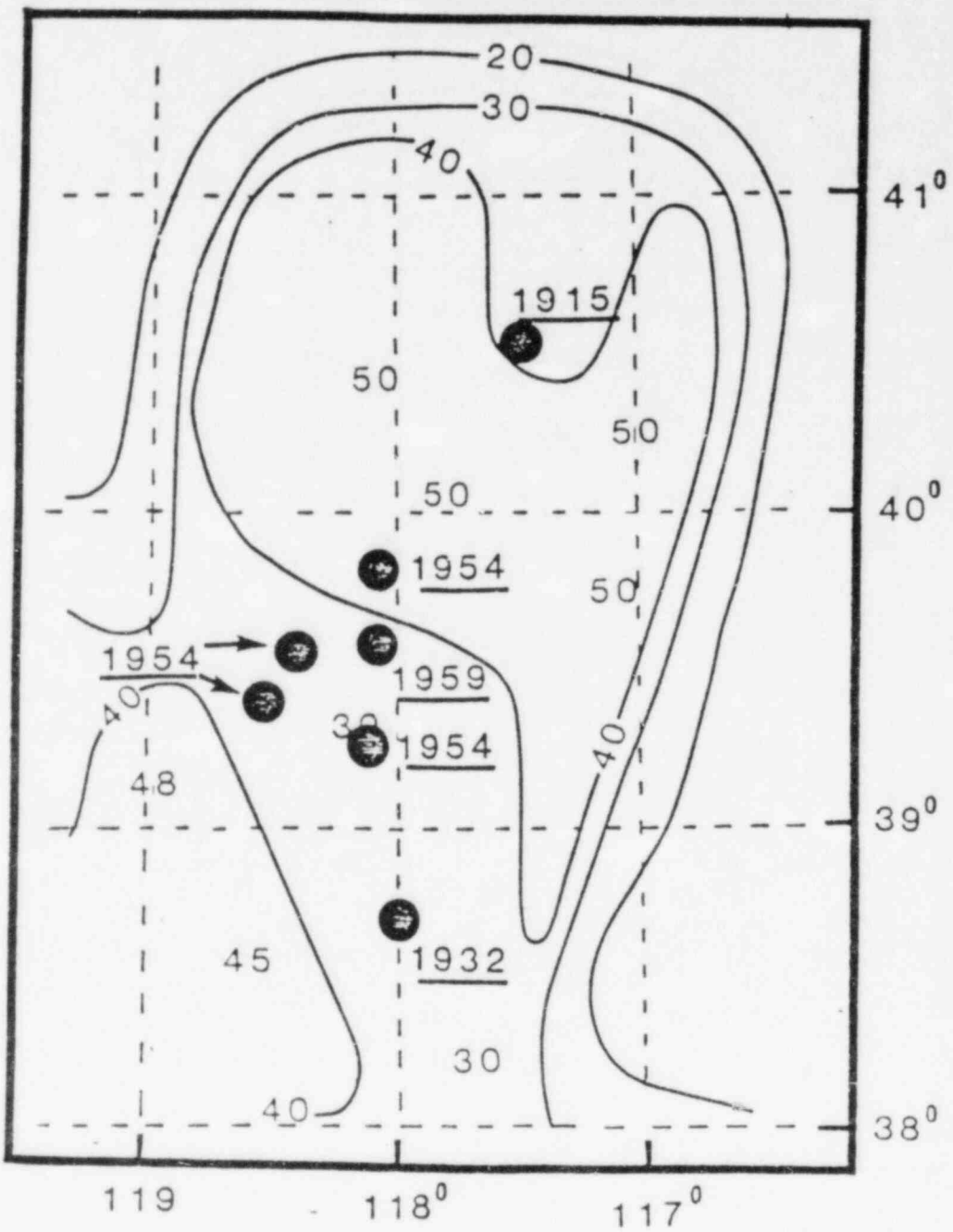

Figure 20 - Velocity (cm/sec) with an exposure time of 250 years and an extreme probability of 90 percent in a portion of the Nevada Seismic Zone. The location of large earthquakes in 1915, 1932, 1954 and 1959 are also shown.

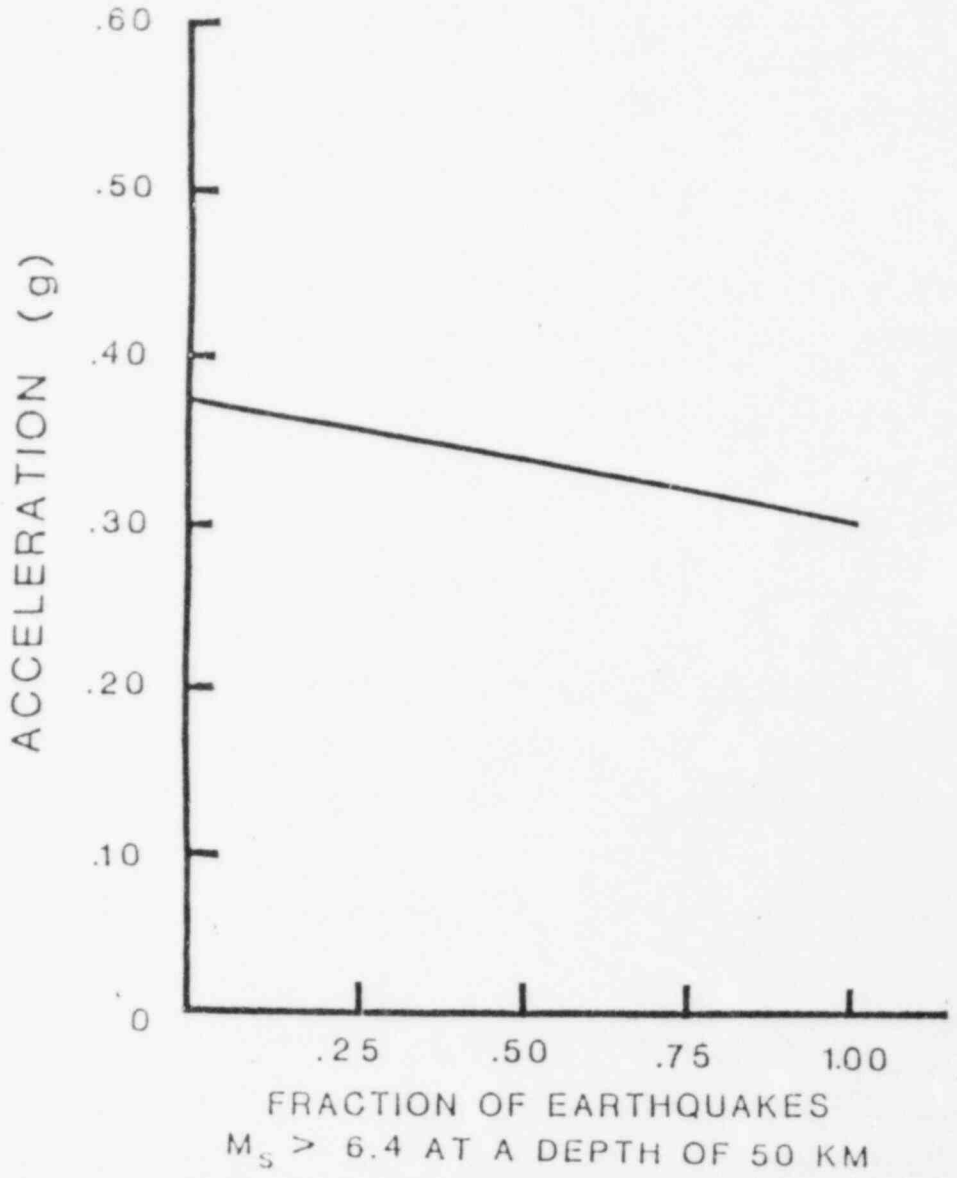

Figure 21 - The acceleration at Seattle, Washington, for an exposure time of 50 years and a 90-percent extreme probability assuming that various percentages of the large earthquakes ($M_S \geq 6.7$) in the magnitude distribution occur at a depth of 60 km. The remainder are assumed to occur at a depth of 10 km.

Ground motion values along the Wasatch fault are higher on the new national maps as compared with the 1976 acceleration map. Recent work on the Wasatch fault that indicates recurrence rates of a few hundred years or less for earthquakes in the magnitude seven range (Swan and others, 1980) has led us to model the Wasatch fault as an individual source zone with fault rupture, rather than as a broad zone of seismicity as in the 1976 map. Modeling the Wasatch fault as a separate zone together with much improved geologic control for the seismic source zones surrounding the Wasatch fault has substantially changed the orientation of the ground motion contours in central Utah on the new maps.

Northern and Central Rocky Mountains (Area D, Figure 4): The general level of ground motion throughout this area remains approximately the same as the 1976 map with some local exceptions. Considerable additional geological input was available as a result of the workshop conducted on the seismotectonics of this area. The resulting broadened seismic source zones and seismic activities in each of the zones tended to reduce the expected ground motion in the Helena, Montana area, a site of several historically damaging shocks and increase the activity in the Flathead Lakes area (zone 064) a recently seismically active region (maximum Modified Mercalli intensity VII earthquakes in 1952 and 1969); (Coffman and von Hake, 1973).

Southern Rocky Mountains and Southern Basin and Range (Area E, Figure 4): Despite extensive revision of seismic source zones for this area for the new national maps, the general level and pattern of ground motion remains approximately the same as for the 1976 map. Exceptions are a decrease (from

the 1976 ground motion levels) in the ground motion in the vicinity of Socorro, New Mexico, and on the New Mexico-Arizona border near 33°N. latitude. The decrease in expected ground motion in the Socorro area results from a reevaluation of the constants a and b in equation 1. The decrease in expected ground motion on the Arizona-New Mexico border results from extensive revision of the seismic source zones.

Great Plains and the Gulf Coast (Area F, Figure 4): The general pattern of expected ground motions is much the same on the new national maps and the 1976 acceleration maps. The expected ground motion associated with the Nemaha Ridge structure (eastern Kansas-Nebraska border area) is lower on the new maps primarily because of a revision of the constants a and b in equation 1. The seismicity is low throughout area F and the value of the constant b in equation 1 was obtained by grouping the seismicity in a number of source zones together to obtain a larger statistical sample (and more statistically reliable b value). The seismicity associated with the zones in the area was not grouped together to obtain a single b value when the 1976 map was developed and the b values in this area used in the computation of the 1976 map are probably less stable.

Central Interior (Area G, Figure 4): The expected levels of ground motion shown on the new national maps are similar to those on the 1976 acceleration map with the exception of the higher expected ground motions in the vicinity of seismic source zone 087 in the New Madrid, Missouri, region. The extensive geological and geophysical investigations program that has been underway in the southeast Missouri area for the past six years has made it possible to

improve our delineation of the most important seismic source zone in the central interior (zone 087). The significance of various earthquake modeling techniques in zone 087 has already been discussed.

Northeast (Area H, Figure 4): The new national maps do not use the Boston-Ottawa trend as a source zone as was the case for the 1976 acceleration map. The Boston-Ottawa zone used in 1976 has been segmented into a number of smaller zones and considerable additional detail has been added to the zones in the Boston-New York City area. The net result for the Northeast on a regional basis is that the expected levels of ground shaking have remained approximately the same as those derived for the 1976 acceleration map, but the general orientations of the contours is now northeast-southwest. More detailed delineation of structures in the Boston area and northwestern New York, and the isolation of specific structures such as the Ramapo fault and the Clarindon-Linden fault, have resulted in about a 30-percent increase in expected ground motion in these areas.

Southeast (Area I, Figure 4): The levels of ground motion for the new national maps are comparable to the levels of expected acceleration shown on the 1976 acceleration map. The causative fault of the 1886 Charleston, South Carolina, earthquake has not been identified and consequently we have retained the philosophy of using historical seismicity to produce a source zone for this area. The uniqueness of the "Charleston zone" (zone 101) as a source of large earthquakes in the southeast United States is an unresolved issue. If, however, the historical seismicity of zone 101 is distributed throughout all of the other zones in the southeast United States, the levels of expected

ground motion would be decreased substantially for the "Charleston zone" but would not increase appreciably throughout the southeast area. The net result of this approach is that, for moderate exposure times (10 to 100 years) of interest for normal commercial construction, the expected ground motions associated with earthquakes would be of only marginal interest. Whether or not the expected ground motions for long exposure times using this distribution of seismicity would be significant remains a largely unresolved problem. The seismicity of the southeast United States is low and because specific seismogenic structures have not been identified, we have chosen to construct the seismic source zones largely on the basis of the spatial distribution of historical seismicity.

CONCLUSIONS

The completion of the six national earthquake hazard maps demonstrates that interdisciplinary efforts with the objective of integrating geological and geophysical data, and interpretations of data, to produce improved estimates of expected ground motion are possible. The level of geological input into the preparation of these new maps is perhaps an order of magnitude greater than was possible in the preparation of the Algermissen and Perkins (1976) probabilistic acceleration map.

Where new geological and geophysical data were available, these data generally had a substantial impact on the ground motion maps. However, in large areas of the United States, particularly in the east, it has not been possible to demonstrate clear relationships between specific structures and earthquake occurrence. A major problem in the probabilistic mapping of ground motion, particularly in the central and eastern United States, is the paucity of data available for the development of suitable attenuation curves.

Statistical variability in the attenuation curves, and uncertainty as to which curves best represent attenuation are the major sources of uncertainty in the mapped ground motions.

The new maps represent an improvement in the application of probabilistic ground motion to earthquake resistant design for two principal reasons: (1) the development of both acceleration and velocity maps makes possible the estimation of a response spectrum at a site and comparison of response spectra at any number of sites under consideration. The response spectrum is the principal method of representing ground motion for earthquake resistant design at the present time. The use of different attenuation relations in the central-eastern U.S. and in the western U.S. properly takes into account, for design purpose, the significant high amplitude-long period ground motion in these parts of the country. (2) The change in earthquake hazard with exposure time can be estimated at any site because ground motion estimates for three exposure times--10, 50, and 250 years are available for every site in the country. It is much easier to select an exposure time (and ground motion) appropriate to the building usage (and cost amortization schedule where life loss is not a factor) when ground-motion estimates are available for a range of exposure times. The probabilistic acceleration and velocity maps are multiple-use maps that can not only be used in building code applications but also for regional land use planning, emergency preparedness, insurance analyses, and preliminary investigations of sites for critical facilities. A simple application of the data contained in the maps is shown in Figure 22 where the maximum accelerations for various exposure times are compared for three cities. Plots of this type facilitate rapid analysis of the relative hazard at any number of locations of interest.

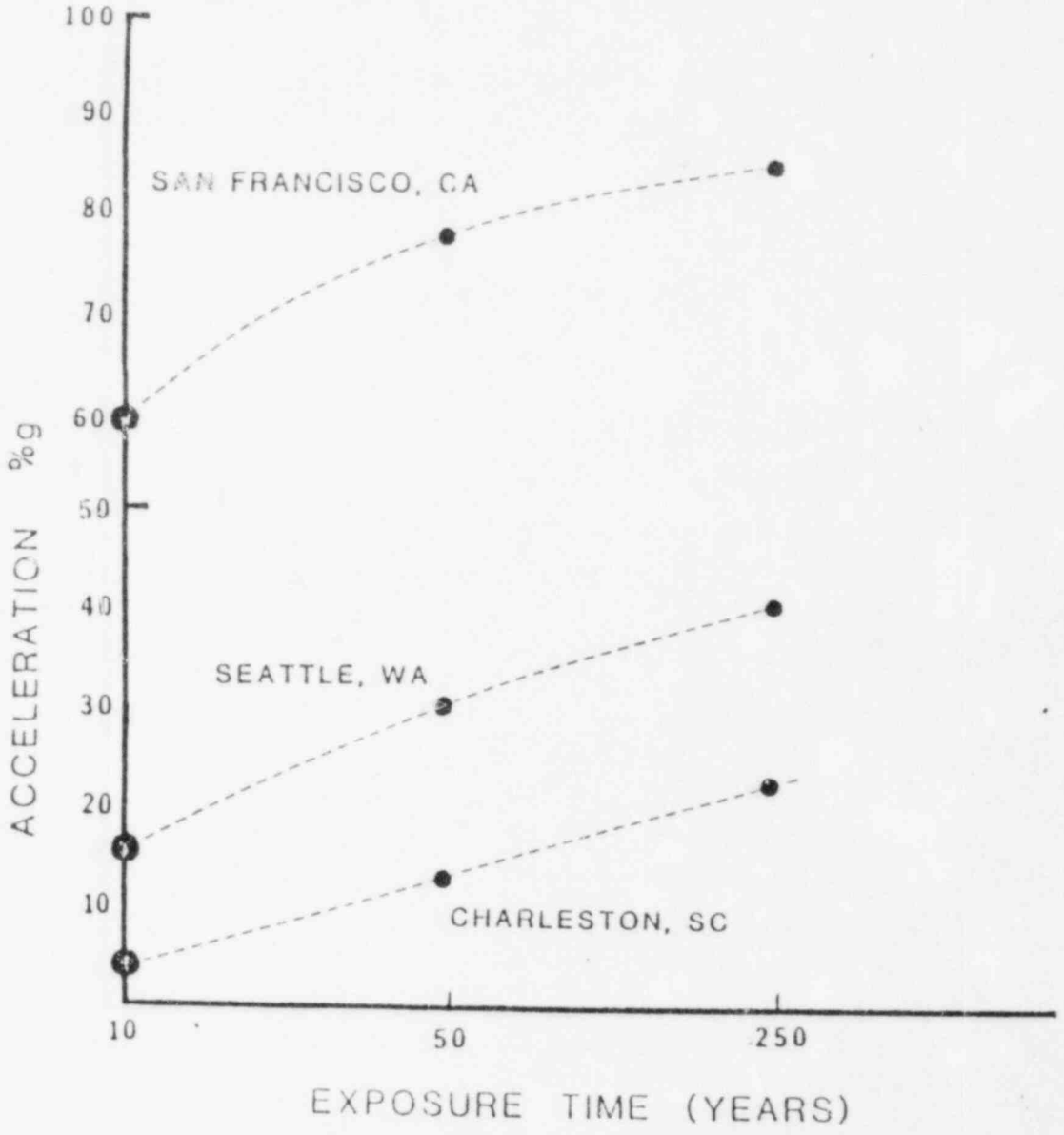

Figure 22 - The estimated acceleration at San Francisco, California, Seattle, Washington, and Charleston, South Carolina, for exposure times of 10, 50 and 250 years with a 90-percent extreme probability.

The present maps are the latest in a series beginning in 1969. Each new version has been motivated by (1) the need to represent hazard in a more useful manner; (2) improvements in the model used to represent ground motion from an earthquake source; and (3) increase in geological information to permit more detailed source zone descriptions.

The maps have not only met strongly voiced user needs, but have also challenged the research community to develop information and techniques to improve the input to maps of this sort. The Algermissen and Perkins (1976) probabilistic acceleration map was crucial to the development of the Applied Technology Council's seismic regulations for buildings (1978). Much of the renewed interest in Holocene and Quaternary geology has been sustained and justified by possible use in hazard maps.

Further improvements in this sort of hazard mapping will come from advances motivated, in part, by the present map. In some states other than California, research in Holocene geology will soon make it possible to produce regional maps at detail approaching that of the California hazard map presented in this paper. A California map can today be begun at even greater detail. Through careful geological investigations of recurrences of major faults it should be possible within the next two years to provide hazard maps which replace the Poisson assumption with time-dependent distributions for which the hazard increases with time from the last large event or an event of interest.

Table 1.--Seismic parameters for source zones

Zone No.*	No. of Modified Mercalli Maximum Intensity V's per year	b_I	Maximum Magnitude M**
p001	0.11010	-0.40	7.3
p002	0.43510	-0.40	7.3
p003	0.12440	-0.54	7.3
p004	0.34840	-0.62	7.3
p005	0.12390	-0.62	7.3
p006	0.02831	-0.62	7.3
p008	0.01642	-0.42	7.3
p009	0.20850	-0.28	7.9
p010	0.45200	-0.28	7.9
p011	0.96370	-0.28	7.9
p012	0.37090	-0.28	7.9
p013	0.69020	-0.28	7.9
p014	0.10940	-0.42	7.3
p015	0.34480	-0.42	7.3
p016	0.04926	-0.42	7.3
p017	0.87860	-0.28	7.9
p018	0.18810	-0.54	7.3
p019	0.04090	-0.54	7.3
c001	0.62770	-0.42	7.3
c002	0.15700	-0.42	7.3
c003	0.31960	-0.42	7.3
c004	0.31960	-0.42	7.3
c005	0.04843	-0.42	6.1
c006	0.15700	-0.42	7.3
c007	0.15700	-0.42	7.3
c008	0.04740	-0.42	6.1
c009	0.04843	-0.42	6.1
c010	0.18190	-0.42	6.1
c011	0.77010	-0.42	7.3
c012	0.19050	-0.42	7.3
c013	0.35840	-0.42	7.3
c014	0.91990	-0.66	7.9
c015	1.49200	-0.45	7.9
c016	0.22560	-0.51	7.9
c017	0.02760	-0.48	7.3
c018	1.09200	-0.49	7.3
c019	0.31980	-0.42	6.7
c020	0.19280	-0.42	6.1
c021	0.10880	-0.42	6.1
c022	0.02422	-0.42	6.1
c023	0.11650	-0.37	7.9
c024	1.97000	-0.43	8.5
c025	0.05085	-0.55	7.3
c026	0.09145	-0.55	7.3

Table 1.--Seismic parameters for source zones--continued

Zone No.*	No. of Modified Mercalli Maximum Intensity V's per year	b_I	Maximum Magnitude M**
c027	0.03437	-0.37	7.3
c028	0.13010	-0.37	7.3
c029	0.02350	-0.37	7.3
c030	0.03630	-0.42	6.7
c031	0.47580	-0.51	6.7
c032	0.55190	-0.45	7.9
c033	0.23070	-0.37	7.9
c034	0.67120	-0.51	7.9
c035	0.02325	-0.60	7.3
c036	0.35220	-0.59	6.7
c037	0.81950	-0.51	6.1
c038	0.82680	-0.54	7.9
c039	0.35810	-0.45	7.9
c040	0.15820	-0.42	6.1
c041	0.08448	-0.37	7.9
001	0.22700	-0.73	7.3
002	0.03600	-0.73	7.3
003	0.08800	-0.73	6.1
004	0.22700	-0.54	7.3
005	0.09100	-0.73	7.3
006	0.13500	-0.73	7.3
007	0.41900	-0.73	7.3
008	0.21100	-0.73	6.1
009	0.19400	-0.54	6.1
010	0.20800	-0.54	7.3
011	0.55100	-0.64	7.3
012	0.34900	-0.64	7.3
013	0.05500	-0.64	7.3
014	0.49000	-0.73	7.3
015	0.01800	-0.73	6.7
016	0.14600	-0.73	6.1
017	0.69300	-0.59	7.3
018	0.26100	-0.54	7.3
019	0.11717	-0.54	7.3
020	1.84900	-0.64	7.3
022	0.19600	-0.64	6.1
023	0.15350	-0.54	7.3
024	0.27400	-0.64	7.3
025	0.16800	-0.64	6.1
026	0.47700	-0.64	6.1
027	0.11100	-0.64	5.5
029	1.31900	-0.64	7.3
030	0.58800	-0.64	7.3
031	1.82685	-0.54	7.3

Table 1.--Seismic parameters for source zones--continued

Zone No.*	No. of Modified Mercalli Maximum Intensity V's per year	b_I	Maximum Magnitude M**
032	0.48114	-0.54	6.1
033	0.08557	-0.54	6.1
034	0.62380	-0.54	7.3
035	0.20070	-0.54	7.3
036	0.01800	-0.58	6.1
037	0.05100	-0.58	7.3
038	0.80600	-0.58	7.3
039	0.12000	-0.58	7.3
040	0.29100	-0.58	7.3
041	0.24400	-0.73	7.3
042	0.01800	-0.73	6.1
043	0.04600	-0.73	7.3
044	0.11300	-0.73	6.1
045	0.45600	-0.73	6.1
046	0.01274	-0.73	6.1
047	0.00427	-0.73	6.1
048	0.00329	-0.73	6.1
049	0.01663	-0.73	6.1
050	0.17000	-0.73	6.1
051	0.01706	-0.73	6.1
052	0.19000	-0.58	7.3
053	0.03600	-0.58	7.3
054	0.01800	-0.58	6.1
055	0.67300	-0.58	7.3
056	0.17700	-0.58	6.1
057	0.66200	-0.58	7.3
058	0.19800	-0.58	7.3
059	0.19200	-0.58	6.1
060	0.03600	-0.58	6.1
061	0.08900	-0.58	7.3
062	0.03600	-0.58	6.1
063	0.12900	-0.58	6.1
064	0.34400	-0.58	7.3
065	0.15200	-0.58	6.1
066	0.01800	-0.73	6.1
067	0.07715	-0.46	6.1
068	0.02894	-0.46	6.1
069	0.00588	-0.46	6.1
070	0.03552	-0.46	6.1
071	0.01176	-0.46	6.1
072	0.02026	-0.46	6.1
073	0.02353	-0.46	6.1
074	0.00270	-0.46	6.1
075	0.06510	-0.46	6.1

Table 1.--Seismic parameters for source zones--continued

Zone No.*	No. of Modified Mercalli Maximum Intensity V's per year	b_I	Maximum Magnitude M**
076	0.14742	-0.46	6.1
077	0.03469	-0.46	6.1
078	0.04389	-0.46	6.1
079	0.03082	-0.46	6.1
080	0.02987	-0.46	6.1
081	0.02044	-0.46	6.1
082	0.03552	-0.46	6.1
083	0.00996	-0.46	6.1
084	0.04117	-0.46	6.1
085	0.03802	-0.46	6.1
086	0.04626	-0.46	6.1
087	0.29865	-0.46	8.5
088	0.09703	-0.46	6.1
089	0.15689	-0.46	6.1
090	0.06103	-0.46	6.1
091	0.00644	-0.46	6.1
092	0.02661	-0.46	6.1
093	0.02680	-0.46	6.1
094	0.10835	-0.46	6.1
095	0.05901	-0.46	6.1
096	0.02675	-0.46	6.1
097	0.01156	-0.46	6.1
098	0.01215	-0.46	6.1
099	0.24830	-0.50	7.3
100	0.42290	-0.50	7.3
101	0.18720	-0.50	7.3
102	0.09532	-0.50	7.3
103	0.33150	-0.50	7.3
104	0.05544	-0.50	7.3
106	0.01952	-0.50	6.7
107	0.19100	-0.50	7.3
108	0.29390	-0.50	6.7
109	0.10650	-0.50	7.9
110	0.30220	-0.50	7.9
111	0.32430	-0.50	7.9
112	0.01532	-0.50	6.7
113	0.07432	-0.50	6.7
114	0.00754	-0.50	6.7
115	0.05834	-0.50	7.3
116	0.06783	-0.50	6.7
117	0.03950	-0.50	7.3
118	0.01334	-0.50	7.3

*The zones are shown in Figures 2 & 3
**See text for definition of M

REFERENCES

Aggarwal, Y. P., and Sykes, L. R., 1978, Earthquakes, faults and nuclear power plants in southern New York and northern New Jersey: Science, v. 200, p. 425-429.

Algermissen, S. T., and Harding, S. T., 1965, Preliminary seismological report, in, The Puget Sound, Washington, earthquake of April 29, 1965: U.S. Department of Commerce, Coast and Geodetic Survey, 51 p.

Algermissen, S. T., 1969, Seismic risk studies in the United States: World Conference on Earthquake Engineering, 4th, Chilean Association for Seismology and Earthquake Engineering, Proceedings, Santiago, Chile, reprint, p. 1-10.

Algermissen, S. T., and Perkins, D. M., 1972, A technique for seismic zoning--General considerations and parameters: Proc. of the Int'l. Conf. Microzonation, Seattle, Washington, p. 865-878.

Algermissen, S. T., and Perkins, D. M., 1976, A probabilistic estimate of maximum acceleration in rock in the contiguous United States: U.S. Geological Survey Open-File Report 76-416, 45 p.

Applied Technology Council, 1978, Tenative provisions for the development of seismic regulations for buildings, National Science Foundation Publication 78-8, 505 p.

Arabasz, W. J., Smith, R. B., Richins, R. B., and William, D., 1979, Earthquake studies in Utah 1850-1878: Special Pub. of the University of Utah Seismograph Stations, Department of Geology and Geophysics, University of Utah, 552 p.

Armbruster, J. G., and Seeber, L., 1981, Intraplate seismicity in the southeastern United States and the Appalachain detachment, in, Beavers, J. E., ed., Earthquakes and Earthquake Engineering--Eastern United States, v. 1, Ann Arbor Science Publishers, Inc., Ann Arbor, Michigan, p. 375-396.

Atwater, T., 1970, Implications of plate tectonics for the Cenozoic tectonic evolution of Western North America: Geological Society of America Bulletin, v. 81, p. 3513-3535.

Bakun, W. H., Stewart, R. M., Bufe, C. G., and Marks, S. M., 1980, Implication of seismicity for failure of a portion of the San Andreas fault: Seismological Society of America Bulletin, v. 70, p. 185-201.

Basham, P. W., Weichert, D. H., and Berry, M. J., 1979, Regional assessment of seismic risk in eastern Canada: Seismological Society of America Bulletin, v. 69, p. 1567-1602.

Bender, B., 1982, Sensitivity analysis for seismic risk using a fault rupture model: U.S. Geological Survey Open-File Report 82-294, 75 p.

Bender, B., and Perkins, D. M., 1982, Seisrisk II--A computer program for earthquake hazard mapping: U.S. Geological Survey Open-File Report 82-293, 103 p.

Bender, B., 1982, Maximum likelihood estimation of b-values for magnitude grouped data [abstract]: Earthquake Notes, v. 53, no. 1, p. 64-65.

Braile, L. W., Hinze, W. J., Keller, G. R., Lidiak, E. G., 1982, The north extension of the New Madrid fault zone, in, McKeown, F. A., and Pakiser, L. C., eds., Investigations of the New Madrid Missouri, Earthquake Region: U.S. Geological Survey Professional Paper 1236

Braile, L. W., Keller, G. R., Hinze, W. J., and Lidiak, E. G., 1982, An ancient rift complex and its relation to contemporary seismicity in the New Madrid Seismic Zone: Tectonics, v. 1, no. 2, p. 225-237.

Buchanan-Banks, J. M., Pampeyan, E. H., Wagner, H. C., McCulloch, D. S., 1978, Preliminary map showing recency of faulting in coastal south-central California: U.S. Geological Survey Miscellaneous Field Studies Map MF-910, 3 pl., scale 1:500,000.

Bucknam, R. C., Algermissen, S. T., and Anderson, R. E., 1980, Patterns of late Quaternary faulting in western Utah and an application in earthquake hazard evaluation in, Proceedings of conference X, earthquake hazards along the Wasatch and Sierra Nevada frontal fault zones: U.S. Geological Survey Open-File Report 80-801, p. 299-314.

Burford, R. O., and Harsh, P. W., 1980, Slip on the San Andreas fault in central California from alinement array surveys: Seismological Society of America Bulletin, v. 70, no. 4, p. 1233-1261.

Campbell, N. P., and Bentley, R. D., 1981, Late Quaternary Deformation of the Toppenish Ridge Uplift in South-Central Washington: Geology, v. 9, p. 519-524.

Coffman, J. J., and von Hake, C. A., 1973, Earthquake history of the United States: U.S. Department of Commerce, National Oceanic and Atmospheric Administration, Publication 41-1, 208 p.

Cook, F. A., Albaugh, D. S., Brown, C. D., Kaufman, S., Oliver, J. E., and Hatcher, R. D., Jr., 1979, Thin-skinned tectonics in the crystalline southern Appalachians; Cocorp seismic relfection profiling of the Blue Ridge and Piedmont: Geology, v. 7, p. 563-567.

Cook, F. A., Brown, L. D., Kaufman, S., Oliver, J. E., and Peterson, T. A., 1981, COCORP seismic profiling of the southern Appalachian orogen beneath the Coastal Plain of Georgia: Geological Society of America Bulletin, pt. 1, v. 92, p. 738-748.

Cornell, C. A., 1968, Engineering seismic risk analysis, Seismolgocial Society of America Bulletin, v. 58, p. 1583-1606.

Crosson, R. S., 1972, Small earthquakes, structure and tectonics of the Puget Sound region: Seismological Society of America Bulletin, v. 62, no. 5, p. 1133-1171.

Diment, W. H., Urban, T. C., and Revetta, F. A., 1972, Some geophysical anomalies in eastern United States, in, Robertson, E. C., ed., The Nature of the Solid Earth: McGraw Hill, New York, p. 544-572.

Evernden, J. F. 1975, Seismic intensities "size" of earthquakes and related parameters: Seismological Society of America Bulletin, vol. 65, p. 1287-1313.

Fletcher, J. B., and Sykes, L. R., 1977, Earthquakes related to hydraulic mining and natural seismic activity in western New York State: Journal of Geophysical Research, v. 82, no. 26, p. 3767-3780.

Gardner, J. K., and Knopoff, L., 1974, Is the sequence of earthquakes in southern California with aftershocks removed, Poissonian?: Seismological Society of America Bulletin, v. 64, p. 1363-1368.

Gawthrop, W., 1975, Seismicity of the central California coastal region: U.S. Geological Survey Open-File Report 75-134, 48 p.

Gower, H. D., 1978, Tectonic map of the Puget Sound Region, Washington: U.S. Geological Survey Open-File Report 78-426, 22 p.

Greensfelder, R. W., 1976, Maximum probable earthquake acceleration on bedrock in the State of Idaho: Research Project No. 79, Idaho Department of Transportation, Division of Highways, 69 p.

Gutenberg, B., and Richter, C. F., 1942, Earthquake magnitude, intensity, energy and acceleration: Seismological Society of America Bulletin, v. 32, p. 163-191.

Hamilton, R. M., Yerkes, R. F., Brown, R. D., Jr., Burford, R. O., DeNoyer, J. M., 1969, Seismicity and associated effects, Santa Barbara region, in, Geology, petroleum development and seismicity of the Santa Barbara channel region, California: U.S. Geological Survey Professional Paper 679, p. 47-77.

Hamilton, R. M., and Russ, D. P., 1981, Seismotectonics of the New Madrid Region, in, Hays, W. W., ed., Proceedings of Conference XIII, Evaluation of Regional Seismic Hazard and Risk: U.S. Geological Open-File Report 81-437, p. 55-73.

Hamilton, R. M., and Zoback, M. D., 1982, Tectonic features of the New Madrid seismic zone from seismic-reflection profiles, in F. A. McKeown and L. C. Pakiser, eds., Investigations of the New Madrid, Missouri, Earthquake Region, U.S. Geological Survey Professional Paper 1236 (in press).

Hammond, P. E., 1979, A tectonic model for evolution of the Cascade Range, in, Armentrout, J. M., Cole, M. R., and Terbest, H., Jr., eds., Cenozoic Paleogeography of the Western United States: Pacific section of the society of economic paleontologists and mineralogists, Pacific Coast Paleogeography Symposium 3, p. 219-237.

Herd, D. G., and Helley, E. J., 1976, Faults with Quaternary displacement northwestern San Francisco Bay region, California: U.S. Geological Survey Miscellaneous Field Studies Map MF-818, 1 plate, scale 1:125,000.

Herrmann, R. B., 1981, Preliminary results of microearthquake studies in the Central Mississippi Valley, in, Hays, W. W., ed., Proceedings of Conference XIII, Evaluation of Regional Hazard and Risk: U.S. Geological Survey Open-File Report 81-437, p. 30-54.

Heyl, A. V., and McKeown, F. A., 1978, Preliminary seismotectonic map of the Central Mississippi Valley and environs: U.S. Geological Survey Miscellaneous Field Studies Map MF-1011, 1 plate, scale 1:500,000.

Hildenbrand, T. G., Kane, M. F., and Stauder, W., 1977, Magnetic and gravity anomalies in the northern Mississippi Embayment and their spatial relation to seismicity: U.S. Geological Survey Miscellaneous Field Studies Map MF-914, 2 plates, scale 1:1,000,000.

Hill, D. P., 1978, Seismic evidence for the structure and Cenozoic tectonics of the Pacific Coast states, in Smith, R. B., and Eaton, G. P., eds., Cenozoic tectonics and regional geophysics of the Western Cordillera: Geological Society of America Memoir 152, p. 145-174.

Hopper, M. G., Algermissen, S. T., Perkins, D. M., Brockman, S. R., Arnold, E. P., 1982, The earthquake of December 14, 1872, in the Pacific Northwest, program of the annual Seismological Society of America Meeting.

Hutchinson, D. R., Pomeroy, P. W., Wold, R. J., Halls, H. C., 1979, A geophysical investigation concerning the continuation of the Clarendon-Linden Fault across Lake Ontario: Geology, v. 7, p. 206-210.

Iverson, W. P., and Smithson, S. B., 1982, Master decollement root zone beneath the Southern Appalachians and crustal balance, Geology, v. 10, p. 241-245.

Kirkham, R. M., and Rogers, W. P., 1981, Earthquake potential in Colorado; a preliminary evaluation: Colorado Geological Survey Bulletin 43, 3 plates, scales 1:100,000, 1:62,500, 171 p.

Kulm, L. D., and Fowler, G. A., 1974, Oregon continental margin structure and stratigraphy--A test of the imbricate thrust model, in, Burk, C. A., and Drake, C. L., eds., The geology of continental margins: New York, Springer-Verlag, p. 261-291.

Lawrence, D. L., 1976, Strike-slip faulting terminates the Basin and Range province in Oregon: Geological Society of America Bulletin, v. 87, p. 846-850.

Lee, W. K., and Vedder, J. G., 1973, Recent earthquake activity in the Santa Barbara channel region: Seismological Society of America Bulletin, v. 63, no. 5, p. 1757-1773.

Leslie, R. B., 1981, Continuity and tectonic implications of the San Simeon-Hosgri Fault Zone, Central California: U.S. Geological Survey Open-File Report 81-430, 54 p.

Machette, M. N., 1978, Geologic map of the Socorro 1 degree x 2 degree quadrange, New Mexico: U.S. Geological Survey Open-File Report 78-607, 1 plate, scale 1:250,000.

Magill, J. R., Wells, R. E., Simpson, R. W., and Cox, A. V., 1982, Post 12 m.y. Rotation of Southwest Washington: Journal of Geophysical Research, v. 87, no. B5, p. 3761-3776.

Mark, R. K., 1977, Application of linear statistical models of earthquake magnitude versus fault length in estimating maximum expectable earthquakes: Geology, v. 5, p. 464-466.

McGuire, R. K., 1978, Seismic ground motion parameter relations: Journal of the Geotechnical Engineering Division, American Society of Civil Engineers, v. 104, p. 481-490.

Moench, R. H., 1973, Down-Basin Fault-Fold Tectonics in Western Maine, with Comparison to the Taconic Klippe, in, DeJong, K. A., and Scholten, R., ed., Gravity and Tectonics: Wiley-Interscience, New York, p. 327-342.

Mooney, H. M., and Morey, G. B., 1981, Seismic history of Minnesota and its geological significance: Seismological Society of America Bulletin, v. 71, no. 1, p. 199-210.

Mudge, M. R., 1970, Origin of the Disturbed Belt, Montana: Geological Society of America Bulletin, v. 81, no. 2, p. 377-392.

Newcomb, R. C., 1970, Tectonic structure of the main part of the basalt of the Columbia River Group Washington, Oregon, and Idaho: U.S. Geological Survey Miscellaneous Geologic Investigations Map I-587.

Nuttli, O., and Herrmann, R. B., 1978, State-of-the-art for assessing earthquake hazards in the United States--Credible earthquakes for the central United States: U.S. Corps of Engineers, Papers 5-13-1, report 12, 99 p.

Nuttli, O. W., and Herrmann, R. B., 1981, Excitation and attenuation of strong ground motion, [Abstract]: 21st General Assembly, IASPEI-AISPIT, London, Canada, July 21-30, 1981.

Pampeyan, E. H., 1979, Preliminary Map showing recency of faulting in coastal North-Central California: U.S. Geological Survey Miscellaneous Field Studies Map MF-1070, 13 pages, 3 plates, scale 1:250,000.

Perkins, D. M., 1980, Outer continental shelf seismic risk, in, Summaries of Technical Reports, v. IX: U.S. Geological Survey Open-File Report 80-6, p. 166-168.

Perkins, D. M., Thenhaus, P. C. Wharton, M. K., Diment, W. K., Hanson, S. L., and Algermissen, S. T., 1979, Probabilistic estimates of maximum seismic horizontal ground motion in rock on the East Coast and the adjacent outer continental shelf: U.S. Geological Survey Interagency Report to the Bureau of Land Management, 18 p., 7 plates, scale 1:2,500,000.

Perkins, D. M., Thenhaus, P. C., Hanson, S. L., Ziony, J. I., and Algermissen, S. T., 1980, Probabilistic estimates of maximum seismic horizontal ground motion on rock in the Pacific Northwest and the adjacent Outer Continental Shelf: U.S. Geological Survey Open-File Report 80-471, 39 p., 7 plates, scale 1:5,000,000.

Qamar, A., and Hawley, B., 1979, Seismic activity near Three Forks Basin, Montana: Seismological Society of America Bulletin, v. 69, no. 6, p. 1917-1929.

Rast, N., 1980, The Avalonian Plate in the Northern Appalachians and Caledonides, in, Wones, D. R., eds., Proceedings of the Caledonides in the USA: Virginia Polytechnic Institute and State University Memoir 2, p. 63-66.

Riddihough, R. P., 1977, A model for recent plate interactions off Canada's west coast: Canadian Journal of Earth Science, v. 14, p. 384-396.

_____1978, The Juan de Fuca plate: EOS (American Geophysical Union, Transactions), v. 59, no. 9, p. 836-842.

Riddihough, R. P., and Hyndman, R. D., 1977, Canada's active western margin--The case for subduction: Geoscience Canada, v. 3, no. 4, p. 269-278.

Russ, D. P., 1979, Late Holocene Faulting and Earthquake Recurrence in the Reelfoot Lake Area, Northwestern Tennessee: Geological Society of America Bulletin, pt. 1, v. 90, p. 1013-1018.

Russ, D. P., 1981, Model for Assessing Earthquake Potential and Fault Activity in the New Madrid Seismic Zone, in, Beavers, J. E., ed., Earthquakes and Earthquake Engineering--Eastern United States: Ann Arbor Science Publishers, Inc., Ann Arbor, Michigan, v. 1, p. 309-319.

Ryall, A. S., 1977, Earthquake hazard in the Nevada region: Seismological Society of America Bulletin, v. 67, no. 2, p. 517-532.

Ryall, A. S., and Van Wormer, J. D., 1980, Estimation of maximum magnitude and recommended seismic zone changes in the western Great Basin: Seismological Society of America Bulletin, v. 70, no. 5, p. 1573-1581.

Ryall, A. S., Slemmons, D. B., and Gedney, L. D., 1966, Seismicity tectonism and surface faulting in the western United States in historic time: Seismological Society of America Bulletin, v. 56, p. 1105-1135.

Sanford, A. R., Olsen, K. H., Jaksha, L. H., 1981, Seismicity of New Mexico-1849 through 1977 in, Hays, W. W., ed., proceedings of the conference on evaluation of regional seismic hazards and risk, August 25-27, 1980, Santa Fe, New Mexico: U.S. Geological Survey Open-File 81-437, p. 74-89.

Sanford, A. R., Olsen, K. H., and Jaksha, L. H., 1979, Seismicity of the Rio Grande Rift, in, Riecker, R. E., ed., Rio Grande Rift, tectonics and magmatism: America Geophysical Union, p. 145-168.

Sbar, M. L., Barazangi, M., Dorman, J., Scholz, C. H., and Smith, R. B., 1972, Tectonics of the Intermountain Seismic Belt, Western United States--Microearthquake seismicity and composite fault plane solutions: Geological Society of America Bulletin, v. 82, p. 13-28.

Sbar, M. L., and Sykes, L. R., 1973, Contemporary stress and seismicity in eastern North America--An example of intraplate tectonics: Geological Society of America Bulletin, v. 84, p. 1861-1862.

Schnabel, P., and Seed, H. B., 1973, Acceleration in rocks for earthquakes in the western United States: Bulletin of Seismological Society of America, v. 63, p. 501-516.

Shoemaker, E. M., Squires, R. L., and Abrams, M. J., 1978, Bright Angel and Mesa Butte Fault Systems of Northern Arizona, in, Smith, R. B., and Eaton, G. P., eds., Cenozoic Tectonics and Regional Geophysics of the Western Cordierlla: Geological Society of America Memoir 152, p. 341-367.

Silver, E. A., 1978a, Geophysical studies and tectonic development of the continental margin off the Western United States, lat. 34° to 48° N., in, Smith, R. B., and Eaton, G. P., eds., Cenozoic tectonics and regional geophysics of the Western Cordillera: Geological Society of America Memoir 152, p. 251-262.

Silver, E. A., 1978b, The San Gregorio-Hosgri Fault Zone: An overview, in Silver, E. A., and Normark, W. R., eds., The San Gregorio-Hosgri Fault Zone: California Division of Mines and Geology, Special Publication 137, p. 1-2.

Simms, P. K., Card, K. D., Morey, G. B., and Peterman, Z. E., 1980, The Great Lakes Tectonic Zone - A major crustal structure in Central North America: Geological Society of America, pt. 1, v. 91, p. 690-698.

Simpson, R. W., and Cox, A. V., 1977, Paleomagnetic evidence for tectonic rotation of the Oregon Coast Range: Geology, v. 5, p. 585-589.

Skehan, J. W., 1965, A continental-oceanic crustal boundary in the Pacific Northwest: Bedford, Mass., Air Force Cambridge Research Laboratories, Office of Aerospace Research, Scientific Report 3, 52 p.

Smith, R. B., and Sbar, M. L., 1974, Contemporary tectonics and seismicity of the Western United States with emphasis on the Intermountain seismic belt: Geological Society of America Bulletin, v. 85, p. 1205-1218.

Smithson, S. B., Brewer, J., Kaufman, S., Oliver, J., and Hurich, C., 1978, Question of the Wind River Thrust, Wyoming, Resolved by COCORP Deep Reflection Data and by Gravity Data: Wyoming Geological Association Guidebook, 30th Annual Field Conference, p. 227-234.

Stacey, R. A., 1973, Gravity anomalies, crustal structure, and plate tectonics in the Canadian cordillera: Canadian Journal of Earth Science, v. 10, p. 615-628.

Stepp, J. C., 1973, Analysis of completeness of the earthquake sample in the Puget Sound area, in Harding, S. T., ed., Contributions to seismic zoning: National Oceanic and Atmospheric Administration Technical Report ERL267-ESL30, p. 16-28.

Stickney, M. C., 1978, Seismicity and Faulting in Western Montana: Northwest Geology, v. 7, p. 1-9.

Stover, C.W., and others, 1979-1981, Seismicity maps of the states of the U. S. Geological Survey Miscellaneous Field Studies maps.

Stuart, W. D., 1979, Strain softening prior to two-dimensional strike-slip earthquakes: Journal of Geological Research, v. 84, no. B3, p. 1063.

Swan, F. H., III, Schwartz, D. P., Cluff, L. S., 1980, Recurrence of moderate to large magnitude earthquakes produced by surface faulting on the Wasatch Fault Zone, Utah: Seismological Society of America Bulletin, v. 70, p. 1431-1462.

Thenhaus, P. C., Perkins, D. M., Ziony, J. I., and Algermissen, S. T., 1980, Probabilistic estimates of maximum seismic horizontal ground motion on rock in coastal California and the adjacent outer continental shelf: U.S. Geological Survey Open-File Report 80-924, 69 p., 7 pls., scale 1:5,000,000.

Thenhaus, P. C., Ziony, J. I., Diment, W. H., Hopper, M. G., Perkins, D. M., Hanson, S. L., and Algermissen, S. T., 1982, Probabilistic estimates of maximum seismic horizontal ground motion on rock in Alaska and the adjacent outer continental shelf in, Coonrad, W. L., ed., U.S. Geological Survey in Alaska--Accomplishments during 1980: U.S. Geological Survey Circular 844, p. 5-9.

Thenhaus, P. C., Algermissen, S. T., and Perkins, D. M., 1982a, A new seismic source zone map for the conterminous United States [abs.]: Geological Society of America Abstracts with Programs, v. 14, no. 7, p. 630.

Thenhaus, P. C., and Wentworth, C. M., 1982b, Map showing zones of similar ages of surface faulting and estimated maximum earthquake size in the Basin and Range Province and selected adjacent areas: U.S. Geological Survey Open-File Report 82-742, 18 p., 1 pl., scale 1:2,500,000.

Thornbury, W. D., 1965, Regional geomorphology of the United States: John Wiley and Sons Inc., 609 p.

Van Wormer, J. D., and Ryall, A. S., 1980, Sierra Nevada-Great Basin boundary zone: Earthquake hazard related to structure, active tectonic processes, and anomalous patterns of earthquake occurrence: Bulletin of the Seismological Society of America, v. 70, no. 5, p. 1557-1572.

Walker, G. W., 1977, Geologic Map of Oregon East of the 21st Meridian: U.S. Geological Survey Miscellaneous Investigations Series, I-902, 2 sheets, scale 1:500,000.

Wallace, R. E., 1977a, Profiles and ages of young fault scarps, north-central Nevada: Geological Society of America Bulletin, v. 88, p. 1267-1281.

Wallace, R. E., 1977b, Time-history analysis of fault scarps and fault traces--a longer view of seismicity in, Ground motion seismicity, seismic risk, and zoning: World Conference on Earthquake Engineering, 6th New Delhi, January 10-14, 1977.

Wallace, R. E., 1978a, Geometry and rates of change of fault-generated range fronts, north-central Nevada: Journal of Research, U.S. Geological Survey, v. 6, no. 5, p. 637-650.

Wallace, R. E., 1978b, Size of larger earthquakes, north-central Nevada [abs.]: Earthquake Notes, v. 49, no. 1, p. 23.

Wallace, R. E., 1978c, Patterns of faulting and seismic gaps in the Great Basin Province, in, Proceedings of Conference VI, Methodology for identifying seismic gaps and soon-to-break gaps: U.S. Geological Survey Open-File Report 78-943, p. 857-868.

Warner, L. A., 1978, The Colorado Lineament A Middle Precambrain Wrench Fault System: Geological Society of America Bulletin, v. 89, p. 161-171.

Wentworth, C. M., and Mergner-Keefer, M., 1981, Reverse faulting along the eastern seaboard and the potential for large earthquakes, in, Beavers, J. E. ed., Earthquakes and Earthquake Engineering--Eastern United States: Ann Arbor Science Publishers, Inc., Ann Arbor, Michigan, v. 1, p. 109-128.

White, C. M., and McBirney, A. R., 1978, Some quantitative aspects of orogenic volcanism in the Oregon Cascades, in Smith, R. B., and Eaton, G. P., eds., Cenozoic tectonics and regional geophysics of the western cordillera, Geological Society of America Memoir 152, p. 369-388.

Witkind, I. J., 1977, Major active faults and seismicity, Northwestern Montana: U.S. Geological Survey Map Miscellaneous Field Studies MF-923, 1 plate, scale 1:500,000.

Woodward-Clyde Consultants, 1980, Seismological Review of the July 16, 1936, Milton-Freewater earthquake source region: report prepared for the Washington Public Power Supply System by Woodward-Clyde Consultants, Contract No. 52028, c.o. 11, Task No. WCC1.

Yang, J. P., and Aggarwal, Y. P., 1981, Seismotectonics of northeastern United States and adjacent Canada: Journal of Geophysical Research, v. 86, no. B6, p. 4981-4998.

Zoback, M. L., and Zoback, M. D., 1980, State of Stress in the Conterminous United States: Journal of Geophysical Research, v. 85, p. 6113-6156.

Zoback, M. D., Hamilton, R. M., Crone, A. J., Russ, D. P., McKeown, F. A., and Brockman, S. R., 1980, Recurrent Intraplate Tectonism in the New Madrid Seismic Zone: Science, v. 209, p. 971-976.

Ziony, J. I., Wentworth, C. M., Buchanan-Banks, J. M., and Wagner, H. C., 1974, Preliminary map showing recency of faulting in coastal southern California: U.S. Geological Survey Miscellaneous Field Studies Map MF-585, 3 pl. scale 1:250,000, 7 p.

Jackson

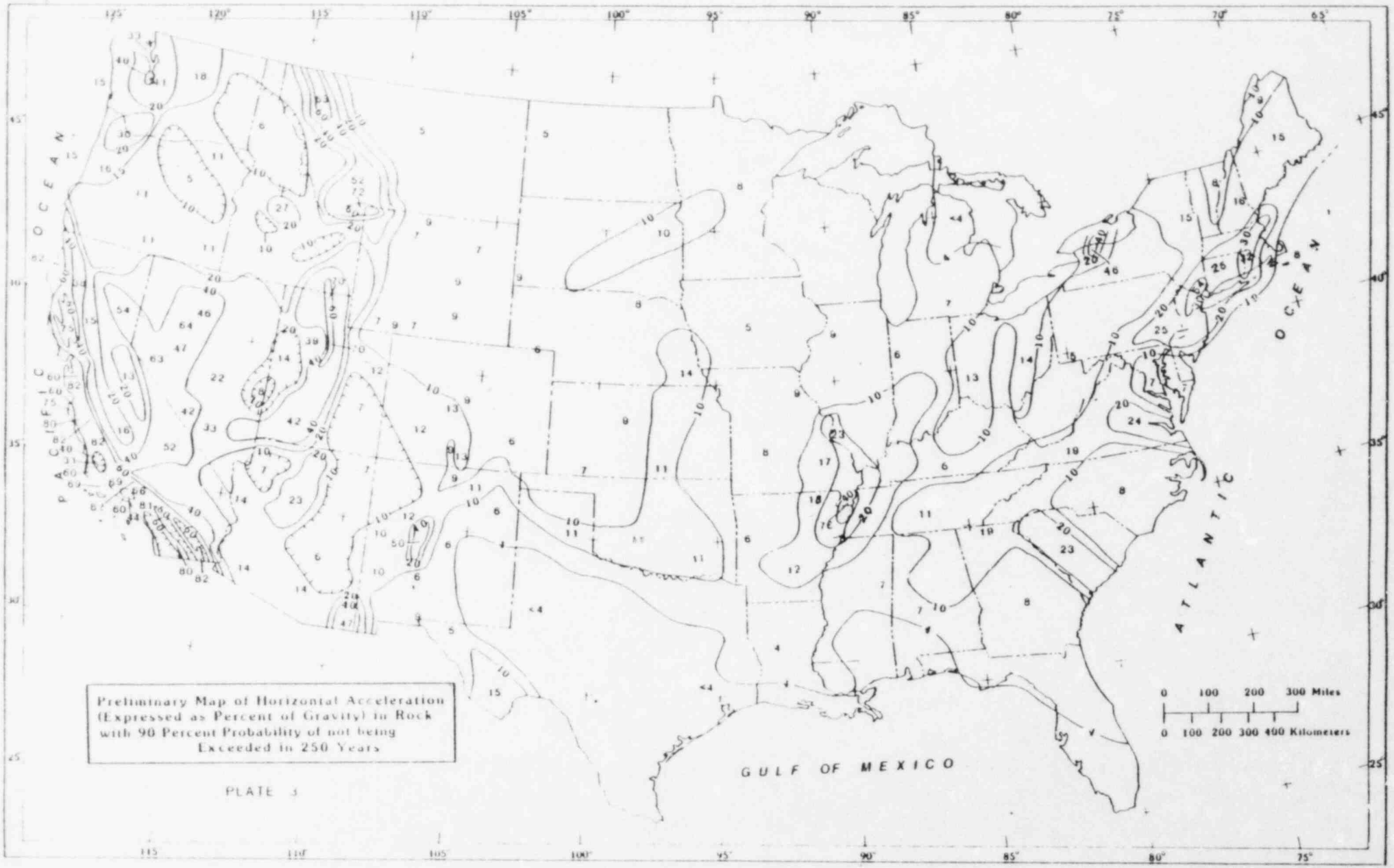

Preliminary Map of Horizontal Acceleration (Expressed as Percent of Gravity) in Rock with 90 Percent Probability of not being Exceeded in 250 Years

PLATE 3

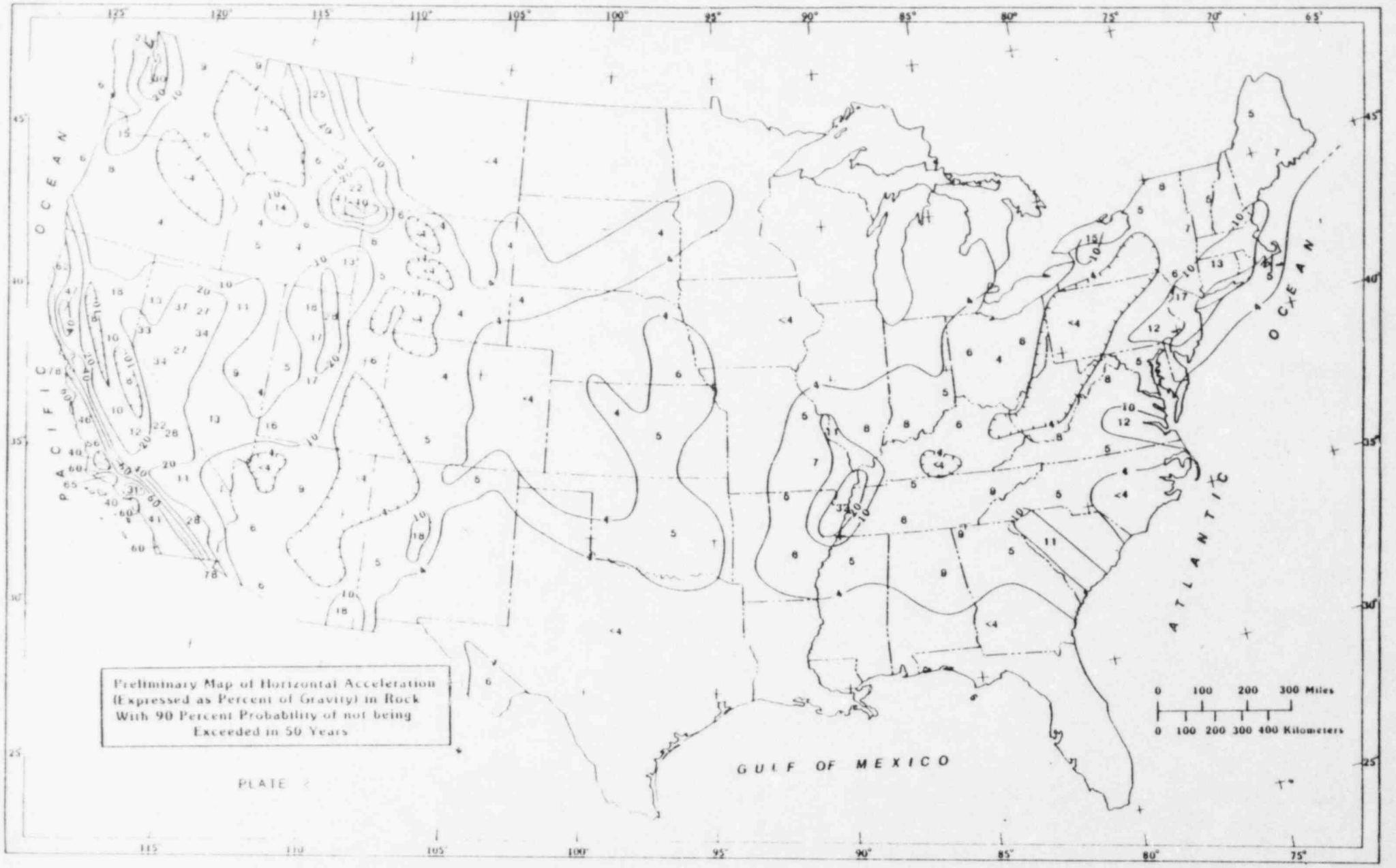
Preliminary Map of Horizontal Acceleration
(Expressed as Percent of Gravity) in Rock
With 90 Percent Probability of not being
Exceeded in 50 Years
PACIFIC OCEAN
ATLANTIC OCEAN
GULF OF MEXICO
0 100 200 300 Miles
0 100 200 300 400 Kilometers
PLATE 2

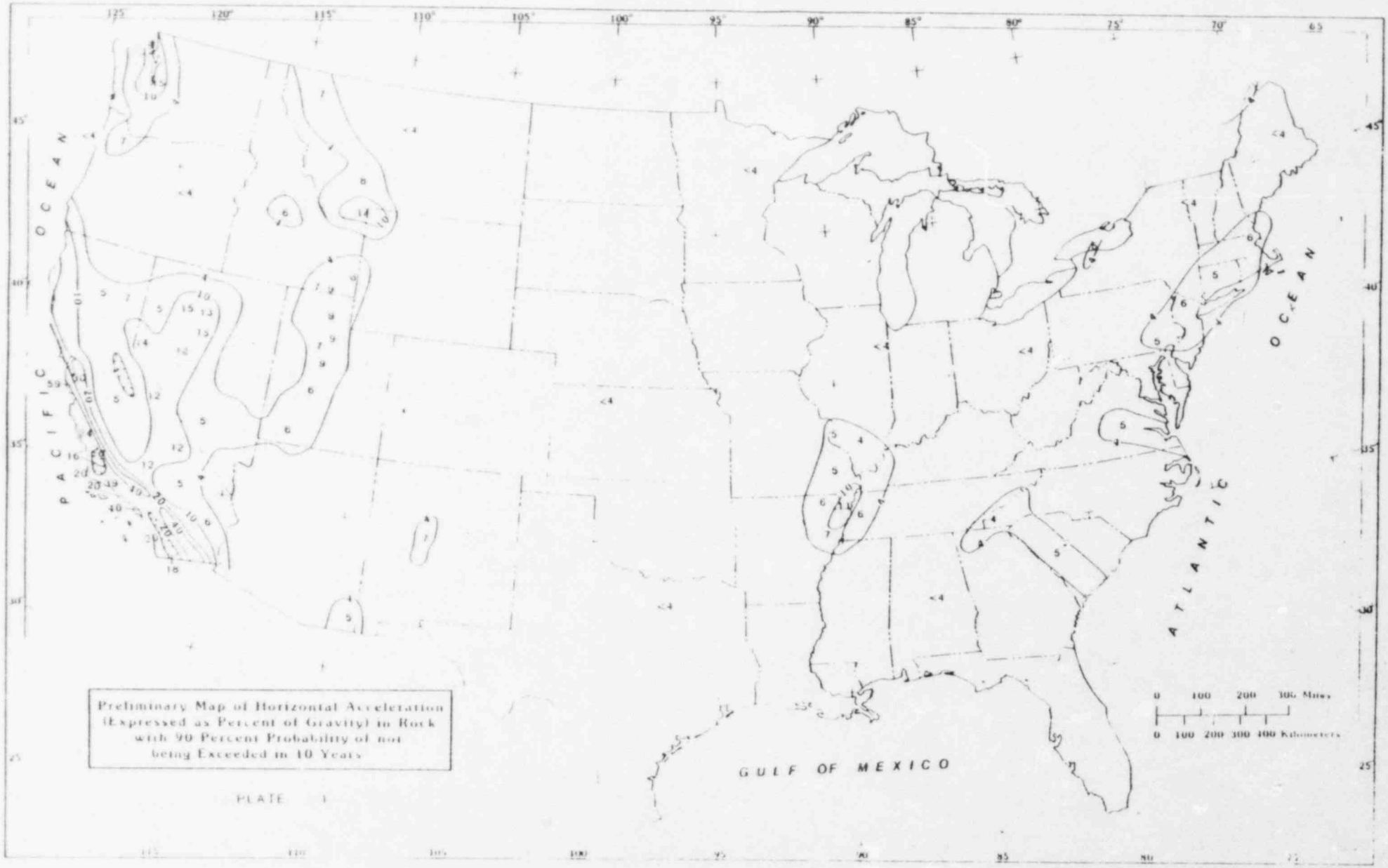

Preliminary Map of Horizontal Acceleration (Expressed as Percent of Gravity) in Rock with 90 Percent Probability of not being Exceeded in 10 Years

PLATE 1

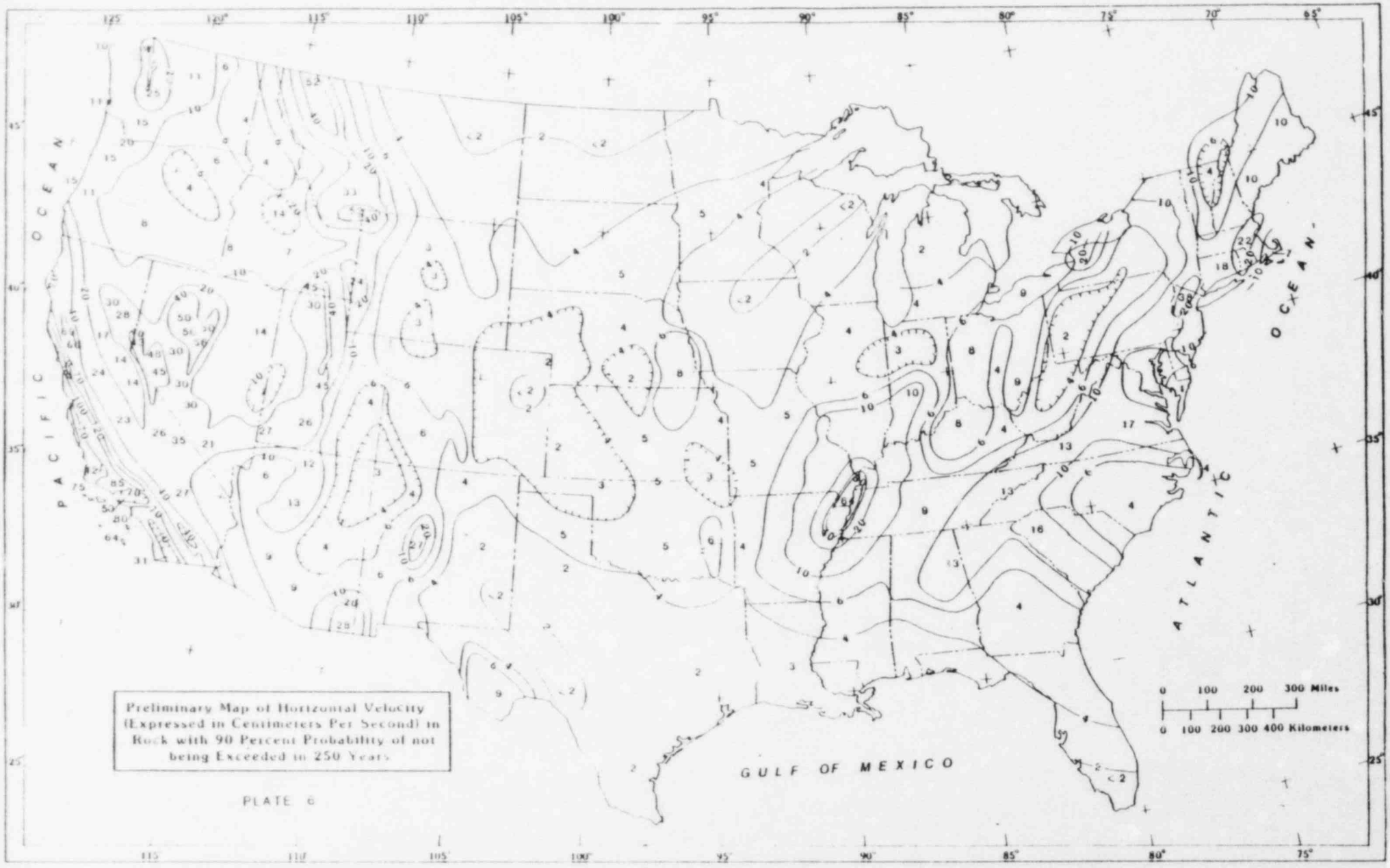

Preliminary Map of Horizontal Velocity (Expressed in Centimeters Per Second) in Rock with 90 Percent Probability of not being Exceeded in 250 Years

PLATE 6

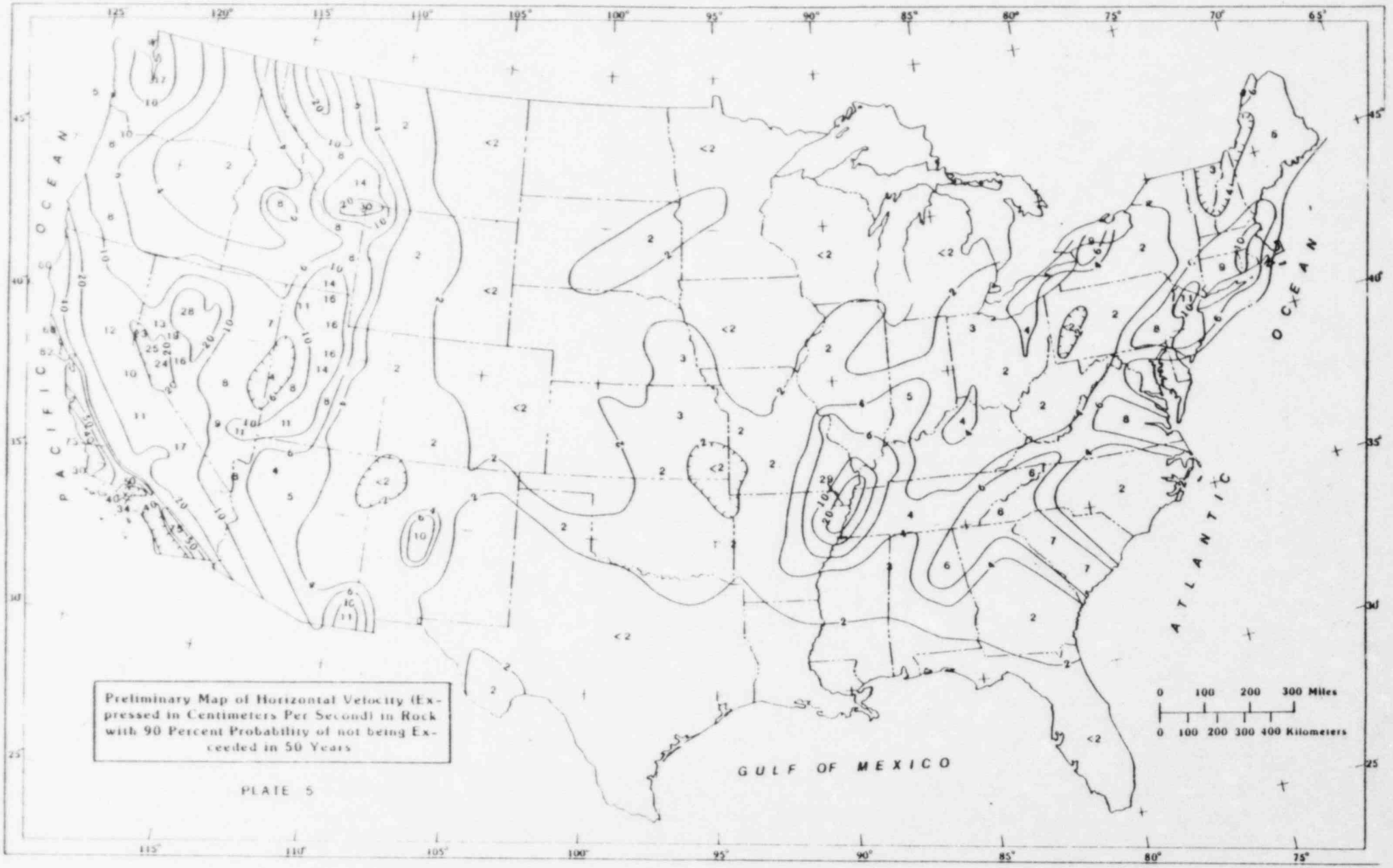

Preliminary Map of Horizontal Velocity (Expressed in Centimeters Per Second) in Rock with 90 Percent Probability of not being Exceeded in 50 Years

PLATE 5

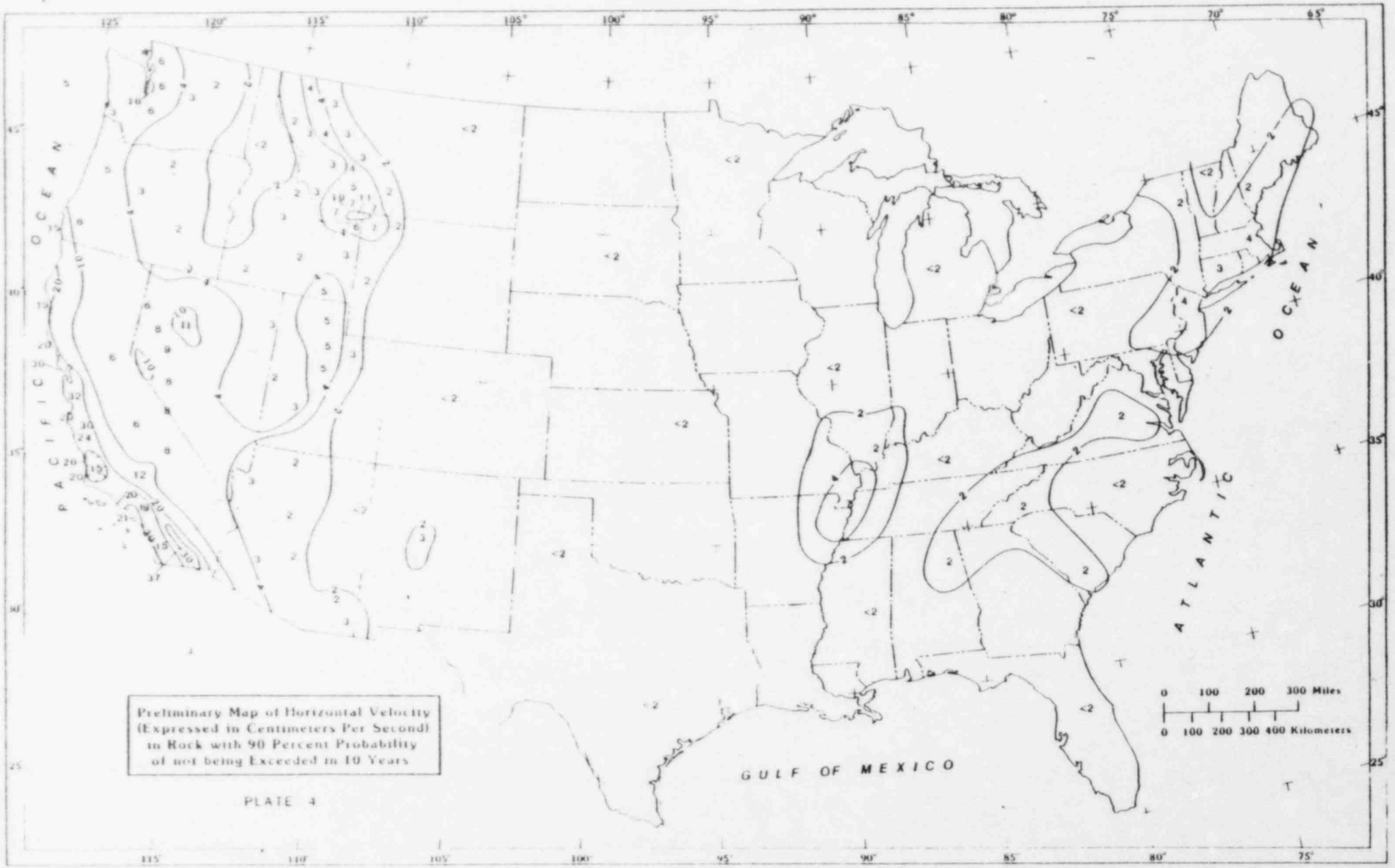

Preliminary Map of Horizontal Velocity (Expressed in Centimeters Per Second) in Rock with 90 Percent Probability of not being Exceeded in 10 Years

PLATE 4

UNITED STATES
NUCLEAR REGULATORY COMMISSION
WASHINGTON, D. C. 20555

DISTRIBUTION FOR BOARD NOTIFICATION

RE: U.S.G.S. OPEN FILE REPORT ON PROBABILISTIC ESTIMATES OF MAXIMUM ACCELERATION AND VELOCITY IN ROCK IN THE U.S. (BOARD NOTIFICATION NO. 82-123)

Docket File -50-133
NRC PDR
LPDR
ORB#2 RDG
ORB#2 BRD FILE
HDenton
ECase
DEisenhut
GLainas
DVassallo
VRooney
SNorris
MJambor
JHard
ABennett-2
ACRS-16
RHartfield
OIE
PPAS
MWilliams
AEOD
JThoma
GMeyer
JGray
JScinto-2
MYoung
SGoldberg
STreby